

University of New Hampshire

University of New Hampshire Scholars' Repository

Master's Theses and Capstones

Student Scholarship

Winter 2014

Automatic Updating Of Structural Models Using Inspection Report Data

Timothy Foy

University of New Hampshire, Durham

Follow this and additional works at: <https://scholars.unh.edu/thesis>

Recommended Citation

Foy, Timothy, "Automatic Updating Of Structural Models Using Inspection Report Data" (2014). *Master's Theses and Capstones*. 986.

<https://scholars.unh.edu/thesis/986>

This Thesis is brought to you for free and open access by the Student Scholarship at University of New Hampshire Scholars' Repository. It has been accepted for inclusion in Master's Theses and Capstones by an authorized administrator of University of New Hampshire Scholars' Repository. For more information, please contact Scholarly.Communication@unh.edu.

AUTOMATIC UPDATING OF STRUCTURAL MODELS
USING INSPECTION REPORT DATA

BY

TIMOTHY FOY

MS, College of Engineering and Physical Sciences, 2014

THESIS

Submitted to the University of New Hampshire
in Partial Fulfillment of
the Requirements for the Degree of

Master of Science
in
Civil Engineering

December 2014

This thesis has been examined and approved in partial fulfillment of the requirements for the degree of Master of Science in Civil Engineering by:

Thesis/Dissertation Director, Dr. Erin Santini-Bell, Associate
Professor, Civil Engineering

Dr. Raymond A. Cook, Associate Professor, Civil Engineering

Dr. Ricardo A. Medina, Associate Professor, Civil Engineering

On November 4, 2014

Original approval signatures are on file with the University of New Hampshire Graduate School.

Chapter 1: Contents

List of Figures	vi
List of Tables	viii
List of Equations.....	viii
ABSTRACT.....	ix
Chapter 1: Introduction	1
1.1 – Social Need.....	1
1.2 – Major Contribution of this Research	2
1.3 – Bridge Inspection	3
1.3.1 – Silver Bridge	4
1.3.2 – National Bridge Inspection Standards	10
1.4 – Structural Health Monitoring.....	11
1.5 – Model Updating	12
1.6 – Case Studies	13
1.6.1 Commodore Barry Memorial Bridge	13
1.6.2 Powder Mill Bridge.....	15
1.6.3 Rollins Road Bridge	16
1.6.4 Tobin Memorial Bridge	19
1.7 – Monitoring Model Creation	20
1.7.1 – Finite Element Modeling.....	21
Chapter 2: Model Updating	23
2.1 – Inspection Reporting.....	23
2.2 – Model Updating Procedures	26
2.2.1 – Visual Basic for Applications	26
2.2.2 – Model Updating Protocols	27
2.2.3 Radius of Gyration	30
2.3 –Structural Model Verification	31
2.4 – Recommended Applications	33
Chapter 3: Introduction to the Maurice J Tobin Memorial Bridge.....	35
3.1 – Instrumentation of the Little Mystic Span	37
3.1.1 Instrumentation Plan	37
3.1.2 Data Collection.....	39
3.2 Installation	39

3.2.1 Preparation Procedure.....	40
3.3 Load Testing.....	40
Chapter 4: Case Study.....	42
4.1 – Testing Plan.....	42
4.2 – Truck Specifications	42
4.3 – Tobin Bridge Finite Element Model	43
4.4 – Truck Load Distribution.....	47
4.5 – Results.....	48
4.5.1 – Chord Members	50
4.5.2 – Diagonals.....	57
4.5.3 – Floor Beams	63
4.5.4 – Verticals.....	69
4.5.5 – Changes to Section Properties.....	79
Chapter 5: Conclusions/Future Work	81
5.1 – Conclusions	81
5.2 – Future Work.....	82
5.2.1 Improved Joint Analysis	82
5.2.1 Improved Acceptance Criteria	83
5.3 – The Future of Bridge Condition Assessment	83
5.4 – The Future of Bridge Modeling.....	85
5.5 – The Future of Bridge Management.....	87
References	89
Appendices.....	93
Appendix 1 User’s Guide.....	94
User’s Guide Table of Contents	94
A1.1 – Introduction	94
A1.2 - Model Setup	94
A1.3 - Spreadsheet Setup	95
A1.4 – Execution	95
A1.5 - Post Processing.....	96
Appendix 2: Sensor Data Sheets.....	96
Appendix 3: Additional Strain vs Time Graphs	104
Appendix 4: VBA Routines	123

Model Updating Protocol.....	123
------------------------------	-----

List of Figures

Figure 1-1: Silver Bridge circa 1966 (Mason County, WV).....	5
Figure 1-2: NTSB Traffic Data at Time of Collapse (National Transportation Safety Board, 1970)	6
Figure 1-3: Bridge Inspection Field Notes, Example (TranSystems, 2008)	7
Figure 1-4: Portion of Silver Bridge Eyebars 330 (National Institute of Standards and Technology, 2009)	8
Figure 1-5: Commodore Barry Bridge, (Dietrich, 2005).....	14
Figure 1-6: Powder Mill Bridge	15
Figure 1-7: Girder 4 top sensor raw, theoretical, and empirical data from April 2008 load test, with three zero-load data points and trend lines included (Sipple and Santini-Bell 2009).....	18
Figure 1-8: Graphical Representation of Parameter Estimation (Bell & Sipple, In-Service Performance Monitoring of a CRFP Reinforced HPC Bridge Deck, 2009)	18
Figure 1-9: Tobin Bridge, Little Mystic Span (MementoMori, 2012).....	20
Figure 2-1 Existing Inspection and Load Rating Procedure	27
Figure 2-2: Model Updater Procedure.....	27
Figure 3-1 Tobin Memorial Bridge (Google, 2013)	35
Figure 3-2: Components of the Tobin Bridge	36
Figure 3-3: Tobin Bridge, Big Mystic Span (Chensiyuan, 2009)	36
Figure 3-4: Elevation view of Little Mystic Span instrument locations (Sanayei, Pfeifer, Brenner, Bell, & Allen, 2010).....	38
Figure 3-5 Example strain rosette in 60° configuration [Efunda 2010]	39
Figure 3-6 Installation of HS Data Acquisition Systems (Sanayei, Pfeifer, Brenner, Bell, & Allen, 2010)	40
Figure 3-7 Strain Gauge Installation Procedure (Sanayei, Pfeifer, Brenner, Bell, & Allen, 2010)	40
Figure 4-1: Trucks Used During Load Test (Sanayei, Pfeifer, Brenner, Bell, & Allen, 2010)	43
Figure 4-2: Basic Model (Sanayei, Pfeifer, Brenner, Bell, & Allen, 2010)	44
Figure 4-3: Piers Model (Sanayei, Pfeifer, Brenner, Bell, & Allen, 2010).....	45
Figure 4-4: Tobin Bridge Shoe Connection	46
Figure 4-5: Tobin Bridge, Hand Holes in Built up Sections	47
Figure 4-6: Truck Wheel Load Locations and Deck Support	48
Figure 4-7: SG-L6U5-E-02, Gap in Collected Data	49
Figure 4-8: SG-L6U7-E-03, Flat-lined Gauge	49
Figure 4-9: Little Mystic Bottom Chord Instrumentation	51
Figure 4-10: SG-L4L5-E-01 Strain vs Time	52
Figure 4-11: SG-L4L5-E-02 Strain vs Time	53
Figure 4-12: SG-L4L5-E-04 Strain vs Time	53
Figure 4-13: SG-L5L6-E-05 Strain vs Time	54
Figure 4-14: SG-L5L6-E-07 Strain vs Time	54
Figure 4-15: SG-L5L6-E-08 Strain vs Time	55
Figure 4-16: SG-L5L6-W-06 Strain vs Time	55
Figure 4-17: SG-L5L6-W-08 Strain vs Time	56
Figure 4-18: SG-L6L7-E-01 Strain vs Time	56

Figure 4-19: SG-L6L7-E-02 Strain vs Time	57
Figure 4-20: SG-L6L7-E-07 Strain vs Time	57
Figure 4-21: Little Mystic Diagonal Instrumentation.....	58
Figure 4-22: SG-L6U5-E-03 Strain vs Time	60
Figure 4-23: SG-L6U5-E-04 Strain vs Time	60
Figure 4-24: SG-L6U5-E-03 Strain vs Time	61
Figure 4-25: SG-L6U5-E-06 Strain vs Time	61
Figure 4-26: SG-L6U5-E-08 Strain vs Time	62
Figure 4-27: SG-L6U7-E-01 Strain vs Time	62
Figure 4-28: SG-L6U7-E-02 Strain vs Time	63
Figure 4-29: SG-L6U7-E-07 Strain vs Time	63
Figure 4-30: SG-FB4-E-01 Strain vs Time	65
Figure 4-31: SG-FB4-E-02 Strain vs Time	66
Figure 4-32: SG-FB4-E-03 Strain vs Time	66
Figure 4-33: SG-FB4-E-04 Strain vs Time	67
Figure 4-34: SG-FB5-E-01 Strain vs Time	67
Figure 4-35: SG-FB5-E-02 Strain vs Time	68
Figure 4-36: SG-FB5-E-03 Strain vs Time	68
Figure 4-37: SG-FB5-E-04 Strain vs Time	69
Figure 4-38: Vertical Member Cross Section.....	69
Figure 4-39: Little Mystic Elevation - Instrumented Verticals	70
Figure 4-40: Little Mystic Sway Frame.....	71
Figure 4-41: Vertical Member Moment Diagram	71
Figure 4-42: SG-L5U5-E-01 Strain vs Time	72
Figure 4-43: SG-L5U5-E-02 Strain vs Time	72
Figure 4-44: SG-L5U5-E-03 Strain vs Time	73
Figure 4-45: SG-L5U5-E-04 Strain vs Time	73
Figure 4-46: SG-L5U5-E-05 Strain vs Time	74
Figure 4-47: SG-L5U5-E-06 Strain vs Time	74
Figure 4-48: SG-L6U6-E-02 Strain vs Time	75
Figure 4-49: SG-L6U6-E-03 Strain vs Time	75
Figure 4-50: SG-L6U6-E-04 Strain vs Time	76
Figure 4-51: SG-L6U6-E-05 Strain vs Time	76
Figure 4-52: SG-L6U6-E-06 Strain vs Time	77
Figure 4-53: SG-L6U6-E-07 Strain vs Time	77
Figure 4-54: SG-L6U6-E-08 Strain vs Time	78
Figure 5-1: Effects of Localizing Deterioration.....	85
Figure 5-2: Subdivided Member U5-L6.....	86
Figure 5-3: Element Based Model Updating and Load Rating Flowchart.....	88
Figure 5-4: Comparison of LRFR and EDM Inventory Factors for Girders 1 through 6 (LeFebvre, 2010)	88

List of Tables

Table 2-1: Sample Inspection Field Notes (TranSystems, 2008).....	25
Table 2-2: Example Model Updater Spreadsheet.....	30
Table 3-1 Instrumentation types and quantities for the Little Mystic Span.....	38
Table 4-1: Changes to Structural Models	50
Table 4-2: Comparison of Section Properties	79

List of Equations

Equation 2-1.....	30
Equation 2-2.....	30
Equation 2-3.....	31
Equation 2-4.....	31
Equation 2-5.....	31
Equation 2-6.....	31
Equation 2-7: Objective Function, J	32

ABSTRACT

AUTOMATIC UPDATING OF STRUCTURAL MODELS
USING INSPECTION REPORT DATA

by

Timothy Foy

University of New Hampshire, December, 2014

In the current economic climate, bridge managers are continually working to maximize the impact of each expense. One way to keep costs down is to streamline maintenance procedures and to first address problems that require immediate attention. Thus, it is important to fully understand the behavior of the bridge. Typically, this assessment is based on regularly scheduled visual bridge inspections. Visual bridge inspections provide valuable information, but are subjective in nature and limited to areas that are visible. Instead bridges should be analyzed and evaluated as a system.

The current procedure used to evaluate bridges is based on assessing each element and requires significant efforts from a data management perspective. The process typically involves manually transcribing inspection field notes, manually calculating member section properties, and manually updating structural models for global analysis and eventual load rating. The research presented in this document describes a proof of concept application for the automatic updating of structural models with inspection report data and creates a platform for inclusion of load test data in structural condition assessment.

Chapter 1: Introduction

1.1 – Social Need

In recent years there has been an increased public awareness pertaining to the structural condition of the infrastructure in the United States. This has come in large part due to the high profile collapse of the I-35W in Minneapolis, Minnesota (2007) and the I-5 Skagit Bridge in Mount Vernon, Washington (2013). This awareness has been reinforced by The American Society of Civil Engineers Infrastructure Report Card for 2013. In this Infrastructure Report Card, the nation's bridges received a grade of C+ (American Society of Civil Engineering, 2013). While this is one of the better grades given to the nation's infrastructure systems, there are more than 500 "Red-Listed" bridges in New Hampshire alone. "Red List" is a category unique to New Hampshire to indicate that a bridge structure is in poor condition and requires immediate action as a rehabilitation, repair or replacement and require more intense inspection procedures until maintenance is performed. These bridges account for about 13% of the nearly 3,800 New Hampshire bridges. (ASCENH, 2011)

The goal of this research was to develop and deploy a protocol that can support more efficient and effective decisions related to bridge maintenance allocations given increasingly limited resources. This protocol includes three parts that are based on current inspection procedures: the first part is a calibrated structural computer model of the target structure, the second component is a detailed visual inspection of the structure, and the final piece is a set of computer applications that automatically update the section properties of the members in the computer model based on the section properties of the inspected structure.

The resulting calibrated structural model verified through collected structural health monitoring data can provide support information for decision-making related to permitting and construction sequencing during rehabilitation for the bridge structure. The major contribution of this research is the third component of the aforementioned protocol. For many large bridges, detailed structural models already exist and inspection data is gathered for all bridges on a two year cycle. As such, this work seeks to leverage what is already done to produce faster, more accurate structural models and load ratings.

1.2 – Major Contribution of this Research

Currently, there exist no commercially available software packages that can automatically update and load rate a bridge by leveraging the information and procedures that are currently used in practice and required by federal guidelines (NBIS, 2014). There are, however, management tools that are used to inventory and analyze statewide infrastructure systems. AASHTOWare Bridge Management Software, formerly PONTIS, is used to keep track of changes in the health of bridges but does not provide any direct link between collected inspection data and structural analysis of bridge. In order to fill this gap, many engineering firms have used Excel Spreadsheets or other electronic means to calculate member section properties. This is done for a variety of reasons but two main reasons stand out. First, is for ease of record keeping. Electronic document storage can be performed far more easily and cheaply than paper documentation. Second, is that once a spreadsheet has been verified as correct, it can be used over and over again with little risk of error.

The second goal of this research is to advance the practice of bridge inspection from an element-by-element evaluation to a system-based condition assessment, which can provide

overload and construction permitting and remaining life prediction incorporating instrumentation, load testing, and structural modeling.

In a typical load rating procedure, after member section properties are calculated, hand calculations are typically performed using approximate methods. While these methods are perfectly fine for design of bridges where conservative values are normally a good thing, during the analysis of existing bridges, being overly conservative could result in limited resources being allocated inappropriately and in restricting bridges unnecessarily. Knowing the actual capacity of the bridge is of critical importance because it allows the bridge owner to direct funds to the bridges that really need work. This methodology may provide a more accurate means of determining bridge capacity.

1.3 – Bridge Inspection

Bridge inspection is an integral part of any bridge manager's toolbox. National standards have been established to govern all publicly owned bridges longer than 20 feet in length. These national standards were developed in the late 1960s and published in 1970. The National Bridge Inspection Standards (NBIS) have been revised many times in the past 40 years. Initially, there were frequent changes to the standards when it was in its infancy. These changes related to the training of bridge inspectors, setting requirements for inspectors, inspection procedures, frequency of inspections, inspection reporting, and bridge inventories. In later years provisions for movable bridges, compliance standards, and culvert inspection were added. Most notably, in 1988, requirements for scour were added which, in turn, required underwater inspections.

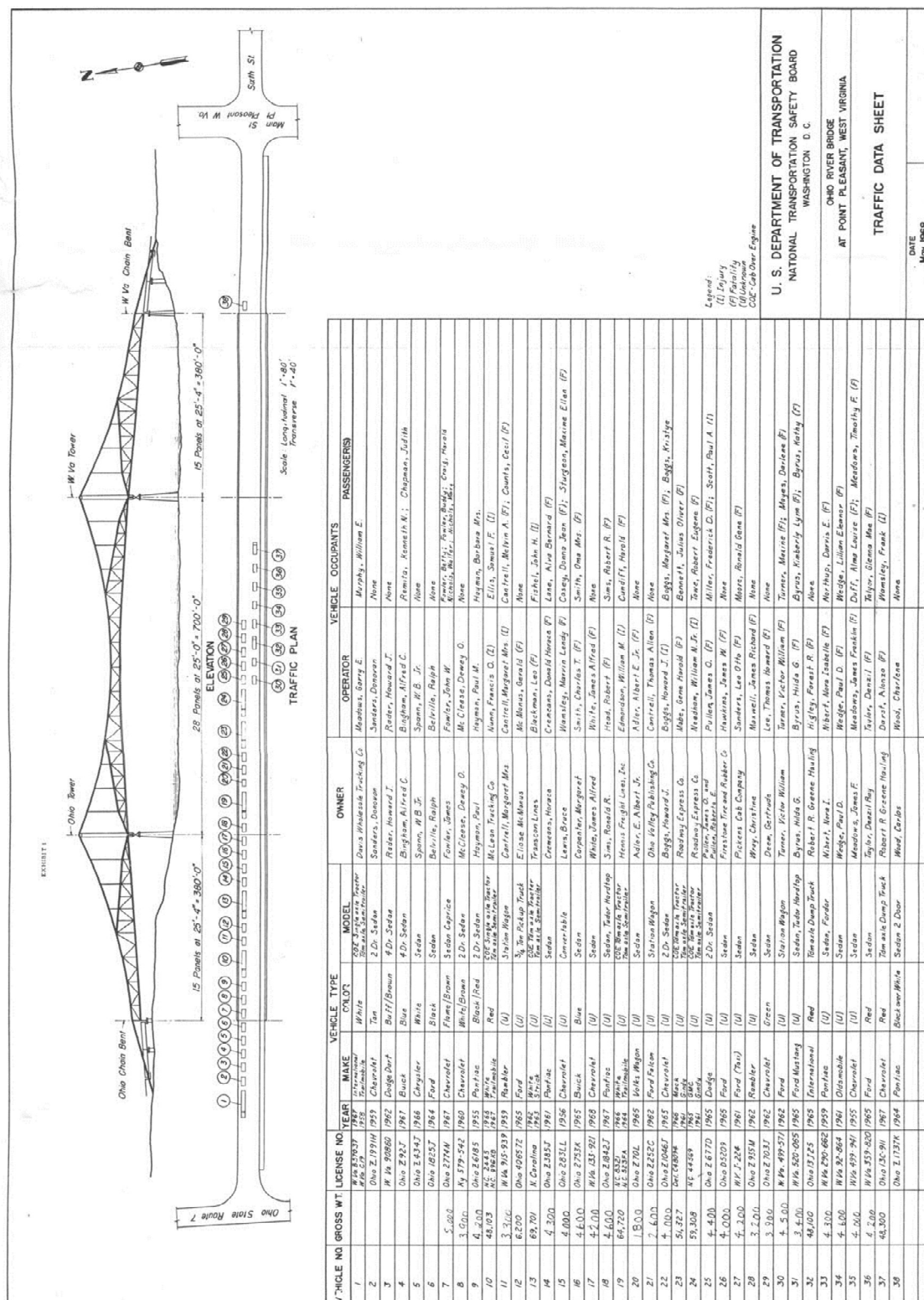
Special requirements for fracture critical members were also added in 1988. Since then, the standards have been updated, but the changes have not been dramatic (Leshko, 2005).

1.3.1 – Silver Bridge

The modern inspection procedures came to fruition after the collapse of the Silver Bridge connecting Point Pleasant, West Virginia to Kanauga, Ohio. The Silver Bridge was an eye-bar change suspension bridge (Figure 1-1). On December 15, 1967, the Silver Bridge collapsed killing 46 people. The total span length of the bridge was 2,235 feet. Each chain link was designed as a 2 inch by 12 inch bar with an 11 inch diameter pin. While steel chain eye bars had been used in the past, most bridges utilized a highly redundant design featuring four to six eye bars creating each link in the chain. The Silver Bridge designers opted for a high strength low redundancy design. Ultimately, each link in the Silver Bridge's chains was made up of only two eye bars. The towers that support the suspension chains were also design in an unorthodox manner. These "rocker" towers were not self-supporting. Rather, the towers depended on the chain for longitudinal stability. Therefore, if any of the main span or secondary span chains were to break, the entire bridge would fail. Additionally, when it was built in 1928, it was designed to support a 40,000 pound truck. At the end of its life, according to NTSB traffic data from the collapse, the bridge was supporting truck loads in excess of 60,000 pounds (Figure 1-2). Note that for the most part data collection and management has not dramatically changed since the late 1960s despite phenomenal advances in technology (Figure 1-3). This research may change that by providing a path forward that builds on current inspection procedures.



Figure 1-1: Silver Bridge circa 1966 (Mason County, WV)



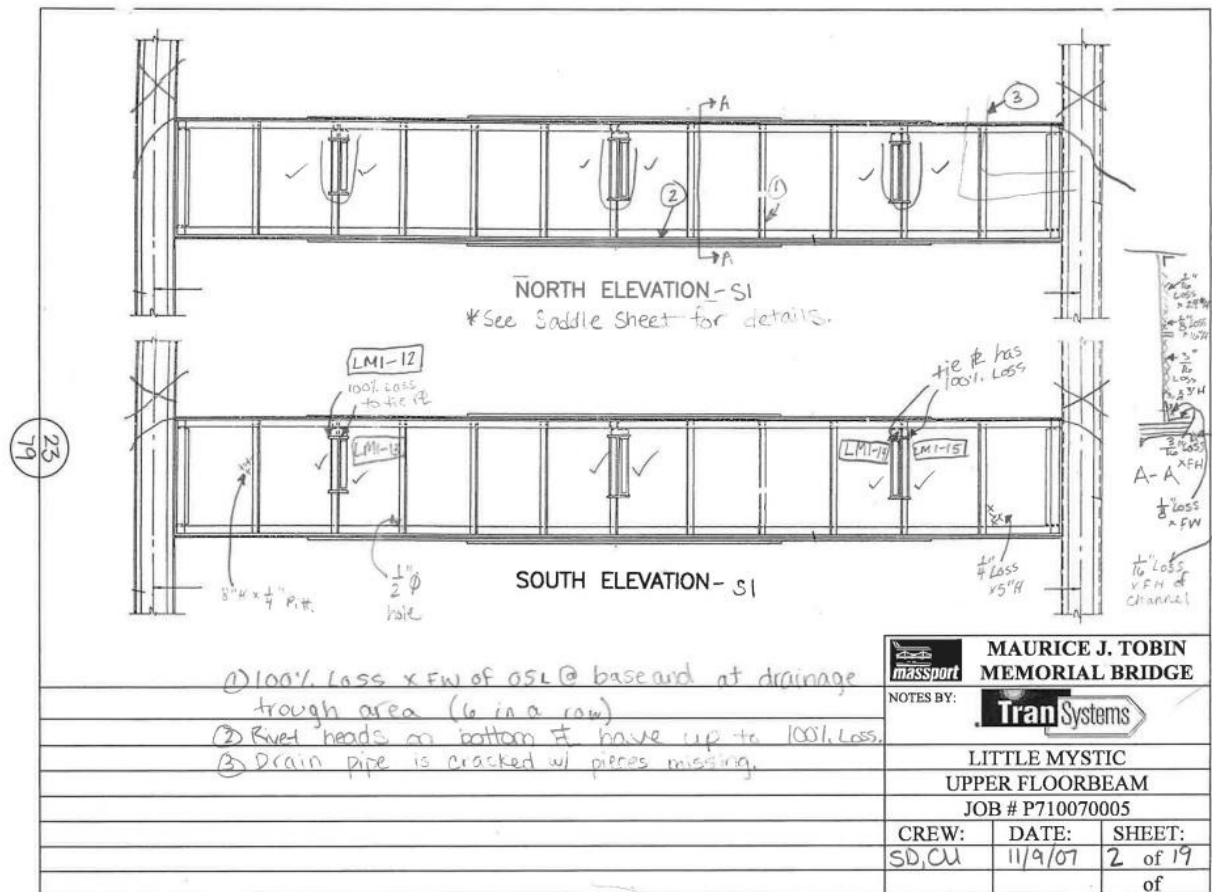


Figure 1-3: Bridge Inspection Field Notes, Example (TranSystems, 2008)

The cause of the Silver Bridge collapse was traced to a 0.1 inch deep defect in one of the steel eye bars. There were three main contributing causes that lead to the defect and failure of the bridge; first, the phenomena that had led to the cracking of the failing eye bar was not fully understood when the bridge was designed; second, the location of the crack, on the inside of the eye bar assembly, was inaccessible; finally, the technology to find cracks that are not visible had not been developed. A portion of Silver Bridge eyebar 330 is show in Figure 1-4: Portion of Silver Bridge Eyebar 330



Figure 1-4: Portion of Silver Bridge Eyebar 330 (National Institute of Standards and Technology, 2009)

In the aftermath of the collapse The National Transportation Safety Board issued recommendations to “expand existing research programs or institute new research programs to:

1. Identify bridge building materials susceptible to slow flaw growth by any of the suspected mechanisms;
2. Determine critical flaw size under various stress levels in bridge building materials;
3. Develop inspection equipment capable of detecting critical or near critical flaws in standing bridge structures;
4. Devise analytical procedures to identify critical locations in bridge structures which require detailed inspection;

5. Develop standards which incorporate appropriate safeguards in the design and fabrication of future bridges to ensure protection against failures of material such as occurred in the Point Pleasant Bridge (The Silver Bridge);
6. Develop standards for the qualification of materials for future bridge structures, using the information disclosed in this investigation;
7. Devise techniques for repair, protection, or salvage of bridges damaged by internal flaws; and
8. Expand the knowledge of loading history and life expectancy of bridges.”

(National Transportation Safety Board, 1970)

Looking back at research that has taken place in the past 40 years regarding these topics, many of them have been addressed through various revisions of the NBIS. Additionally, many of them are still being studied. Specifically, this research directly relates to items number 4 and 8 illustrating that these research areas are still relevant more than 50 years after the collapse of the Silver Bridge.

The NTSB also recommended the “Secretary of Transportation explore the alternatives for action to assure mandatory application of the bridge safety requirements of the 1968 Federal-Aid-Highway Act to all highway bridges in the United States, since the majority of older bridges in the country are not in the Federal-Aid-Highway System and these bridges are most susceptible to extensive repair or replacement; including such alternative courses of action as urging the adoption by the States of mandatory standards, or the enactment of Federal legislation applicable to all highway bridges.” (National Transportation Safety Board, 1970) This

particular recommendation has led directly to the establishment of the National Bridge Inspection Standards that are used today.

Finally, the NTSB recommended that the “Secretary of Transportation consider the advisability of proposing a program of Federal aid to ensure the adequate repair of all bridges not in the Federal-Aid-System.” (National Transportation Safety Board, 1970)

1.3.2 – National Bridge Inspection Standards

The National Bridge Inspection Standards set forth rules for bridges that must be inspected, who should inspect them, how they should be inspected, and when they should be inspected.

Within these rules are the seven main types of bridge inspections. These inspection types are initial, routine, damage, in-depth, fracture-critical, underwater, and special (AASHTO, 2011).

The first main type is an initial inspection. Initial inspections occur when a new bridge is opened or when a bridge undergoes significant rehabilitation. As part of this inspection, the bridge must be assigned a load carrying capacity and a scour critical determination. The initial inspection sets the baseline for all bridge inspections that will follow for a given bridge.

A routine inspection is used to determine the overall health of the bridge as it ages. Routine inspections typically occur every 24 months, however that frequency may be exceeded based on past reports, performance history, and analysis (AASHTO, 2011). Routine inspections may include other inspection types depending on the type of bridge and its location. For instance, a bridge that crosses a river may require an underwater inspection. Additionally, a routine inspection could trigger one of the other inspection types such as an in-depth inspection.

Routine inspections generally do not require special equipment as most bridges can be

satisfactorily inspected from the top of the deck, from the water level, and from permanent work platforms.

In-depth inspections are also known as hands-on inspection. The hands-on terminology comes from the idea that during the inspections, each element should be within an arm's reach so that all deficiencies that are not detectable through routine inspection procedures may be uncovered. If the bridge in question is small, the entire structure can be inspected using this method. For larger structures, sections of the bridge, categories of elements, or connections may be inspected separately from the rest of the structure.

Damage inspections are performed after an event that causes harm to the bridge. Damage inspections are, of course, unscheduled and must be adequate to determine if emergency repairs or load restriction are required for the bridge. An in-depth inspection will typically follow a damage inspection to verify field measurements and calculations.

The inspection of fracture critical members should be in accordance with the NBIS. Fracture critical members are those in which failure of the member could result in failure of a large portion of the bridge or the whole bridge (AASHTO, 2011). Testing of fracture critical material should be performed if mechanical properties are not available. The member or part in question may need to be specially cleaned or testing by means of x-ray or ultrasonic methods.

1.4 – Structural Health Monitoring

In the past 15 years, structural health monitoring systems have been used for many different purposes. Most notably, structural health monitoring systems are being used on bridges in an attempt to gauge the structural health of the bridge as it ages. Additionally, structural health monitoring systems can be used to verify the design of the bridge when innovative materials

(Bowman, 2002) or innovative construction techniques are used (LeFebvre, 2010). Structural health monitoring, when combined with other technologies, can help to greatly increase bridge owners ability to make accurate decisions regarding the allocation of maintenance funds. While some may argue that structural bridge engineers are capable of predicting the behavior of bridges, numerous recent research projects and publications demonstrate that structural health monitoring systems have allowed engineers to calibrate models to produce results that more accurately reflect the behavior of the system. (Santini-Bell, Lefebvre, Sanayei, Brenner, Sipple, & Peddle, 2013) (Schlune, Plos, & Gylltoft, 2009) (Zhang & Aktan, 1997)

1.5 – Model Updating

While finite element models are typically used by practicing engineers to design structures, they can also be used to verify the design of an existing structure. In the latter case, the task is coupled with the use of data measured in the field. Finite element model updating is the process of correcting assumptions selected during model creation while avoiding arbitrary changes to the model that would “correct” the finite element model (Schlune, Plos, & Gylltoft, 2009).

There are two main types of model updating procedures. The first is manual model updating. Manual model updating is just as it sounds, the user manually changes certain parameters of the model in an attempt to achieve a result that more closely matches field observations. This can be as simple as changing the compressive strength of a concrete bridge deck from the design value to the value determined during concrete testing at the time that the deck was poured or inserting spring elements into the model to represent neoprene bearing pads at the boundary conditions.

The second type of model updating is automatic updating. This procedure can be complex and computationally intensive. It typically involves writing computer software that uses an optimization routine to minimize an objective function to update a set of structural parameters to thus resulting in a model that more accurately reflects the experimental data. In many cases, an attempt is made to “find” damage in the bridge by matching the response of the bridge model due to modeled damage (Sanayei, Bell, Javdekar, Edelman, & Slavsky, 2006).

The procedures presented herein are a combination of the two. A semiautomatic procedure is presented that utilizes techniques widely used throughout the industry and combines it with a manual model updating technique.

1.6 – Case Studies

This research advances the work of researchers who have specialized in both automatic and manual model updating. There are several examples of structural condition assessment on in-service structures. Four key examples that are relevant to this research are presented here.

1.6.1 *Commodore Barry Memorial Bridge*

The Commodore Barry Memorial Bridge is a long span cantilever bridge with many simple span beam type approach spans as well as simple span deck truss approach bridges (Figure 1-5). The total span of the bridge is just less than 14,000 feet with the main span coming in at just over 1,600 feet. The average approach span is between 90 and 125 feet in length while the deck truss approach spans are 366.5 feet in length. (Structurae, 1999)



Figure 1-5: Commodore Barry Bridge, (Dietrich, 2005)

The Commodore Barry Bridge was instrumented by Barrish, Grimmelsman, and Aktan. The goals of the Commodore Barry Bridge instrumentation are quite similar to the goals of this research. The goals of Commodore Barry Bridge instrumentation are as follows:

- *“To provide a continuously operating monitor for long-term measurement of the operational and load environment and the critical responses of the structure.*
- *To complement the continuous monitor by intermittent controlled tests and short duration monitoring at necessary*
- *Locations and during relevant events.*
- *To gain insight into the structure's behavior for use in FE modeling and calibration.*
- *To collect, analyze and interpret data necessary for objectively evaluating the structure.*
- *To provide the Delaware River Port Authority with long-term data that may assist in management decisions for the Commodore Barry Bridge.” (Barrish, Grimmelsman, & Aktan, 2000)*

1.6.2 Powder Mill Bridge

The Powder Mill Bridge (PMB) (Figure 1-6) is located in Barre, MA. The PMB is in a unique situation because it is owned by a small town and offers many unique opportunities for research. Additionally, the bridge is located near a landfill which causes a large amount of truck traffic over the bridge (Fay, Spoffard, & Thorndike, LLC, 2007).



Figure 1-6: Powder Mill Bridge

The PMB is a 150 foot 3 span bridge with a 75' center span. The main span crosses the Warre River while the two approach spans are over the bridge embankments. When the PMB was in the process of being replaced, The University of New Hampshire as well as Tufts University were given the opportunity to instrument the bridge under the Federal Government's "Whatever Happened to Long Term Bridge Design?" program. Its instrumentation is considered by many to be one of the densest in the nation.

In creating a more accurate finite element model for the PMB, some initial steps were taken to correct obvious assumptions in the analytical model that was used to design the bridge. First,

the actual compressive strength of the concrete deck was used for the material property of the deck elements. Because the modulus of elasticity of concrete is calculated based on compressive strength, this inclusion changed the stiffness of the concrete deck. Next, additional concrete elements sidewalks and curbs were directly attached to the deck. The sidewalks and curbs are directly connected to the decking with reinforcing steel. The final change that was made was much less obvious, it involved accounting for the asphalt topping as a structural component in the model. This is a highly variable component as the asphalt will wear significantly faster than the concrete deck. However, as an academic exercise, it did produce more accurate results (LeFebvre, 2010). These additional elements created a finite element model that is more reflective of actual bridge conditions. All of these model updates until this point have been manual changes. This manual updating was complimented by an FRF-based modal updating protocol developed at the University of New Hampshire as shown in (Garcia-Palencia & Santini-Bell, A Frequency Response Functions-Based Model Updating Algorithm for Condition Assessment of In-Service Bridges, 2014).

1.6.3 Rollins Road Bridge

The Rollins Road Bridge is located in Rollinsford, NH and carries Rollins Road over Main St and one set of rail road tracks. The bridge is a single span concrete carbon fiber reinforced polymer (CFRP) deck supported on five concrete New England bulb tee beams. The bridge was built in 2000 with funding from the Innovative Bridge Research and Construction (IBRC) program. Under this program, the bridge was to be constructed using innovative materials under the stipulation that the results of the construction must be disseminated to others. In order to objectively capture the results of the bridge, a SHM system was installed during construction.

A bridge load test was performed in April 2009. The collected data was post-processed to account for temperature impacts, and then used to update a structural finite element model of the bridge (Figure 1-7). The Rollins Road Bridge research used model updating protocols to determine the appropriate stiffness of the elastomeric bearing pads as well as the performance of the innovative CFRP concrete deck. The parameters used in each case were varied along a scaled until reasonable agreement with the collected strain data was achieved. (Bell & Sipple, In-Service Performance Monitoring of a CRFP Reinforced HPC Bridge Deck, 2009). The SHM system is continuously collecting data and storing it to and saving it to a web based service for later analysis.

Another technique that was used for the Rollins Road project involved the use of parameter estimation (Figure 1-8). In this process, the mechanical and material properties, such as rotational stiffness of connections or modulus of elasticity, of the bridge are back calculated based on the results of the experimental values obtained through a nondestructive testing (NDT).

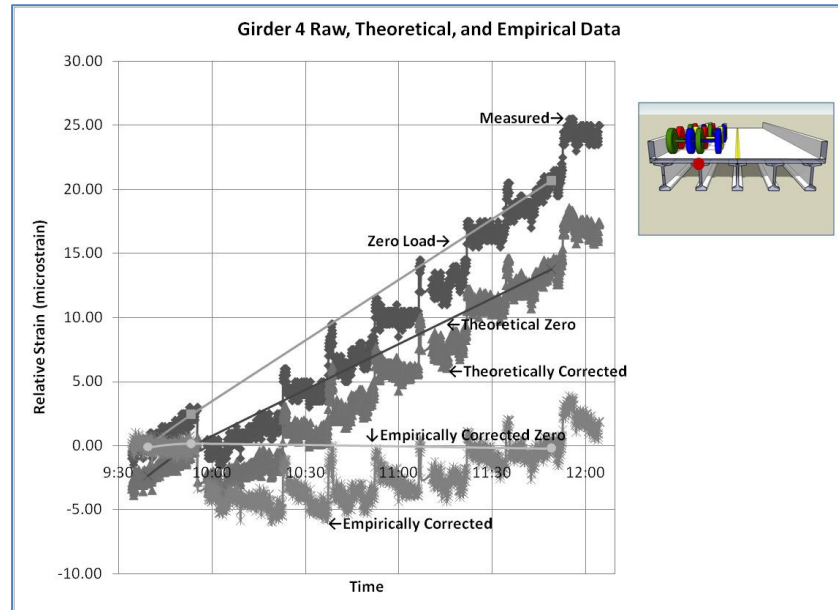


Figure 1-7: Girder 4 top sensor raw, theoretical, and empirical data from April 2008 load test, with three zero-load data points and trend lines included (Sipple and Santini-Bell 2009)

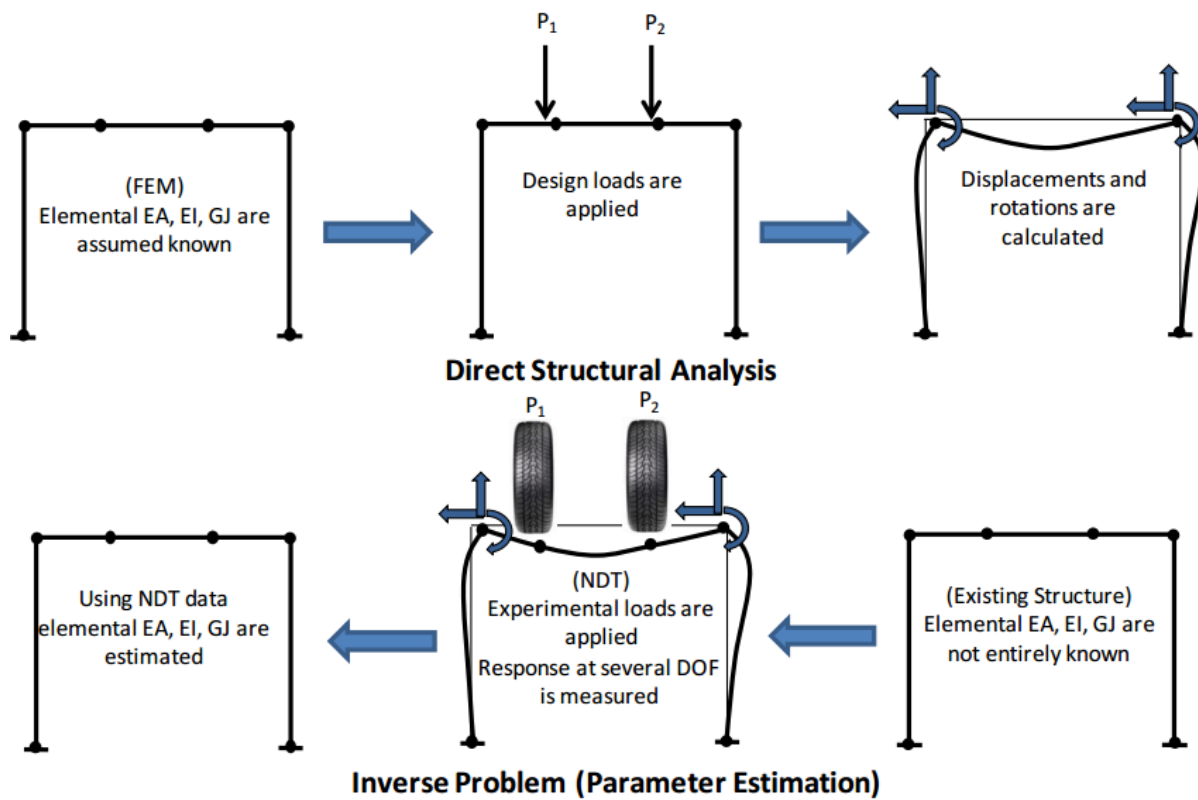


Figure 1-8: Graphical Representation of Parameter Estimation (Bell & Sipple, In-Service Performance Monitoring of a CRFP Reinforced HPC Bridge Deck, 2009)

1.6.4 Tobin Memorial Bridge

The closure of large scale, signature bridge structures has a significant impact on the travelling public and local economy. The Maurice J Tobin Memorial Bridge connects the Charlestown section of Boston to Chelsea, MA by carrying US Route 1 over the Mystic River. The signature spans of the bridge are the Big Mystic Span, which is a cantilever truss bridge and the Little Mystic Span which is a 400' through type truss bridge (Figure 1-9).

In combination with the research presented in this paper, the Little Mystic Span was instrumented with more than 80 strain gauges and strain rosettes, accelerometers, tilt gauges, and a weather station by the research team. This instrumentation was used to validate a structural model that was created using innovative techniques. The procedures used in this research created a simple means for developing a 3D finite element model of a truss bridge. They involved exporting the geometry of a 3D AutoCAD model of the bridge to a Microsoft Excel spreadsheet where the user could assign section properties and boundary conditions before the final step. The last step in this process is to import the data from the Excel sheet to a structural analysis package, in this case, SAP2000. The routines would allow this model creation tool to automate the process. This research expands on this project to incorporating visual inspection information.



Figure 1-9: Tobin Bridge, Little Mystic Span (MementoMori, 2012)

1.7 – Monitoring Model Creation

Analytical computer models are frequently used to design and verify the design of structures. Their use during design and assessment has become extraordinarily common over the past two decades. Furthermore, analytical modeling has moved toward structure specialization. Software such as CSI Bridge is used exclusively to design bridges. It contains tools that will create an entire bridge model in a matter of minutes rather than several hours or even days. Non-analytical software has also increased in usage. Previously, CAD software would mimic the action of manually drawing a bridge, whereas BIM (Building Information Modeling) and BrIM

(Bridge Information Modeling) solutions like AutoDesk's Revit, allow the user to assign much more information to a designed element. BIM solutions can allow a bridge owner to create a "living" model of the bridge: a model that tracks all of the information associated with it. Documents like construction sketches, inspection reports, maintenance records, and testing data can be linked into a BIM model. This allows the owner an unparalleled ability to view the "whole" picture when making decisions about maintenance and fund distribution. This research leverages the existing inspection report data so that it may be used beyond the traditional visual assessment.

For small structures, advanced structural models are typically not required. The bridges may be simple enough that creating a model is more time consuming than simply performing the required work by hand. For structures that are larger or more complicated a decision must be made concerning how much data is required to complete the design or evaluation task. This decision is required because as structural complexity increases, so does the time required to create, run, and post process the model. Efforts have been made to reduce the amount of time that is required to create the models, such as converting three dimensional AutoCAD models into three dimensional analytical models. (Sanayei, Pheifer, Brenner, Bell, & Allen, 2010)

1.7.1 – Finite Element Modeling

The American Association of State Highway and Transportation Officials (AASHTO) offers two main types of analysis for bridges. The first is an approximate method in which distribution factors are used to determine the relative interaction between all of the beams acting in the system. Alternatively, a finite element method (FEM) may be used. A FEM is a numerical method that can be used to analyze a structure. This method can produce results that are more

accurate than results obtained using the approximate method and it allows engineers to analyze structures with a much higher degree of complexity.

FEM was developed in the 1940s but did not become popular until digital computing power could be used to perform the complex matrix algebra necessary to solve large problems.

One main downside of FEM is commonly referred to as the black box effect. This problem arises when the engineer does not adequately understand what the model is doing to produce the output that it has created. One way to deal with this issue is to calibrate the model using an existing structure as a baseline. This helps to ensure that the model is producing results that coincide with the physical structure.

Chapter 2: Model Updating

There are two different types of model updating, automatic and manual. Manual model updating involves changing key aspects of the model based on measured or calculated aspect of the model. (LeFebvre, 2010). Alternatively, automatic updating typically depends on sophisticated, custom written computer software to interpret the results of non-destructive testing on the structure and change key parameters of the model. This process is typically performed a number of times until the model more precisely reflects the existing structure (Lord, Ventura, & Dascotte, 2004). This automatic refinement technique typically involves the use of an error function (Garcia-Palencia & Santini-Bell, A Frequency Response Functions-Based Model Updating Algorithm for Condition Assessment of In-Service Bridges, 2014). In situations involving dynamic data and testing, calculating the error function could involve calculating the inverse of large matrices. The calculations are computationally intense and require high levels of processing power and it is likely not ready to be used on full scale projects (Garcia-Palencia & Santini-Bell, Structural Model Updating Using Dynamic Data, 2013). The work described in this paper lies between the two techniques in that it uses visual observations from inspection reports to refine the structural model. The exact procedure is presented in Section 2.2.2 – Model Updating Protocols.

2.1 – Inspection Reporting

Typically, when a bridge is inspected, notes will be made on paper and photographs are taken to document the condition of a specific structural member or connection. All of the notes are then compiled into a set and brought back to the office where each sheet of notes will be incorporated into some form of digital document as shown in Table 2-1 (TranSystems, 2008).

This most often takes the form of spreadsheets though databases can also be used. From that point, the analysis of the digital data can begin. For most bridges, this analysis is performed using AASHTO's approximate methods for bridge design and analysis (AASHTO, 2011). However, for especially large bridges, computer models take over the complex calculations required to analyze highly indeterminate structures.

Table 2-1: Sample Inspection Field Notes (TranSystems, 2008)

CONDITION SUMMARY LITTLE MYSTIC - TRUSS				
Location	Ref	Photo	Member	Condition
L0	70		East Truss	<input type="checkbox"/> Vertical gusset plate has up to ¼" loss throughout truss. <input type="checkbox"/> Truss bearing has random areas of heavy rust with up to ¼" loss on faces of anchor bolt nuts. <input type="checkbox"/> Up to ½" impacted rust between double gusset plates on east and west side. <input type="checkbox"/> Up to 5/8" gap between pin plate and vertical gusset plate on east and west side. <input type="checkbox"/> Up to 1/16" pitting, full height of pin plate on east face. <input type="checkbox"/> 1/16" pitting, 3" high on exterior of west web plate.
			West Truss	<input type="checkbox"/> Up to 1" impacted rust between double gusset plates on east and west side.
L0U1	70		East Truss	<input type="checkbox"/> Deteriorated cross section - see field note.
	65		West Truss	<input type="checkbox"/> Up to ¼" impacted rust between box angle, web plate and cover plates.
L0L1	70		East Truss	<input type="checkbox"/> Deteriorated cross section - see field note. <input type="checkbox"/> Debris inside of truss member.
	67		West Truss	<input type="checkbox"/> Deteriorated cross section - see field note.
L1	67		West Truss	<input type="checkbox"/> Up to ¾" impacted rust between gusset plates and vertical on east and west side.
L1U1	70		East Truss	<input type="checkbox"/> Up to ½" impacted rust between exterior cover plate and flange angles. <input type="checkbox"/> Deteriorated cross section - see field note.
	65		West Truss	<input type="checkbox"/> Up to ½" impacted rust between exterior cover plate and flange angles. <input type="checkbox"/> Deteriorated cross sections - see field notes.
	67			
L1L2	70		East Truss	<input type="checkbox"/> Deteriorated cross sections - see field notes.
	67		West Truss	<input type="checkbox"/> Deteriorated cross sections - see field notes.
L2	70		East Truss	<input type="checkbox"/> Gusset plates have random areas of up to ¼" loss.
	67		West Truss	<input type="checkbox"/> Up to ¼" impacted rust between gusset plate and truss member.
L2U1	66		East Truss	<input type="checkbox"/> Deteriorated cross sections - see field notes.
	70		West Truss	<input type="checkbox"/> Deteriorated cross section - see field note.
	67			

The protocol presented in this research builds on the existing structural analysis programs that are commercially available. This protocol is a new way to update an existing structural computer models reducing the risk of human error and data-entry time required to manually update the model and provides “inspection to inspection” continuity between structural models. If these models are calibrated with collected field data for general correlation, then the results from these models can be used for load rating, overload permitting and predicted remaining life, assuming a linear elastic behavior.

2.2 – Model Updating Procedures

The use of inspection report data in conjunction with model updating protocols has been shown to produce acceptable results (Jang, Li, & Spencer, 2013). However, this previous research was conducted using data collected by accelerometers. Additionally, the inspection that was performed on the test structure was a specialized inspection using ASTM standards that are more than 25 years old. These standards are elaborate tests requiring considerable time and are not practical for routine inspections of in service bridges. The verification that is used in this research was acquired using traditional inspection techniques by bridge inspectors that are trained by the National Institute for Certification in Engineering Technologies during regularly scheduled inspections.

2.2.1 – Visual Basic for Applications

The model updating procedure described in this paper is written entirely using Microsoft Visual Basic for Applications (VBA). VBA is an event-driven programming language that is implemented in most Microsoft Office applications (Microsoft, 2010). The Microsoft Office application used,

in this case, is Microsoft Excel. VBA-based modules can interface with the structural modeling program SAP2000®, which is the platform used to create structural model used in this research.

2.2.2 – Model Updating Protocols

A flowchart depicting the actions taken by the model updating script can be found in Figure 2-2. Using the model updater requires several elements to function. These components are a bridge structure, a bridge inspection report, a calibrated finite element model of the bridge, and instrumentation and load test data to validate and calibrate the predicted response of the finite element model.

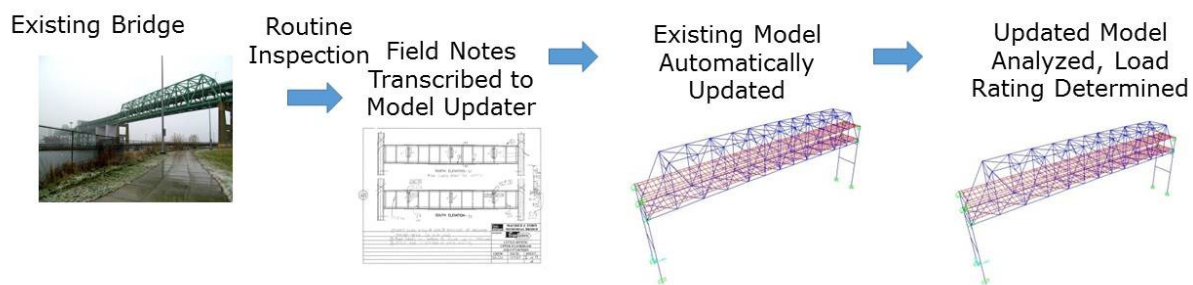


Figure 2-1 Existing Inspection and Load Rating Procedure

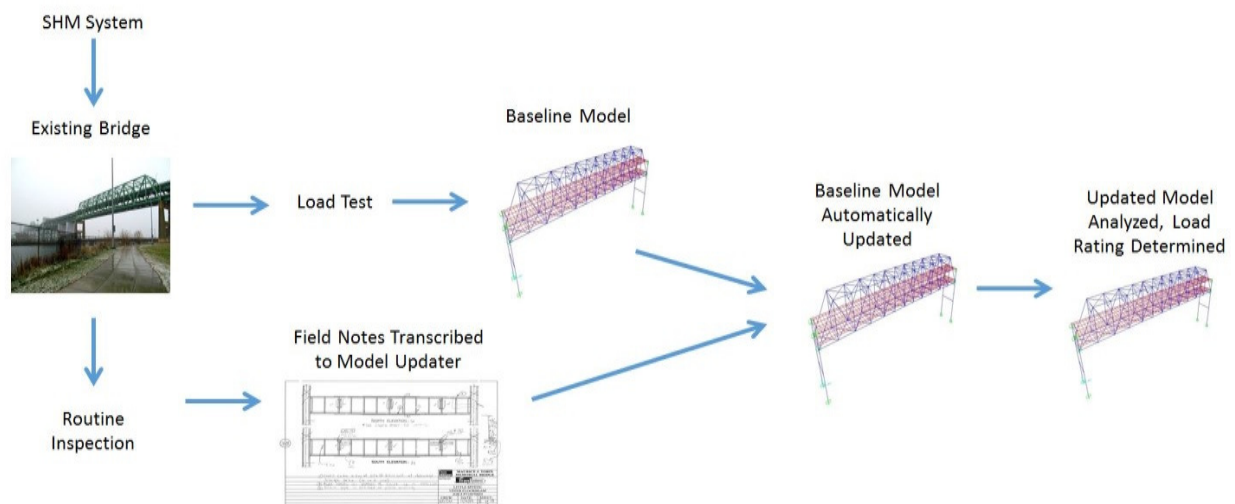


Figure 2-2: Model Updater Procedure

The first two items of the procedure can be performed concurrently. These two tasks are to perform a detailed bridge inspection and create a structural finite element model of the inspected bridge. If the bridge structural finite element model exists, the second step can be ignored.

The model updating program requires that each inspection element have a unique name. The inspected structural elements are entered into the member name section of the model updater spreadsheet. From this stage, the model updater is prepared to accept the results of the inspection procedure.

The bridge inspection must be conducted using applicable industry standard according to the AASHTO Bridge Inspection Manual and any local inspection guidelines or procedures. In the United States, this standard conforms to the National Bridge Inspection Standards. After completing the inspection, the resulting observations are entered into the model updater spreadsheet. These results must be in the form of units of the structural model, in this case square inches. Table 2-2 depicts the information that is obtained from the model through the use of the SAP2000's Open Application Programming Interface (OAPI) or information that is calculated based on data input by the user or obtained through the OAPI.

In Table 2-2, the "Member" column is reserved for the unique member name that is assigned to each element of the model. "Geometry" defines the general shape of the member and is used simply for the user's benefit. "Inspected Area" is the cross sectional area that is determined from the bridge inspection. The "Inspected Area Modifier" is used to convert the raw inspected area into property modifier which is more easily updated in the SAP2000 API. This method was chosen because the routine to update property modifiers is less complex than changing the

member properties. Additionally, the research team had previously chosen to define all of the members on the bridge with the same member properties, but change each element's property modifiers. The "Member Area from SAP" term is the value of the property modifier that is currently assigned this value will be change to the value found in the "Inspected Area" column when the updated terms are sent back to SAP2000. For instance, each member in the Little Mystic Span model has the same cross sectional area, 0.0459 square feet. However this area is modified for each of the elements based on the value of the area property modifier.

It should be noted that until this stage, the procedure has produced a minor level of additional work for the bridge inspection team, either in-house department of transportation or consultant. In many cases, complex bridges such as truss bridges are normally analyzed and load rated based on results from a three-dimensional structural finite element model of the bridge. For smaller, overpass bridge, such a model may not be available but given the advances in structural analysis software packages, such as CSIBridge® in SAP2000®, as well as previous research (Sanayei, Pheifer, Brenner, Bell, & Allen, 2010), the model creation does not require a significant effort in terms of personal or computational effort to create.

After the information is placed into the appropriate location in the Excel spreadsheet, the user executes the model updater module and the structural section properties of the finite element model are updated to reflect the inspected conditions.

Table 2-2: Example Model Updater Spreadsheet

Member	Geometry	Inspected Cross Sectional Area (in ²)	Inspected Area Modifier	Member Area from SAP	FROM SAP I33 Axis (Local y)	FROM SAP I22 Axis (Local x)
L0-U1	Box	136.3	20.62	20.96	110.95	2073.75
U1-L2	Box	84.25	12.75	13.78	80.22	1246.15
L2-U3	Box	81.05	12.26	14.26	89.37	1397.28
U3-L4	Box	48.18	7.29	8.62	34.70	772.82
L4-U5	Box	43.45	6.57	7.78	27.21	678.92
U5-L6	Box	32	4.84	6.31	16.68	467.67
L6-U7	Box	32	4.84	6.31	16.68	467.67
U7-L8	Box	42.7	6.46	7.78	27.21	678.92
L8-U9	Box	49.18	7.44	8.62	34.70	772.82
U9-L10	Box	79.6	12.04	13.53	84.39	1326.45
L10-U11	Box	89.86	13.60	14.16	83.02	1278.22
L12-U11	Box	129.1	19.53	18.91	100.27	1878.36
L0-L1	Box	68.63	10.38	13.01	86.97	1250.61
L1-L2	Box	73	11.04	13.01	86.97	1250.61
L2-L3	Box	143.9	21.77	23.16	117.35	2169.39
L3-L4	Box	143.78	21.75	23.16	117.35	2169.39

2.2.3 Radius of Gyration

The main assumption of the model updater modules is that given small reductions in cross sectional area, the radius of gyration will remain constant. The radius of gyration is given by Equation 2-1.

$$r = \sqrt{\frac{I}{A}}$$

Equation 2-1

By considering small changes in cross sectional area, Equation 2-1 becomes:

$$r = \sqrt{\frac{I - \delta I}{A - \delta A}}$$

Equation 2-2

The proof can be simplified by assuming a rectangular cross section where b is the width of the section and d is the depth:

$$I = \frac{bd^3}{12}$$

Equation 2-3

$$A = bd$$

Equation 2-4

Substituting Equation 2-3 and Equation 2-4 into Equation 2-2 yields:

$$r = \sqrt{\frac{(b - \delta b)(d - \delta d)^3}{12[(b - \delta b)(d - \delta d)]}}$$

Equation 2-5

By simplifying Equation 2-5, r becomes:

$$r = \sqrt{\frac{d^2 - d\delta d + \delta d^2}{12}}$$

Equation 2-6

While considering small changes to the cross sectional area, the squared term δd and $d\delta d$ will approach zero, leaving d as the only variable.

Using this assumption, the moments of inertia can be updating by utilizing the reduced cross sectional areas that are sometimes provided in inspection reports (TranSystems, 2008).

2.3 –Structural Model Verification

Before a model should be updated based on visual inspection data, it should be verified with field-collected structural responses from a load test or some other controlled-excitation procedure. This provides a level of confidence that the model is providing results that are in agreement with the structure that is being investigated. The load test data available for this project was static strain data collected on key structural elements in the Little Mystic span of

the Tobin Bridge The exact location and orientation of these gauges and details of the load test will be discussed in Chapter 4:.

An objective function, J , is frequently used to compare the results of a bridge load test to the performance of a structural model (Equation 2-7), (Sanayei, Bell, Javdekar, Edelmann, & Slavsky, 2006), (Garcia-Palencia & Santini-Bell, A Frequency Response Functions-Based Model Updating Algorithm for Condition Assessment of In-Service Bridges, 2014).

$$J = \sum_{i=1}^k w_k \frac{\sum_{j=1}^{n_k} |Z_{k,nj} - Z_{k,ej}|}{\sum_{j=1}^{n_k} |Z_{k,ej}|}$$

Equation 2-7: Objective Function, J

In Equation 2-7:

J = Objective function

w = Weighting factor

n = Number of responses

$Z_{k,nj}$ = Predicted response

$Z_{k,ej}$ = Actual response

In this equation, the analytical and experimental responses can be any response of the structure such as deflection, strain, acceleration, or velocity. The objective function is a measure of a finite element model's effectiveness. This effectiveness is defined as a single number for the entire bridge. It allows a bridge manager to quickly and easily see how accurately the virtual bridge represents the actual bridge. There are several issues with the objective function. The first issue is possibly one of its greatest strengths, J is a single number. There are unique benefits to providing a single number to a bridge manager to illustrate year to

year changes in performance of a bridge. However, due to the normalization techniques that are used during the calculation process, J takes all of the errors and inconsistencies associated with the model and lumps them into a single number. This makes year to year changes in performance difficult to judge. For instance, a 10% change in J does not necessarily mean that there is a 10% change in the performance of the bridge.

The second issue is that each bridge is affiliated with a single J . The solution to the objective functions cannot be compared with one another with any sort of efficiency. For instance, if a bridge manager would like to compare one bridge to another, they have completely different J values and the comparison would mean nothing. To further complicate things, for highly indeterminate structures it is possible to look at the acceptability of each member, with each member's J value being completely independent from the other members.

It is for these reasons that the acceptability of the structural model has been simplified to be a visual inspection of influence lines for each gauge location. The criterion that has been considered is the overall geometry of the influence line and its closeness to the experimental data. Any differentials that are larger than 10% were considered to not be a good fit.

2.4 – Recommended Applications

Finally, it should be noted that these protocols are not recommended or warranted for simple bridges. In fact, if hand calculations can easily be performed, they likely should be. However, if the bridge is complicated, highly indeterminate, and large, these protocols have the potential to save considerable amounts of time. Due to the ease of modeling a typical overpass bridge a structural model may be sufficient for condition assessment without this complex updating procedure. For example, the previously discussed Powder Mill Bridge, which was modelled

using Computer and Structure's CSI Bridge, would not be a good candidate for the model updater presented within this paper. Part of this relates to the high complexity with which the girders are modeled and part of it relates to the use of the CSI Bridge software itself. The CSI Bridge software assigns the node, frame, and element numbers based on a seemingly random process. This complicates the model updating procedure as the member names cannot be known easily. Furthermore, renaming the elements would require the user to locate the element and rename it manually. For models with hundreds or thousands of elements this is a time consuming process. However, using other model creation software (Sanayei, Pfeifer, Brenner, Bell, & Allen, 2010) will allow the user to easily predict the names of the elements and update the model quickly and easily.

Chapter 3: Introduction to the Maurice J Tobin Memorial Bridge

The testing platform for this research is the Maurice J Tobin Memorial Bridge (Tobin Bridge).

The Tobin Bridge spans the Mystic River connecting Chelsea, MA to Boston, MA. The bridge carries US Route 1 over both the Big Mystic River and the Little Mystic River (Figure 3-1). The Tobin Bridge carries 3 lanes of traffic in each direction on two separate decks. Throughout the length of the bridge, US Route 1 southbound is carried on the upper deck of the bridge while US Route 1 Northbound is carried by the lower deck. The main span (Big Mystic Span) of the bridge crosses the Big Mystic River and is of steel truss cantilever construction with 361' anchor spans, 206' cantilever arms, and a 387' suspended span for a total length of 1524'. The secondary span (Little Mystic Span) of the bridge crosses the Little Mystic River and is a through type steel truss bridge. It has a clear span of 439' (Figure 3-2: Components of the Tobin Bridge).

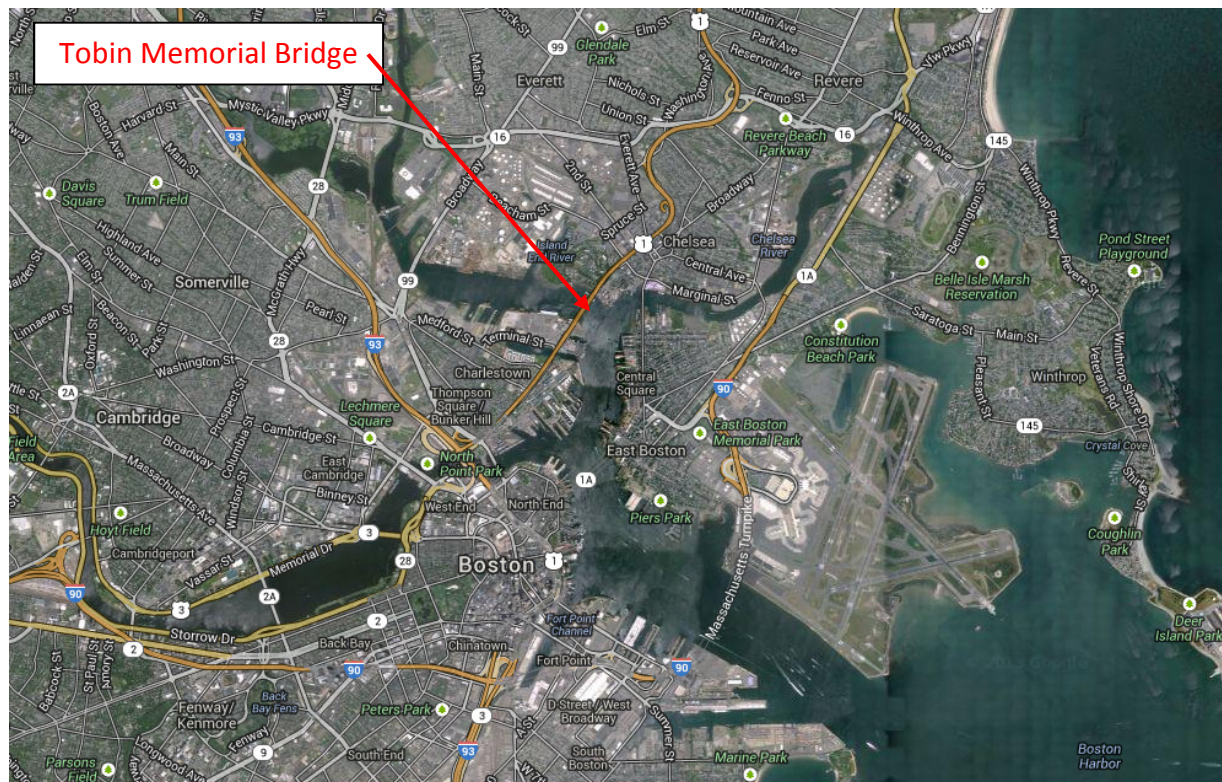


Figure 3-1 Tobin Memorial Bridge (Google, 2013)



Figure 3-2: Components of the Tobin Bridge



Figure 3-3: Tobin Bridge, Big Mystic Span (Chensiyuan, 2009)

The Tobin Bridge was constructed in the late 1940s and opened to the public on February 27, 1950 (Wilhelm Ernst & Sohn Verlag, 2014). It is constructed up riveted steel box sections for the chords and diagonals. The verticals of the trusses are built up rolled sections with caps channels riveted to the flanges. Bottom chord side trusses are connected by built up floor beams. The floor beams support wide flange stringers which support wide flange purlins which in turn support the reinforced concrete deck.

3.1 – Instrumentation of the Little Mystic Span

The Little Mystic Span of the Maurice J Tobin Memorial Bridge was instrumented with various types of sensors by Geocomp Corporation Inc. (Sanayei, Pheifer, Brenner, Bell, & Allen, 2010). The locations for each of the sensors were chosen based on the anticipated loading conditions for a future field test of the bridge.

3.1.1 Instrumentation Plan

Each instrument location was chosen based on preliminary analysis of the structure and engineering judgment. The members that were chosen to be instrumented were those that would experience the largest forces when the bridge was loaded at the midspan. These loads were predicted using a preliminary finite element model of the bridge with two 35 kip trucks placed at the midspan. Four gauges were installed at each instrumentation location, one gauge was installed on each face of the member; top, bottom, inside face, and outside face.

Additionally, members near specific connections were instrumented in order to investigate the behavior of the connection.

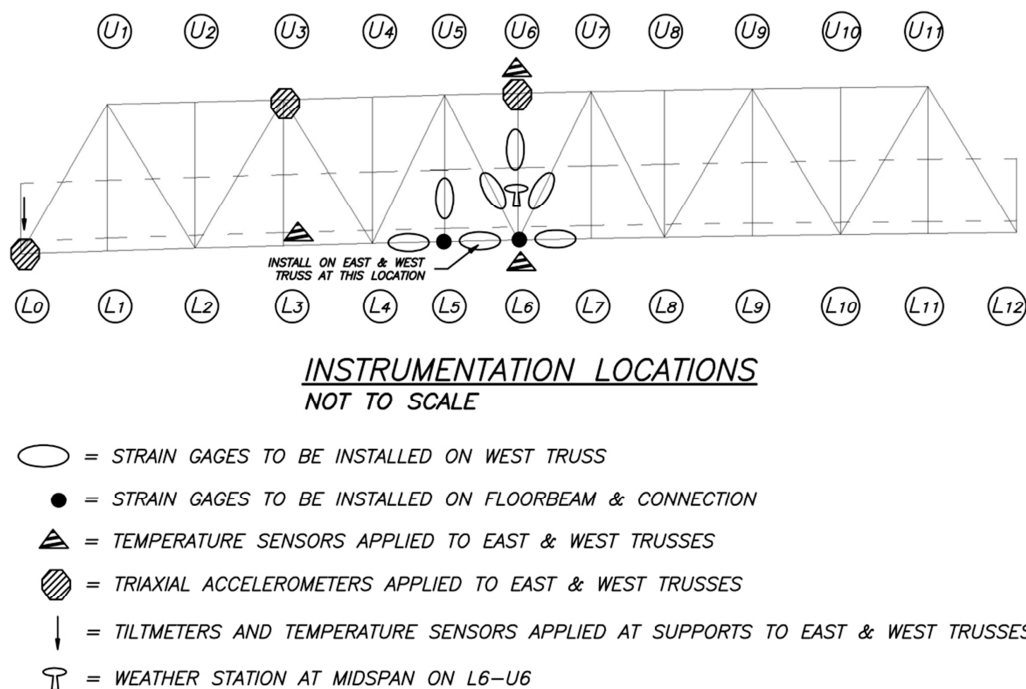


Figure 3-4: Elevation view of Little Mystic Span instrument locations (Sanayei, Pheifer, Brenner, Bell, & Allen, 2010)

Locally, care was taken not to place gauges too close to locations of predicted stress concentrations. These stress concentrations were predicted to be located near the hand holes that were cut into the plate-work when riveting together the built up sections. Additionally, care was taken to keep the gauges far enough away from connections to allow for the stresses to stabilize, thus minimizing any appearance of shear lag. Sensor types and quantities are located in Table 3-1.

Table 3-1 Instrumentation types and quantities for the Little Mystic Span

Instrument Type	Number of Instruments
Strain Gauge - Member	80
Strain Gauge Rosettes - Connection	12
Tiltmeters w/Temperature Sensor	2
Accelerometers	6
Temperature Sensors	6
Weather Station	1

The stain gauges and strain rosettes that were chosen for this project are quarter bridge strain gauges from Omega Engineering. Strain rosettes utilize 3 separate strain gauges integrated onto

the same instrument to measure strain in each of the principal directions, ϵ_x , ϵ_y , and ϵ_{xy} . These gauges were placed on the gusset plates of the bridge to capture the rotational fixity of the connections as well as the behavior of the gusset plates (Rosenstrauch, Sanayei, & Brenner, 2013). Figure 3-5 shows an example 60° strain rosette, and the resulting formulas for the components of plane strain.

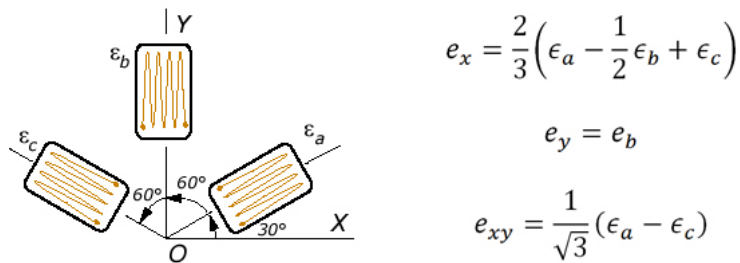


Figure 3-5 Example strain rosette in 60° configuration [Efunda 2010]

3.1.2 Data Collection

There are two means of data collection for the structural health monitoring systems installed on the Little Mystic Span. The first involves logging into the iSite web interface where this data is constantly collected and data for any period of time can be acquired using this system. The data collection rate for this method is 1Hz.

The second method for data collection involves connecting a computer directly to the data acquisition system. This method allows for much higher data collection rates. Sampling rates using this interface can be defined up to 200Hz.

3.2 Installation

The installation of the instruments was performed by GeoComp Corporation. GeoComp is a structural health monitoring firm that specializes in geotechnical applications, however they are also fully capable of instrumenting steel and concrete systems.



Figure 3-6 Installation of HS Data Acquisition Systems (Sanayei, Pheifer, Brenner, Bell, & Allen, 2010)

3.2.1 Preparation Procedure

The strain gauge installation process is a simplified version of the manufacturer's instructions and is more suited to field installation conditions. The process involves: (a) grinding the paint to reveal bare steel, (b) gluing the strain gauge, (c) epoxy and (d) weatherproofing are applied to improve the sensors' durability (Figure 3-7).

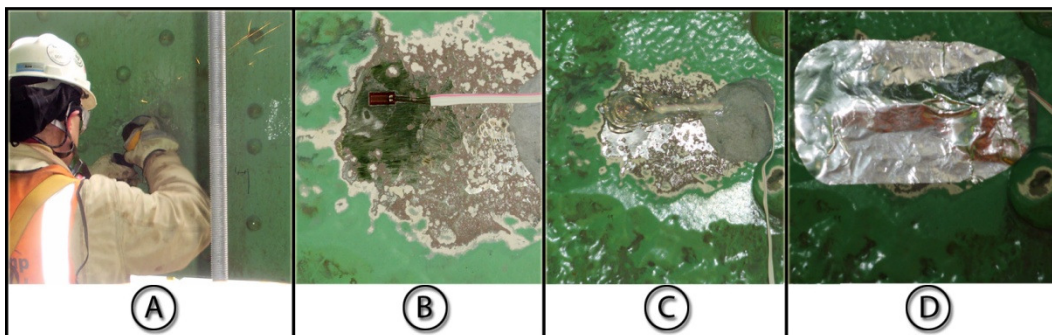


Figure 3-7 Strain Gauge Installation Procedure (Sanayei, Pheifer, Brenner, Bell, & Allen, 2010)

3.3 Load Testing

The load testing of the bridge took place during a scheduled bridge closure. This proved to be one of the greatest challenges of the load test. Because the bridge is a highly travelled road, the load test had to be conducted efficiently and quickly. The speed at which the load test was run proved to be a problem because there was not time to troubleshoot any problems. The issue that was encountered was the lack of high speed data connectivity to the iSite box. This

resulted in the low speed data collection being the only means of data acquisition. The low speed data collection collects at a rate of 1Hz, while the high speed data collection is capable of collecting data at a rate of 200Hz. Despite the issues related to the load test, the collected data was used to calibrate the 3D structural model of the Little Mystic Span.

Chapter 4: Case Study

4.1 – Testing Plan

The goal of this test was to collect high speed (200Hz) data for a relatively extended period time while the two trucks were near the midspan of the bridge, see Figure 3-2. This was accomplished by parking the trucks near the toll plaza area on the lower deck. After the bridge was closed, the trucks began moving at a crawl speed of about 4 miles per hour. The trucks continued until they reached the relative midspan of the bridge. At this point the trucks were stopped and the engines were kept running. The trucks remained in this position for about 20 seconds after which they moved at a crawl speed until they were off the bridge. While the test was taking place, the trucks were tracked using automatic motorized total stations. The survey equipment was used to track the location of the truck in 3d space each second. By combining this data with the strain data that was collected using iSite data collection systems, one can correlate the strain data with the location of the truck allowing for the collection of influence lines for strain for each strain gauge. All of these actions were required to be performed in a short period of time. The bridge was closed for about 20 minutes.

4.2 – Truck Specifications

The trucks used in the load test were owned by MassPort. These trucks are typically used as plow trucks used for snow removal and spreading deicing salts or sand, Figure 4-1. At the time of the load test, each truck was loaded with sand to a gross vehicle weight of about 35,000 pounds (35kip).



Figure 4-1: Trucks Used During Load Test (Sanayei, Pheifer, Brenner, Bell, & Allen, 2010)

4.3 – Tobin Bridge Finite Element Model

The finite element models that were used in this research were created using a three dimensional AutoCAD model of the bridge. An AutoLisp script was written that would convert the AutoCAD model into a data file. The data file was then be used to create a model in SAP2000 or GTStrudl. (Sanayei, Pheifer, Brenner, Bell, & Allen, 2010)

The models that were used in this research were created using SAP2000. In previous research, four models were created: the Basic model, the Deck model, the Piers model, and the Stiffness Reduction Factor model (SRF Model). The Basic model can be seen in Figure 4-2. The Basic model consists of 927 nodes, 1387 frame elements and 552 zero stiffness deck elements. Zero stiffness area elements were used to distribute the truck loads to the adjacent frame members. Zero stiffness area elements were used because it was not known if the deck was acting compositely with the rest of the bridge. In calibrating the Basic model, the decision was made that the frame elements that make up the truss are not acting as fully pinned truss members. They are in fact much more closely related to fully fixed frame elements (Sanayei, Pheifer,

Brenner, Bell, & Allen, 2010) in that they resist moment. This behavior was captured in the collected data and will be discussed in Section 4.5 – Results.

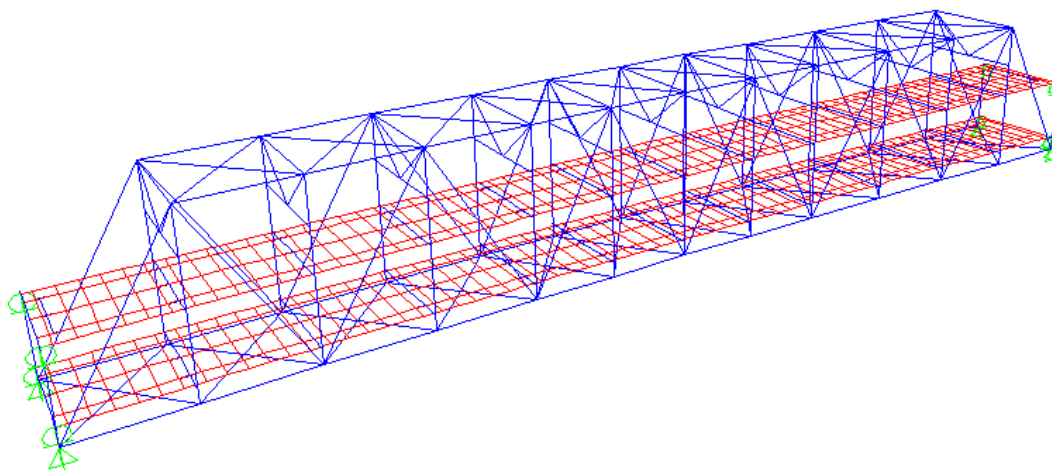


Figure 4-2: Basic Model (Sanayei, Pheifer, Brenner, Bell, & Allen, 2010)

The deck model is visual identical to the basic model and can be seen in Figure 4-2. The Deck model contains 927 nodes, 1387 frame elements, and 552 area elements. The difference between the Basic model and Deck model is that the Deck model contains area elements that were assigned a stiffness value. The area elements have been modified so that they mimic the action of the poured concrete deck. The choice to make this change was made based on the change in the value of an objective function. The objective function is discussed in greater detail in 2.3 –Structural Model Verification and also in previous research (Sanayei, Pheifer, Brenner, Bell, & Allen, 2010).

The Piers model can be seen in Figure 4-3. The difference between the Piers model and the Deck model is that the Piers model includes additional frame elements to capture the action of the concrete piers that support the bridge. Considering that these piers are just over 100 feet in length it is a reasonable presumption to assume that they influence the response of the truss members. This assumption was proven through the use of the same objective function used in the Deck model. The piers are modeled using concrete frame elements. They are fixed at the base and pinned to the structure. Pins were chosen for the connection to truss span due to the use of pin elements at the top of the pier, see Figure 4-4. The Piers model has 939 nodes, 1403 frame elements, and 552 area elements.

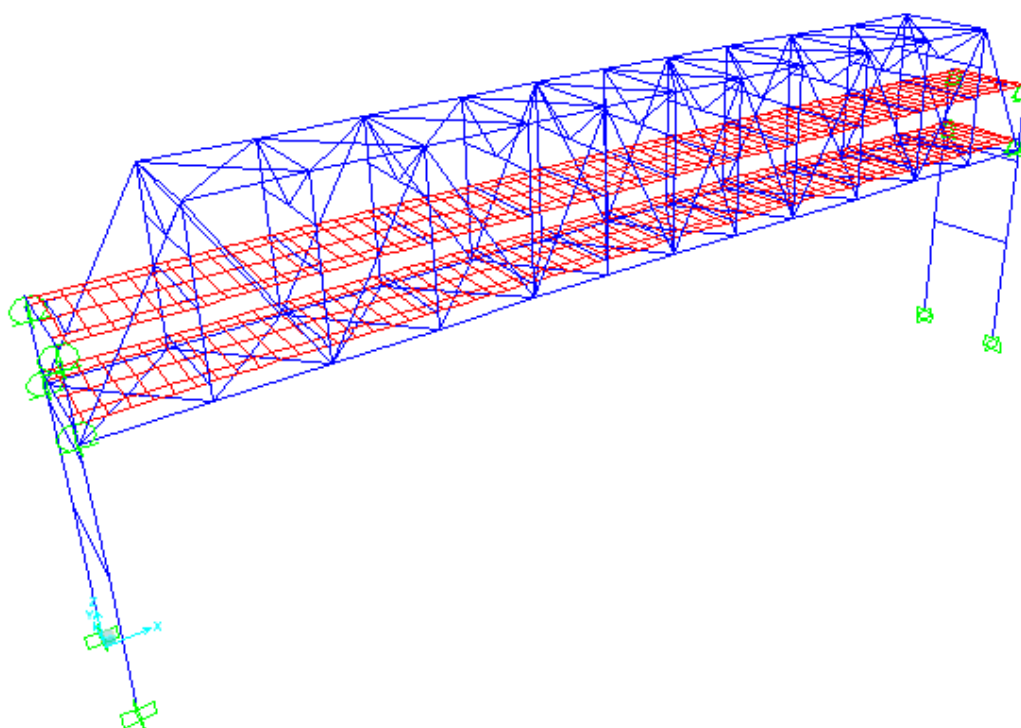


Figure 4-3: Piers Model (Sanayei, Pheifer, Brenner, Bell, & Allen, 2010)



Figure 4-4: Tobin Bridge Shoe Connection

When creating the SRF model, there was a need to consider bridge construction procedures.

When the box shaped built up members were created, they were connected using rivets. When driving rivets, one end of the rivet must be held while the other end is hammered flat (Salmon & Johnson, 1996). In order to gain access to the non-hammered end of the rivet, holes were cut into the face of the member, see Figure 4-5. These holes have an impact on the overall stiffness of the member. A special study was conducted during previous research in order to determine the size of the stiffness reduction factor (SRF), (Sanayei, Pheifer, Brenner, Bell, & Allen, 2010). In this case, the piers model has been modified to reduce the stiffness of the box shaped members. The stiffness reduction factor is 97.7%, this means that on average, a solid box shaped member would be about 3% stiffer than one that has hand holes in it.



Figure 4-5: Tobin Bridge, Hand Holes in Built up Sections

The next logical step in creating a more accurate model is to consider any losses to the structural members that may cause a decrease in performance. The inspected model has been run through the Model Updater in order to better represent the response of the structure.

4.4 – Truck Load Distribution

The truck wheel loads were distributed to the truss through the use of an external finite element model (Figure 4-6). This model consisted of a grid of frame elements connected at nodes. Each of these nodes shown represented as black dots is a support point for the purlins. The frame elements support shell elements that represent the bridge deck. The shell elements were loaded using the truck weights and wheel locations, shown in orange (Figure 4-6). The exact wheel location is shown as coordinates near each orange marker and the magnitude of each wheel load is adjacent to the orange markers. After analyzing the isolated portion of the bridge, the resulting reactions were then used to load the global model of the Tobin Bridge. (Sanayei, Pheifer, Brenner, Bell, & Allen, 2010)

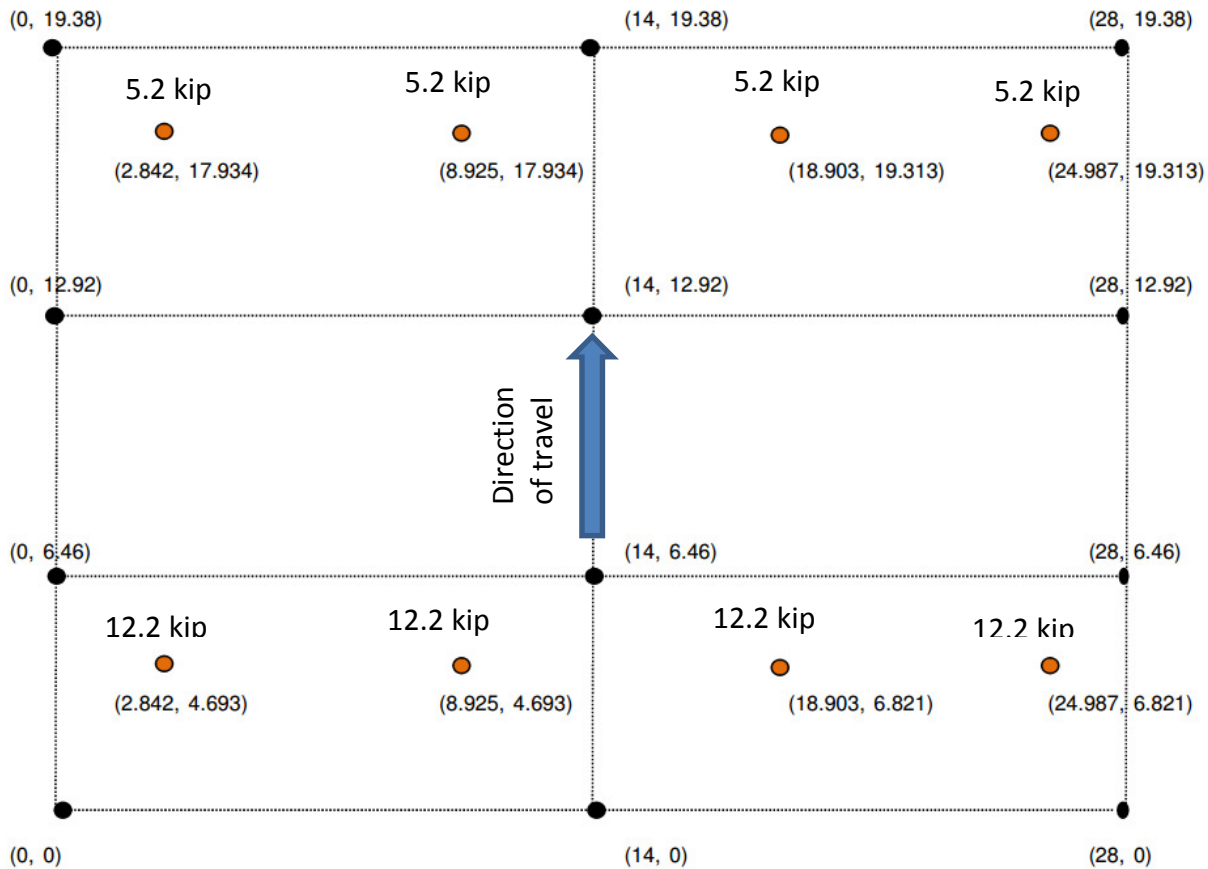


Figure 4-6: Truck Wheel Load Locations and Deck Support

The location and magnitude of each reaction was then placed into an Excel spreadsheet and the SAP2000 API was used to step this grid of loads across the bridge. The output of each load step was recorded into a spreadsheet for further analysis.

4.5 – Results

Because of issues with the data collection system that were discussed earlier, gauges that were deemed to have collected meaningless or poor data were not included in the collection of gauges. Examples of poorly collected data include, but are not limited to “flat lined” gauges or gauges with gaps in the collected data. See Figure 4-7 and Figure 4-8 for examples of discarded gauges.

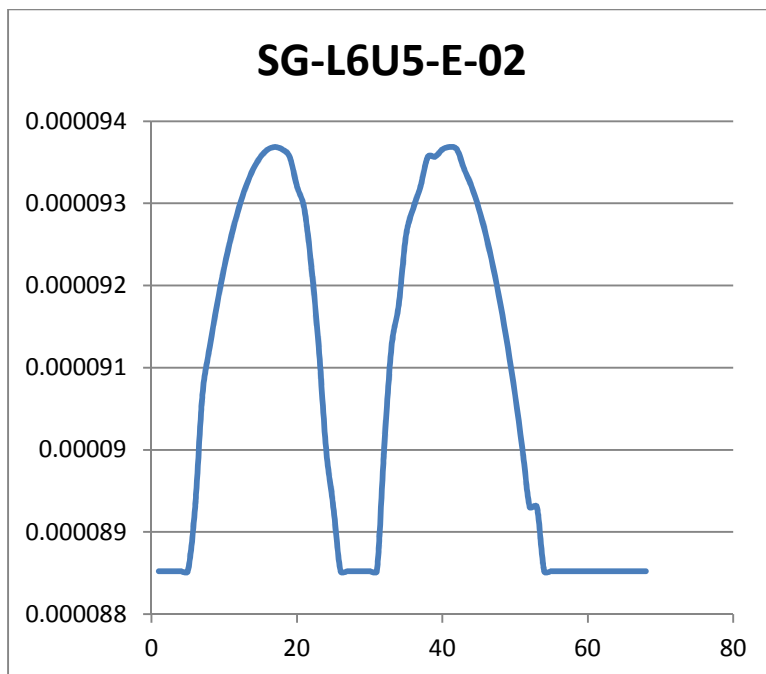


Figure 4-7: SG-L6U5-E-02, Gap in Collected Data

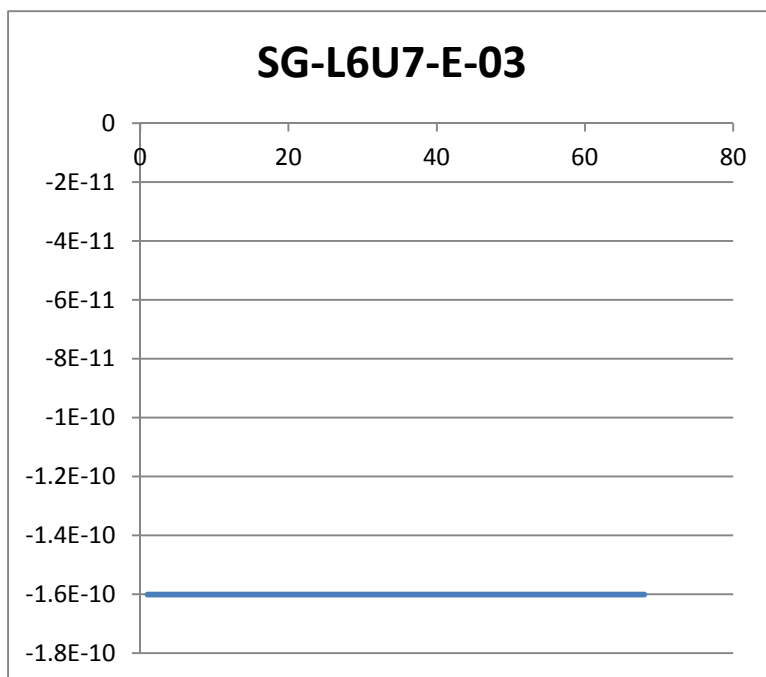


Figure 4-8: SG-L6U7-E-03, Flat-lined Gauge

The following sections outline the results of the model updating procedure and compare it to the collected data from the load test. The sections are broken up by member so that each gauge may be addressed individually.

The results that are displayed in the following sections contain six different data sets. The first set represents the data that was collected during the load test on the Tobin Bridge, this set is referred to as “Collected”. The next 4 data sets represent the models that were created from previous research; they are referred to as “Basic”, “Deck”, “Piers”, and “SRF”. The final data set is from the model that was created from this research, that model is labeled as “Inspected”. See

Table 4-1: Changes to Structural Models for a summary of the changes to the structural models.

Table 4-1: Changes to Structural Models

<u>Model Name</u>	<u>Changes</u>
Basic	Baseline model
Deck	Adds concrete deck as a structural element
Piers	Adds concrete piers to the model
SRF	Reduces section properties based on hand holes
Inspected	Includes updated section properties from inspection report data (Final Model)

4.5.1 – Chord Members

The bottom chord members of the truss are built up box shaped members. The members that are instrumented on the Little Mystic Span are members L4L5, L5L6, L5L6-W, and L6L7 (Figure 4-9). Each of these members is instrumented with a gauge near the i-joint of the member and also near the j-joint of the member. In all cases, the i-joint of the member is the lower node number associated with the member name. For instance, the i-joint of the member L4L5 is at panel point number 4 and the j-joint is at panel point number 5. With the exception of L5L6-W, all of the instrumented members are located on the east side of the bridge.

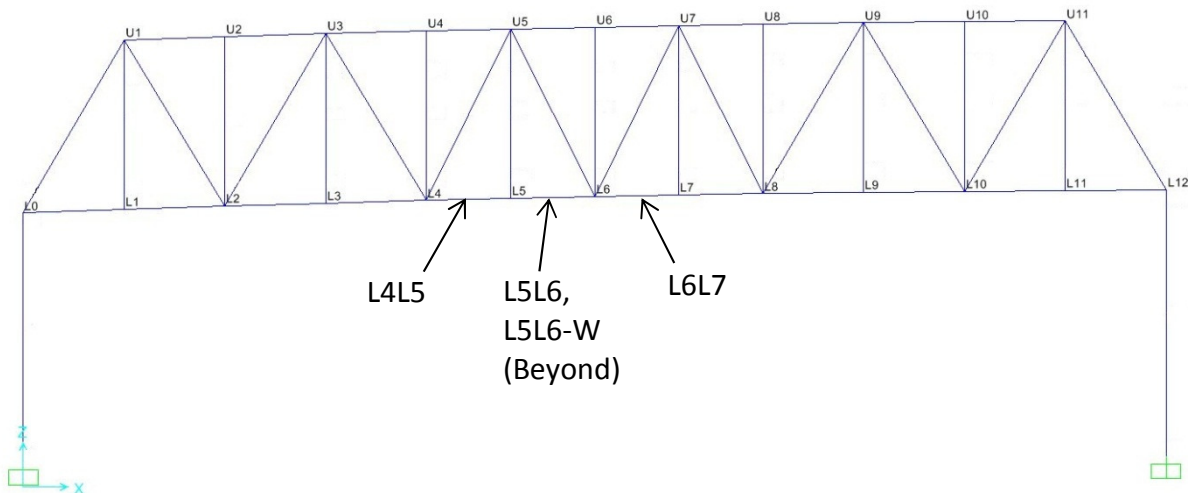


Figure 4-9: Little Mystic Bottom Chord Instrumentation

Because these members are chord members of the truss, they experience increasing strain from the time that the trucks enter the bridge. The strain that these members experience is fairly low as the steel manufactured during the time period when the Tobin Bridge was built would yield at over 1000 microstrain.

Figure 4-10 shows that there is agreement between collected data and the analytical data. The gauge that collected the data in Figure 4-10 is located on the side of the member. The experimental results that are found in Figure 4-11 appear to have higher values than those in Figure 4-10 as well as the analytical data. This can be explained by recognizing that each of the chord members undergoes localized bending as the truck moves over the location where the gauges are installed. By considering that the strain gets higher in Figure 4-11 compared with Figure 4-10, the bending must be positive as it is putting more tension in the bottom of the member. Predictably, the localized effects can be observed by investigating the opposite face of the member. As seen in Figure 4-12, as the truck moves across this location, strain is deducted from the global effects. By considering that the gauges in Figure 4-11 and Figure 4-12 are installed on the same member at the same location but on opposite faces, it can be deduced

that the bridge is experiencing this localized bending that has not been captured in the modeling. Similar behavior can be seen in Figure 4-15. The magnitude of this concentrated load can be estimated as 4 to 5 microstrain. Because the maximum strain in a gauge located on the side of the member is about 8 microstrain, this additional strain caused by bending cannot be ignored. This result proves that the bridge is not a pure truss; a fact previously proven (Sanayei, Pheifer, Brenner, Bell, & Allen, 2010).

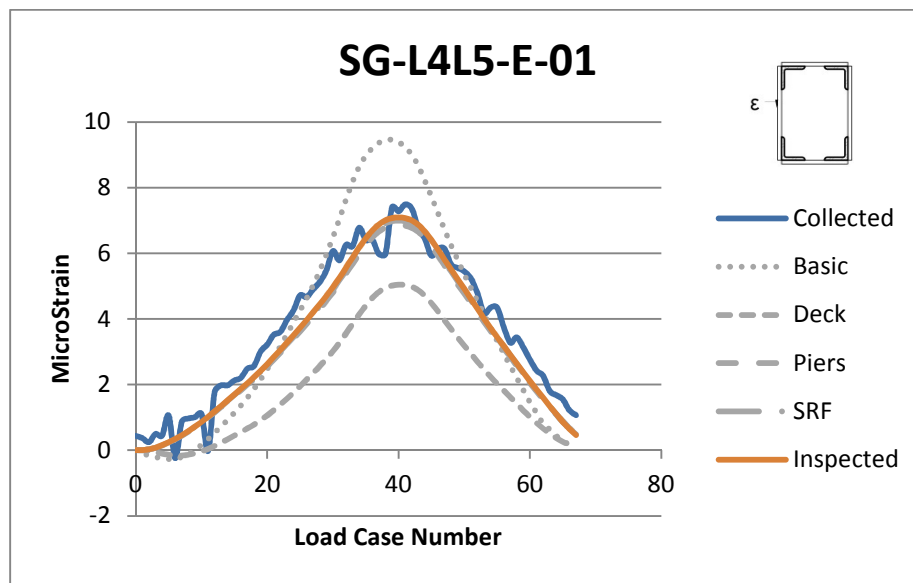


Figure 4-10: SG-L4L5-E-01 Strain vs Time

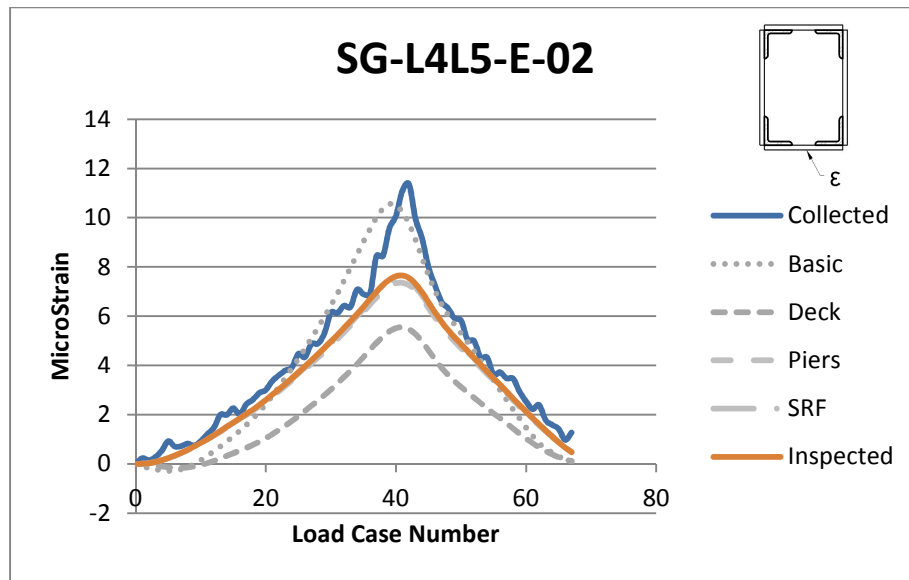


Figure 4-11: SG-L4L5-E-02 Strain vs Time

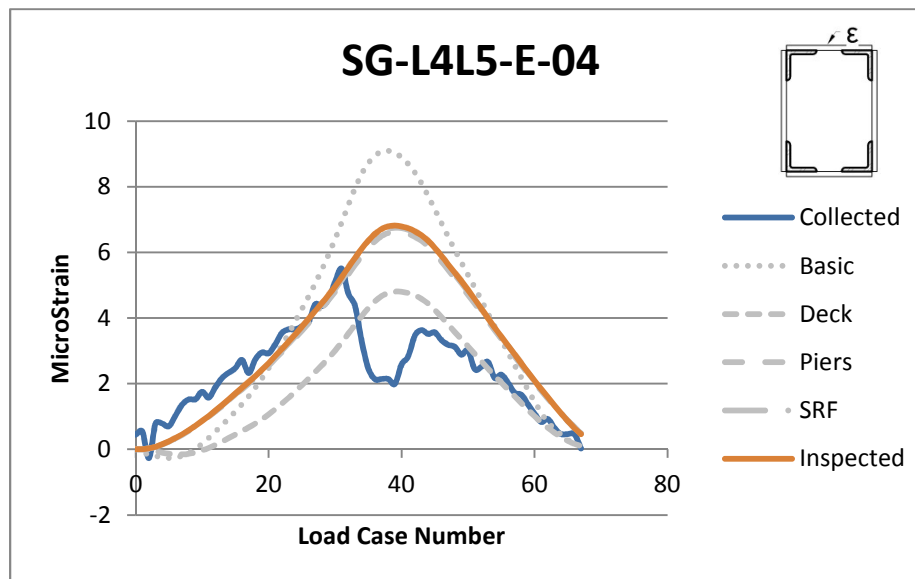


Figure 4-12: SG-L4L5-E-04 Strain vs Time

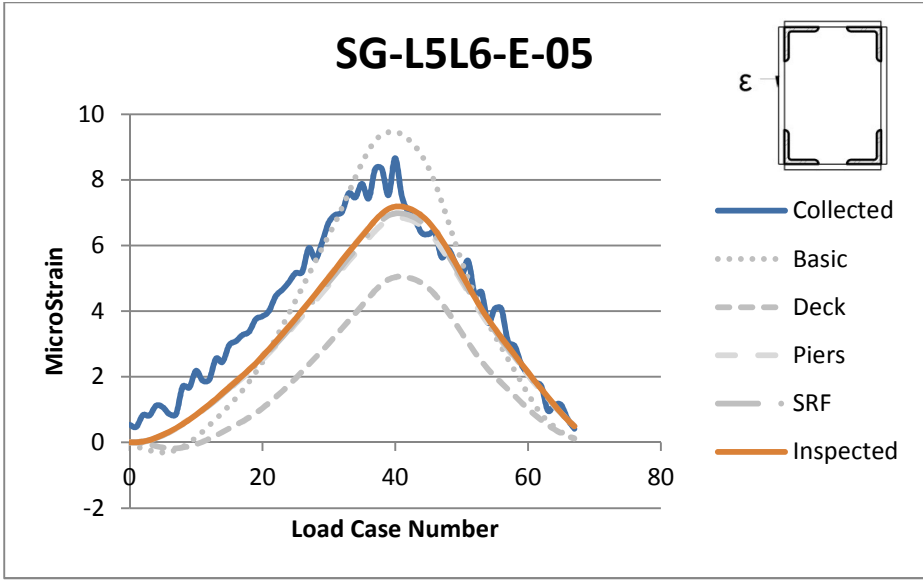


Figure 4-13: SG-L5L6-E-05 Strain vs Time

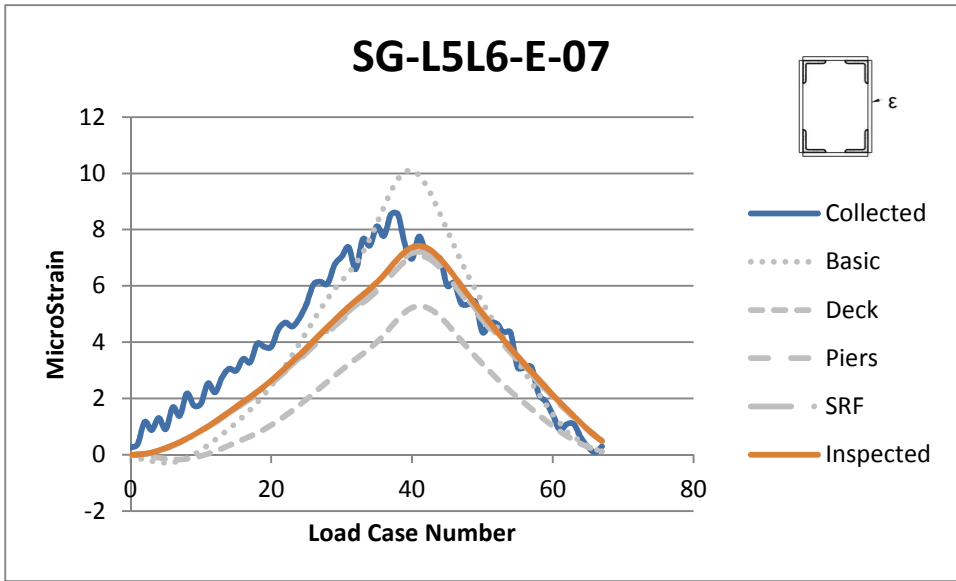


Figure 4-14 SG-L5L6-E-07 Strain vs Time

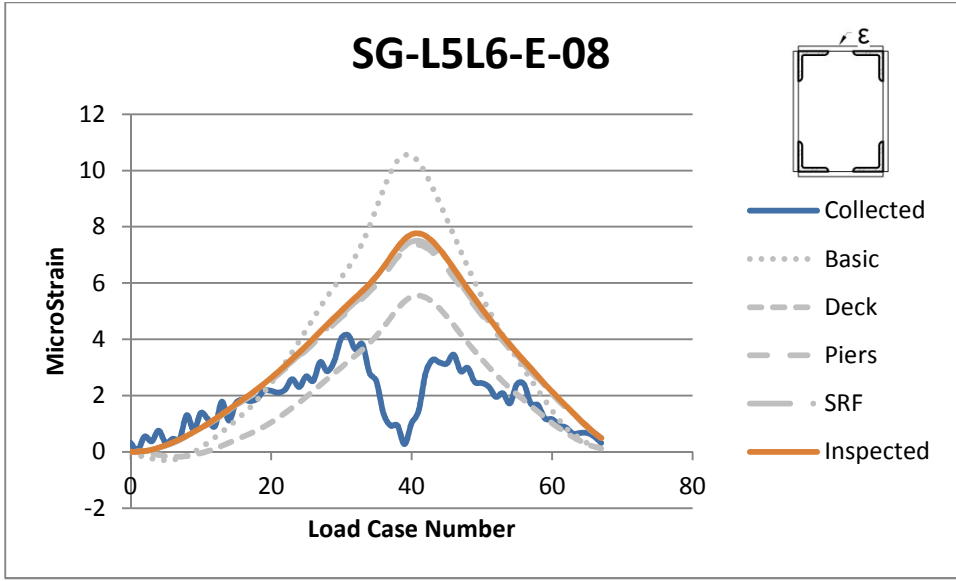


Figure 4-15: SG-L5L6-E-08 Strain vs Time

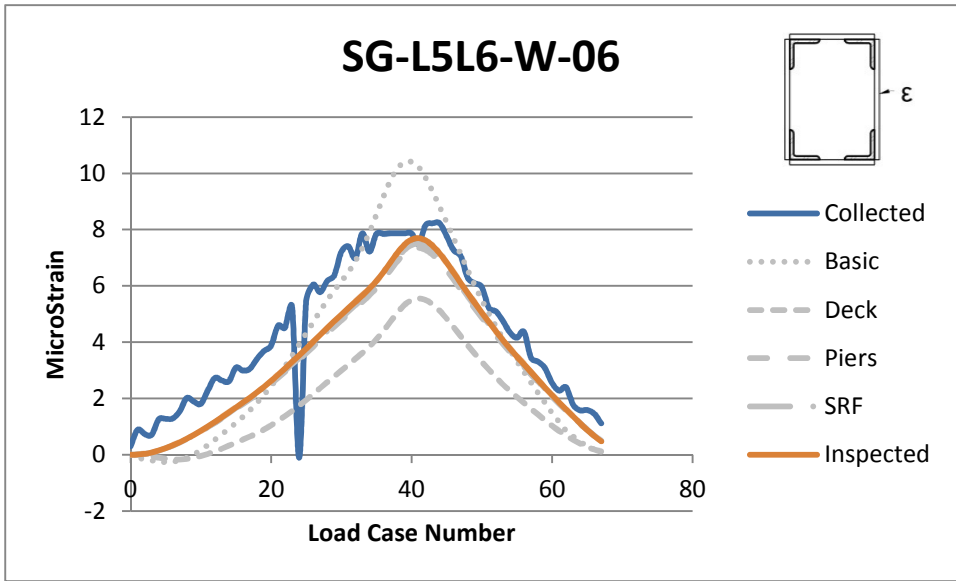


Figure 4-16: SG-L5L6-W-06 Strain vs Time

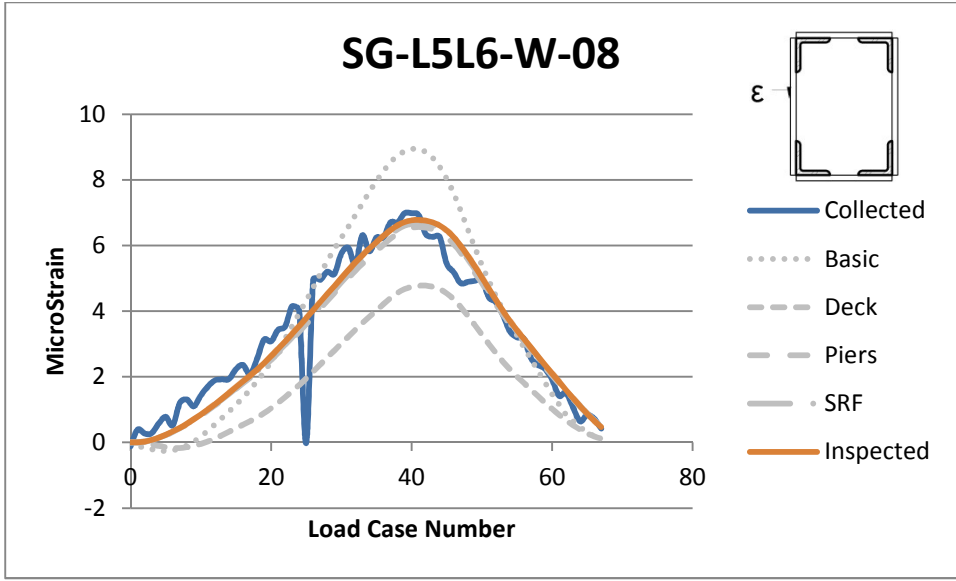


Figure 4-17: SG-L5L6-W-08 Strain vs Time

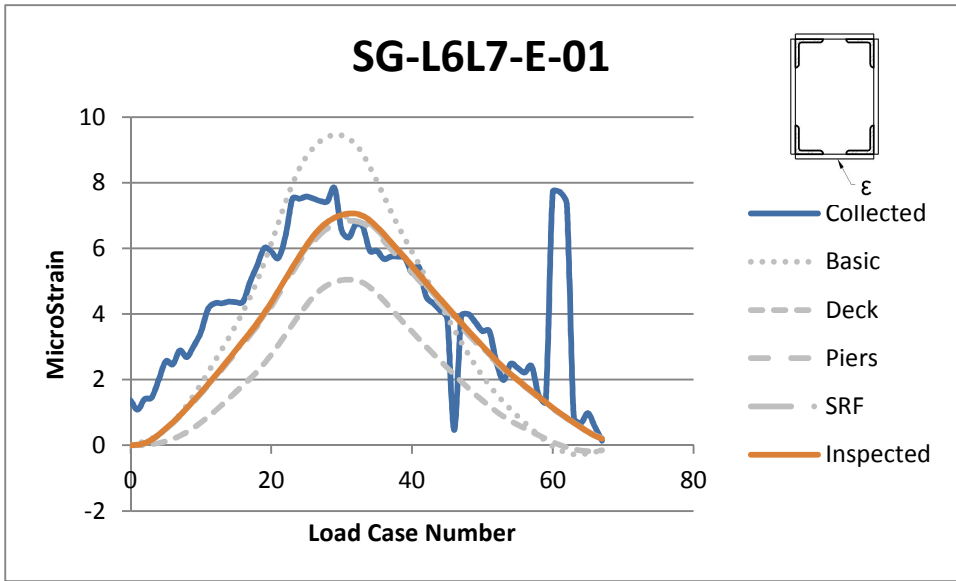


Figure 4-18: SG-L6L7-E-01 Strain vs Time

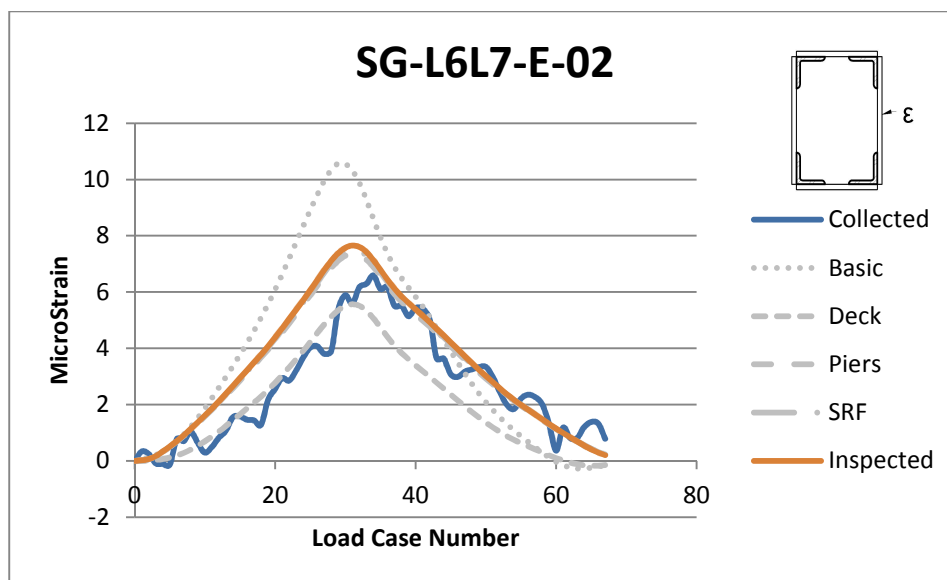


Figure 4-19: SG-L6L7-E-02 Strain vs Time

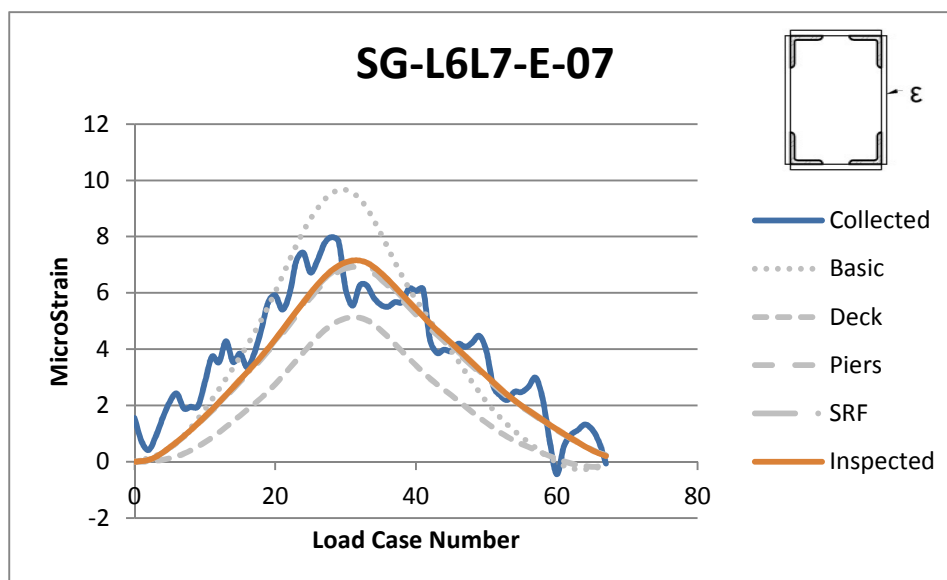


Figure 4-20: SG-L6L7-E-07 Strain vs Time

4.5.2 – Diagonals

The diagonals of the Little Mystic Span are built up box-shaped members similar in construction to the chord members. Also similar to the chords, diagonals have hand holes to facilitate the built up construction. The diagonals are connected to the chords using gusset plates and only two sides of the diagonal are connected to the truss.

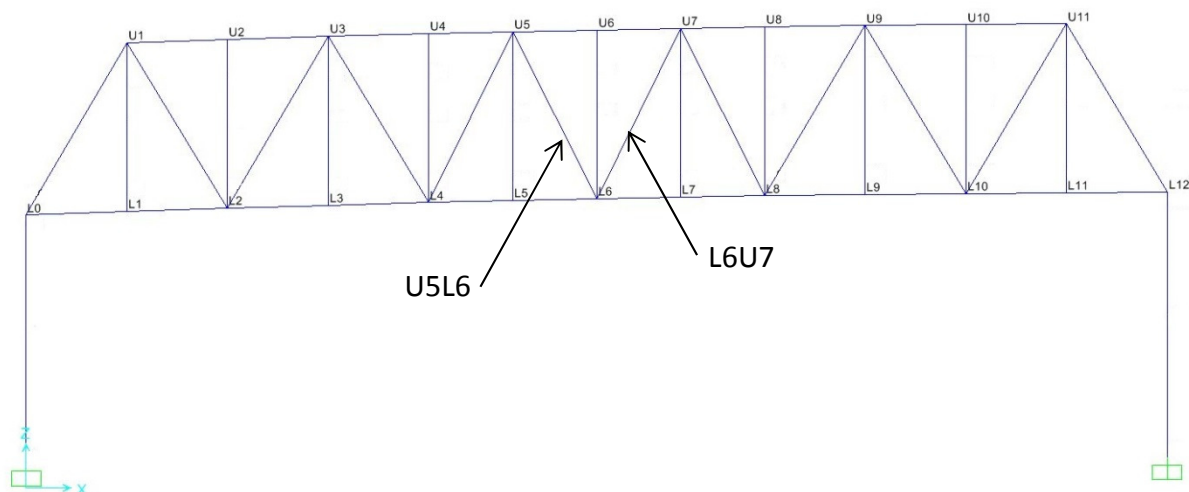


Figure 4-21: Little Mystic Diagonal Instrumentation

Two diagonal members of the truss were instrumented. Member U5L6 is a diagonal truss member located between panel points 5 and 6. The low point of the diagonal is located at the 6th panel point while the high point is located at the 5th panel point. L6U7 is located between the 6th and 7th panel points. The low point of the diagonal shares a truss node with member U5L6 and the high point is located at the 7th panel point. See Figure 4-21.

The start of the load test is located near panel 12 and moved to panel 1.. As such, member U5L6 starts in axial tension (Figure 4-22). After the truck passes the 5th panel point, the strain begins to transition down to a negative maximum at the 6th panel point after which it increases back to zero. The analytical models show a sharp transition while with the collected data, the transition is smoother. This is because while the trucks are passing over the 5th and 6th panels, the bottom chords are taking the truck loads in bending.

Because only two sides of the box shaped diagonal member are connected to the gusset plate the diagonal members experience shear lag. Shear lag occurs when not all the elements of a member are connected to another member. Shear lag is most commonly considered when

designing tension members. This is because shear lag causes stress concentrations at the ends of the member which are amplified by the reduced cross sectional area across bolted or riveted connections. Despite the fact that shear lag is mainly considered only for tension members, it could be extrapolated to compression members if certain criteria are met. First and most importantly, the ends of the members that are connected cannot bear on one other. If the surfaces of the adjoining members are milled for bearing and the members are properly constructed so that there is no gap between the members. When the members experience compression, strain from one member will be directly transferred to the adjoining member. Member U5L6 however, like all the diagonal members of this truss, does not bear on the other members in the L6 node. Because of this fact, the compression must enter the member via gusset plates and rivets and the behavior will be similar to shear lag in tension members. Proof of this can be found by comparing the strain in the gauges that are mounted on the inside and outside faces of the member with the strain in the gauges that are mounted on the longitudinal sides of the member. This can be seen most explicitly by comparing strain levels in Figure 4-22 with the strain levels in Figure 4-23. It can also be noted that there is a slight increase in tension on SG-L6U5-E-03 as the truck approaches the 6th panel point and the transition from tension to compression. This increase is due to the floor beam engaging the diagonal to take the torsional load in the bottom chord. This will be discussed in greater detail in later sections.

In most cases, the gauges are numbered following the same pattern. The even numbered gauges are typically located on the inside and outside faces while the odd numbered gauges are on the longitudinal faces. The gauge location figures for each gauge's chart reflects this change.

This problem is not present on member L6U7 and the odd numbered gauges are installed on the inside and outside faces of the member for both the i-joint and the j-joint.

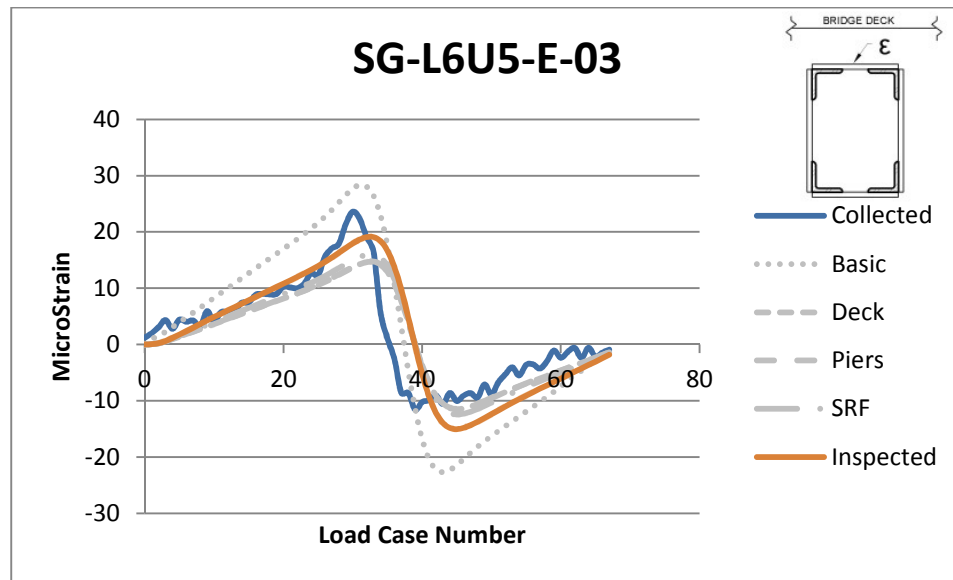


Figure 4-22: SG-L6U5-E-03 Strain vs Time

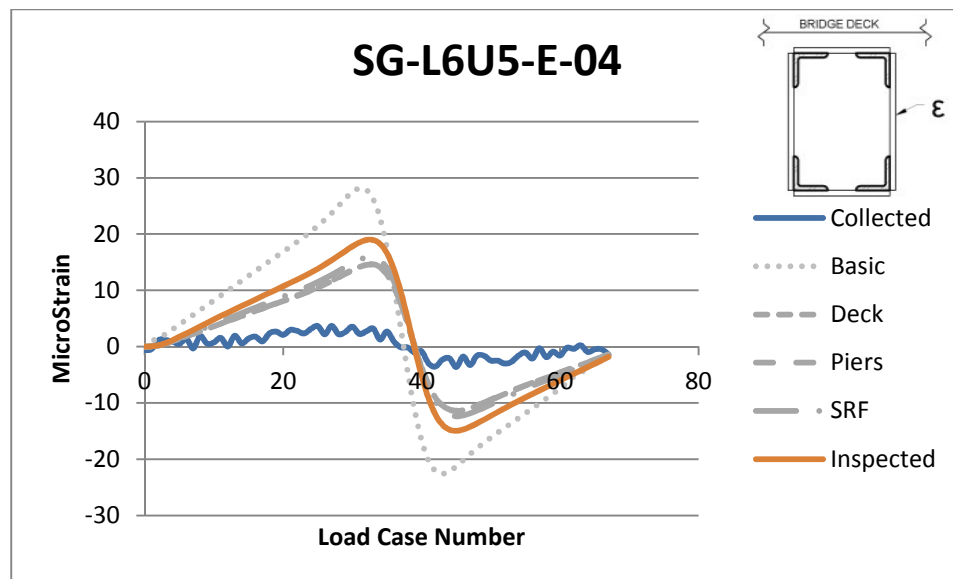


Figure 4-23: SG-L6U5-E-04 Strain vs Time

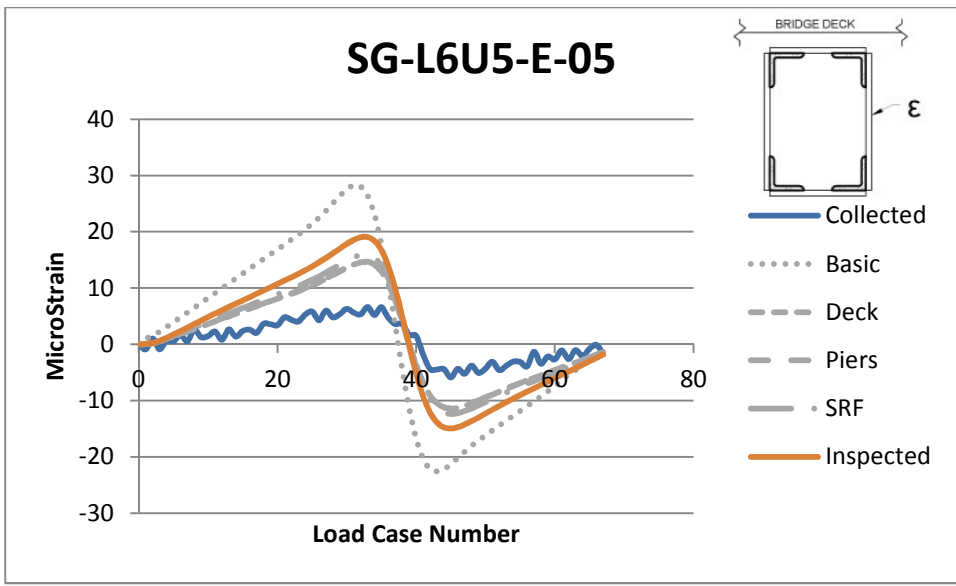


Figure 4-24: SG-L6U5-E-03 Strain vs Time

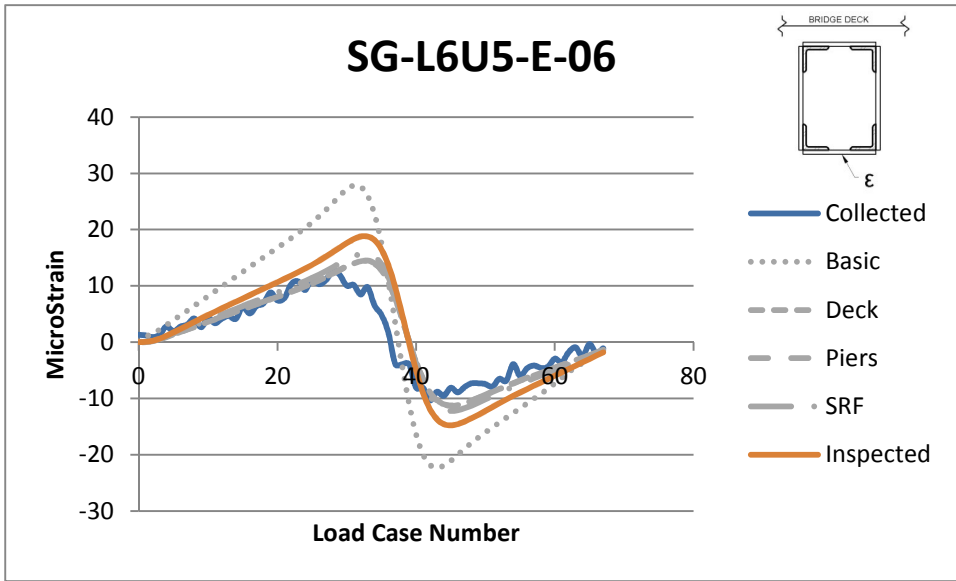


Figure 4-25: SG-L6U5-E-06 Strain vs Time

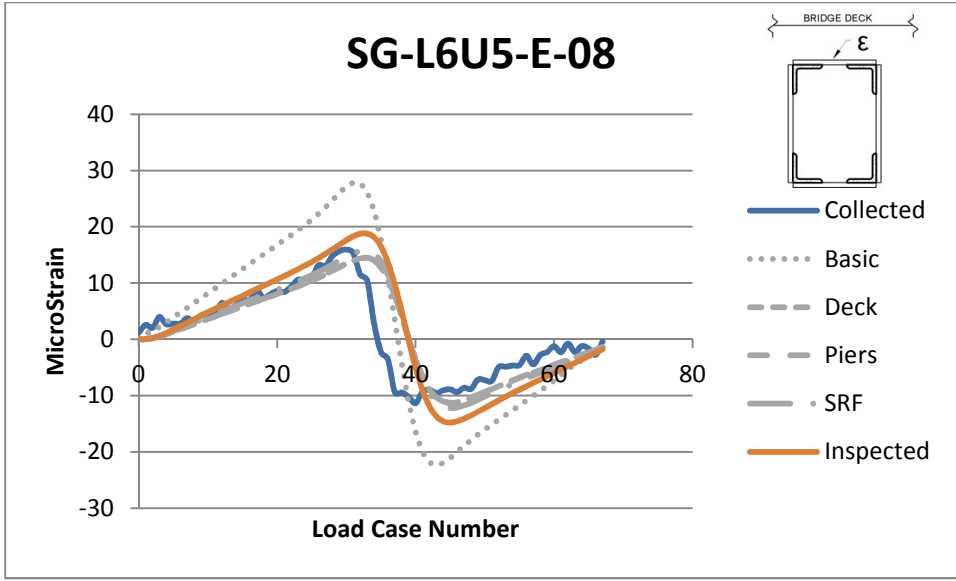


Figure 4-26: SG-L6U5-E-08 Strain vs Time

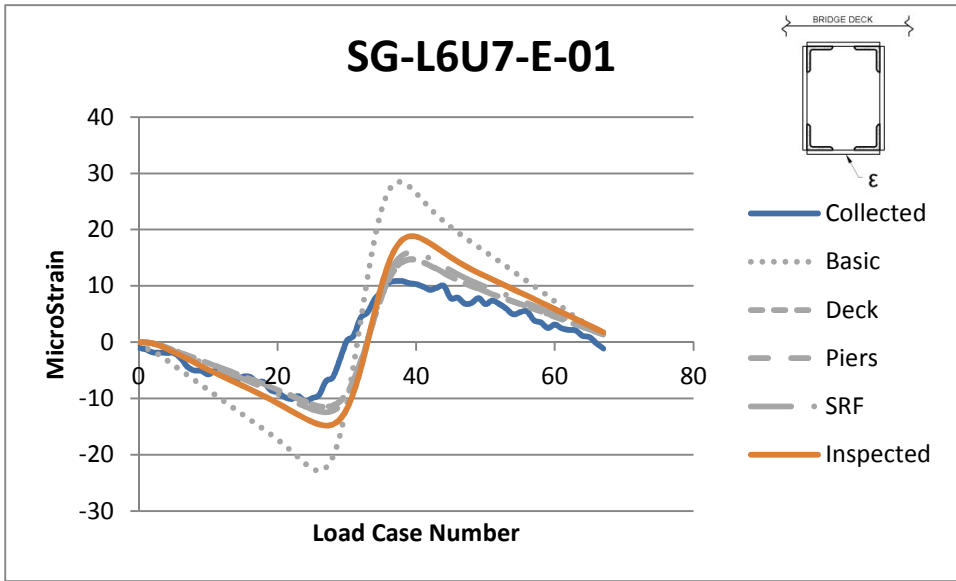


Figure 4-27: SG-L6U7-E-01 Strain vs Time

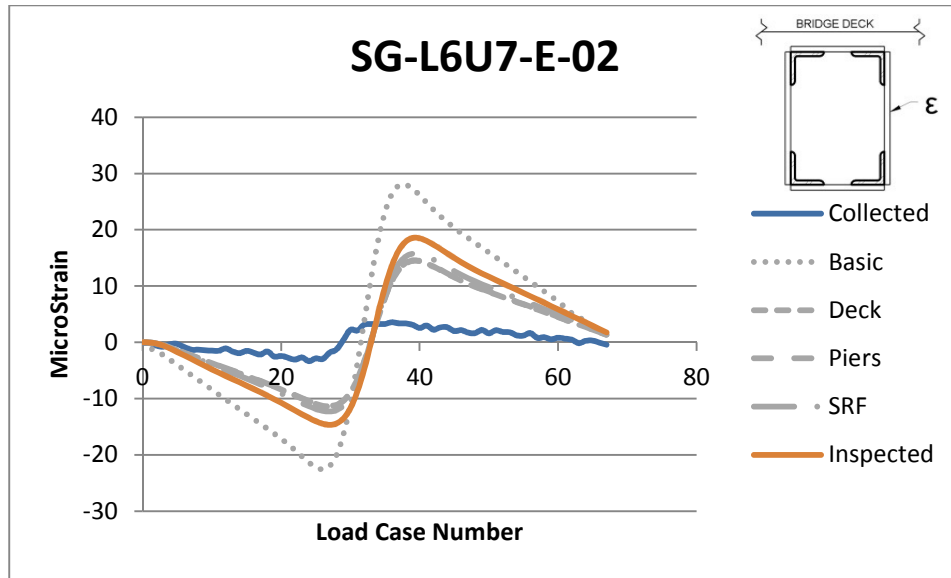


Figure 4-28: SG-L6U7-E-02 Strain vs Time

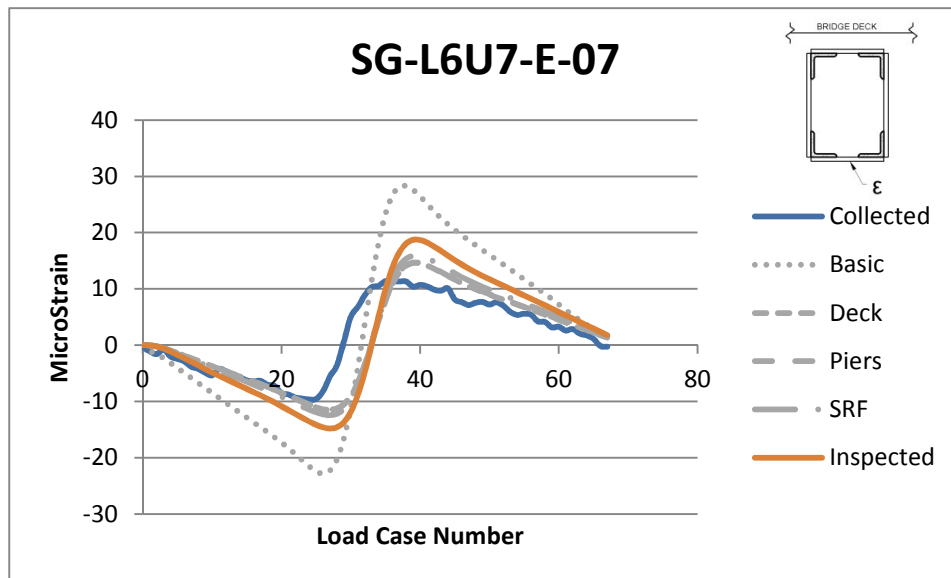
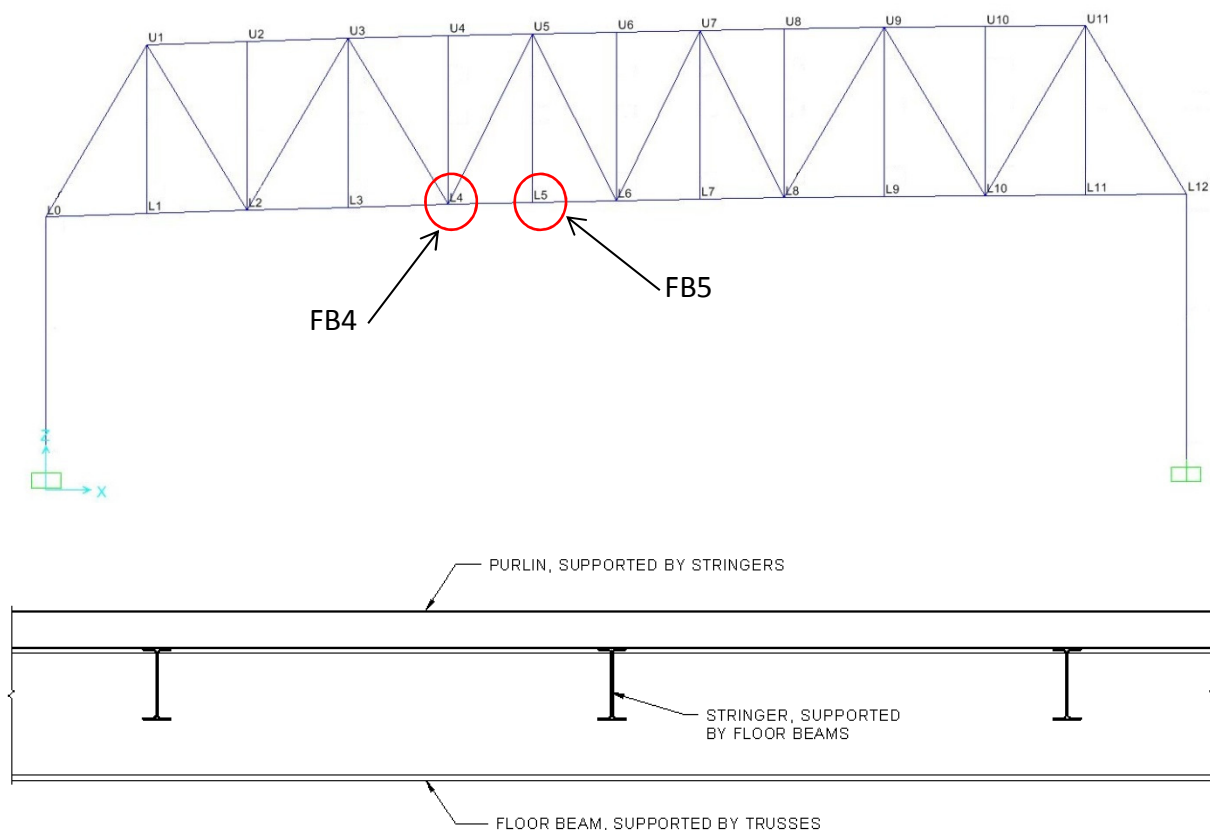


Figure 4-29: SG-L6U7-E-07 Strain vs Time

4.5.3 – Floor Beams

Two floor beams have been instrumented as part of this research. The two beams are floor beam number 4 (FB4) and floor beam number 5 (FB5). These beams are located at the 4th and 5th panel points and connect the bottom chord of the east and west side trusses. The floor

beams support the bridge stringers which in turn support purlin beams which support the bridge deck.



Strain vs Time graphs are included in Figure 4-30, Figure 4-31, Figure 4-32, and Figure 4-33.

These gauges are located roughly 3 feet from the centerline of the west side truss. In comparing the analytical data with the experimental data it can be seen that the experimental data has produced far larger responses than the analytical data. Much of this could be due to the proximity of the gauges to the gusset plate that connects the beam to the side truss. No as-built drawings were provided to confirm the installation location of the strain gauges but installation drawings are available and the gauges are assumed to have been installed in the intended location. In the case of the floor beams, the gauges were to be installed approximately 6 feet

from the centerline of the bottom chord of the truss. The beam is connected using a simple shear connection on the web and bottom flange plates. This, in conjunction with the use of rivets, creates a partially restrained moment connection. It is possible that gauges are experiencing strains due to stress concentrations relating to the uneven distribution of forces around the rivet holes. While the connection plates end after just a few feet, the member's cap plates are riveted through the length of the floor beam. With that in mind, avoiding stress concentrations would be difficult.

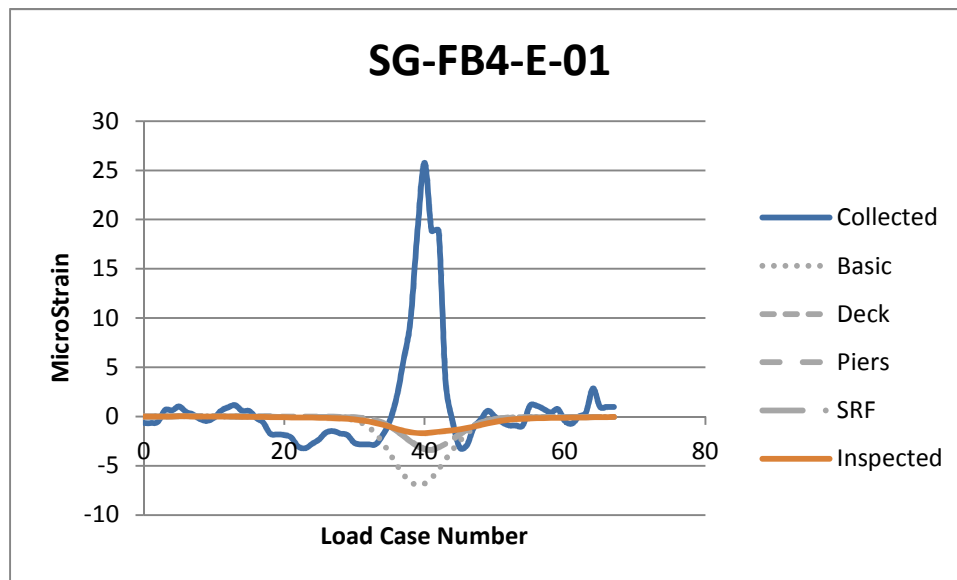


Figure 4-30: SG-FB4-E-01 Strain vs Time

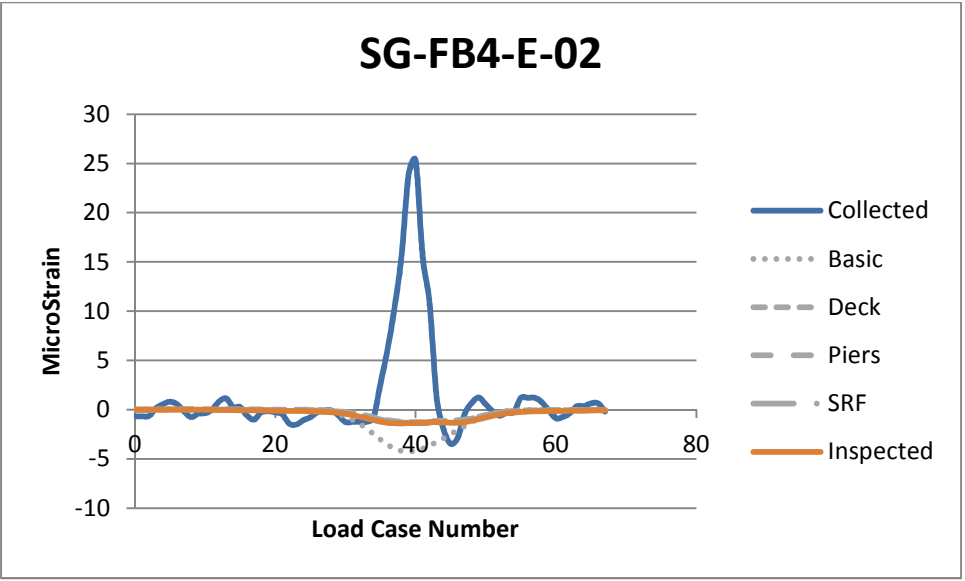


Figure 4-31: SG-FB4-E-02 Strain vs Time

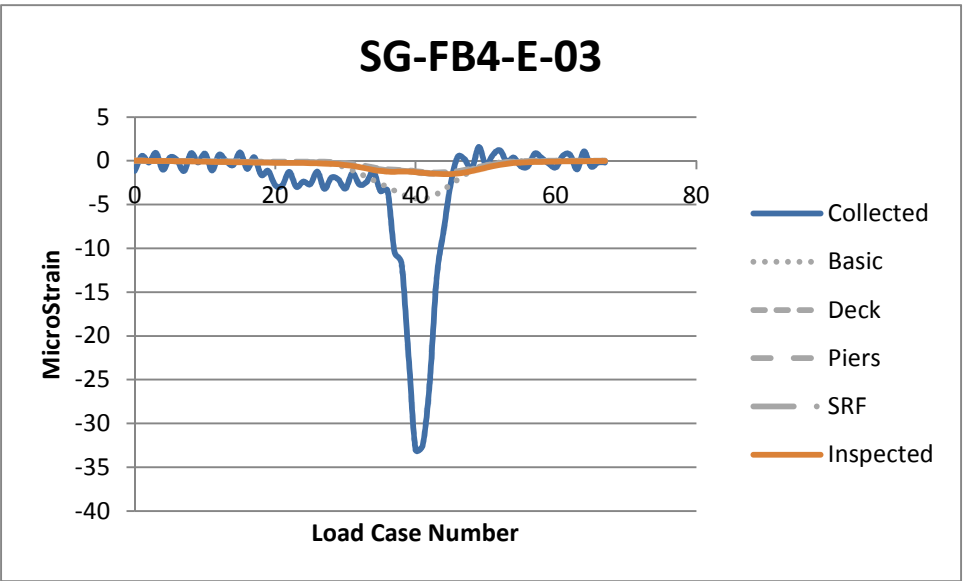


Figure 4-32: SG-FB4-E-03 Strain vs Time

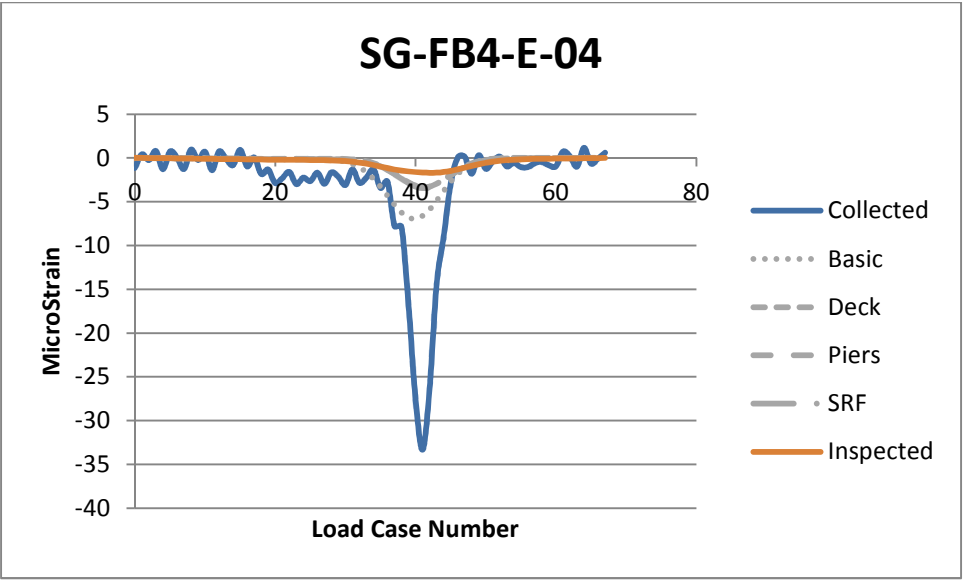


Figure 4-33: SG-FB4-E-04 Strain vs Time

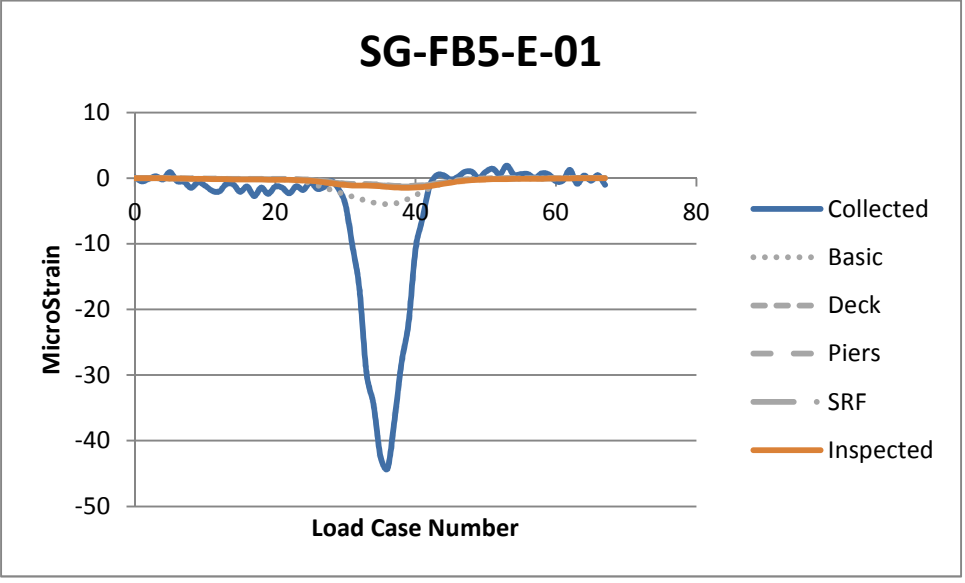


Figure 4-34: SG-FB5-E-01 Strain vs Time

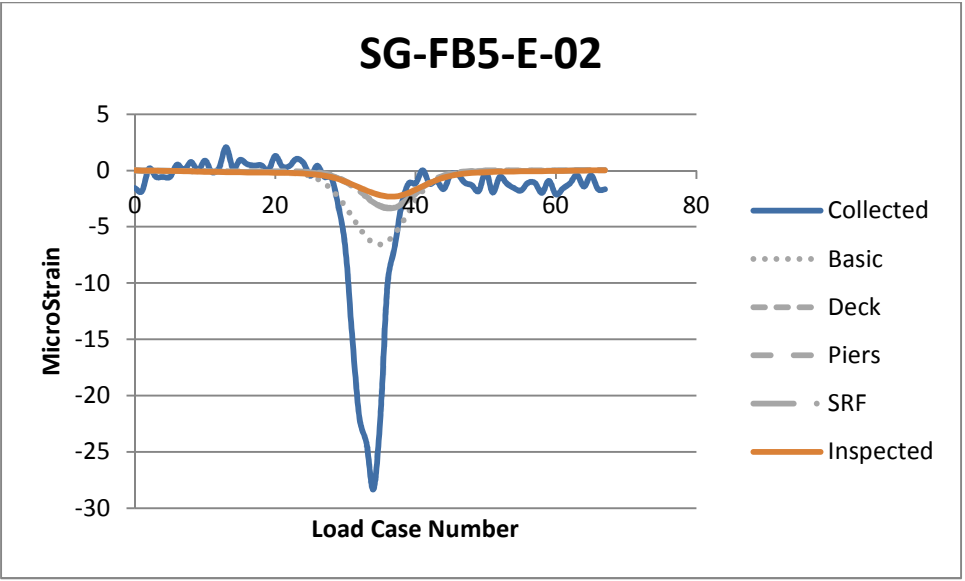


Figure 4-35: SG-FB5-E-02 Strain vs Time

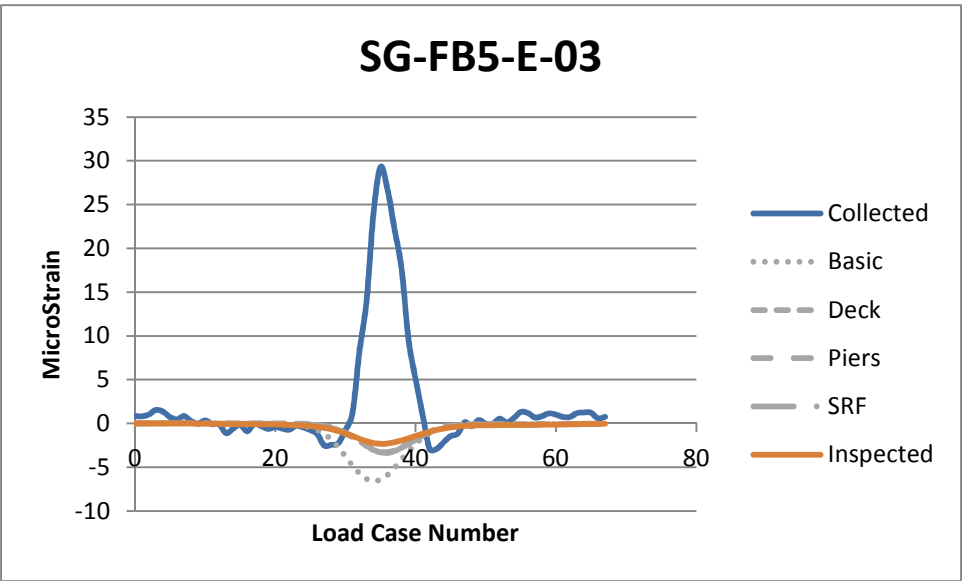


Figure 4-36: SG-FB5-E-03 Strain vs Time

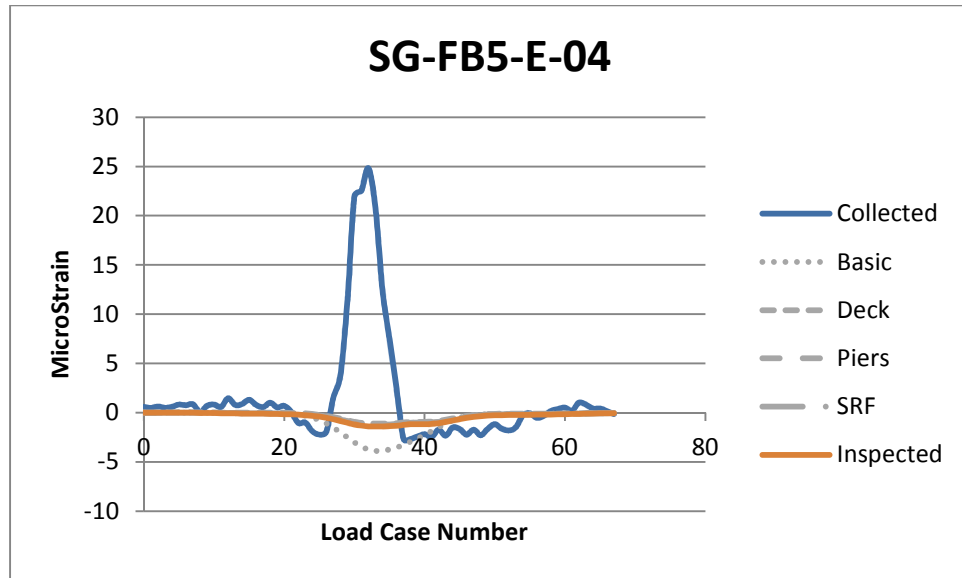


Figure 4-37: SG-FB5-E-04 Strain vs Time

4.5.4 – Verticals

Two vertical members of the bridge were instrumented with strain gauge. They are members L5U5 and L6U6, located at panels 5 and 6 respectively. Both members are located on the east side of the bridge. The vertical members are built up sections created using WF18x57 main members with C18x27.5 cap channels (Figure 4-38). L5-U5 has 6 functional gauges while L6-U6 has 8 functional gauges. The gauges are mounted to the inside of the cap channels.

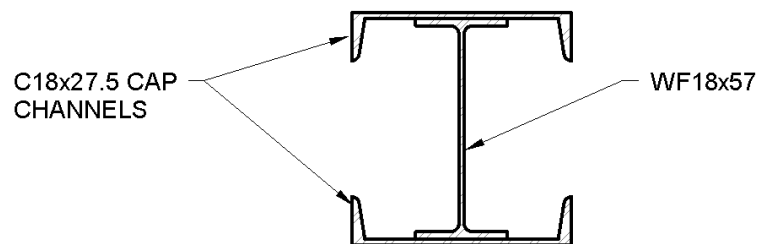


Figure 4-38: Vertical Member Cross Section

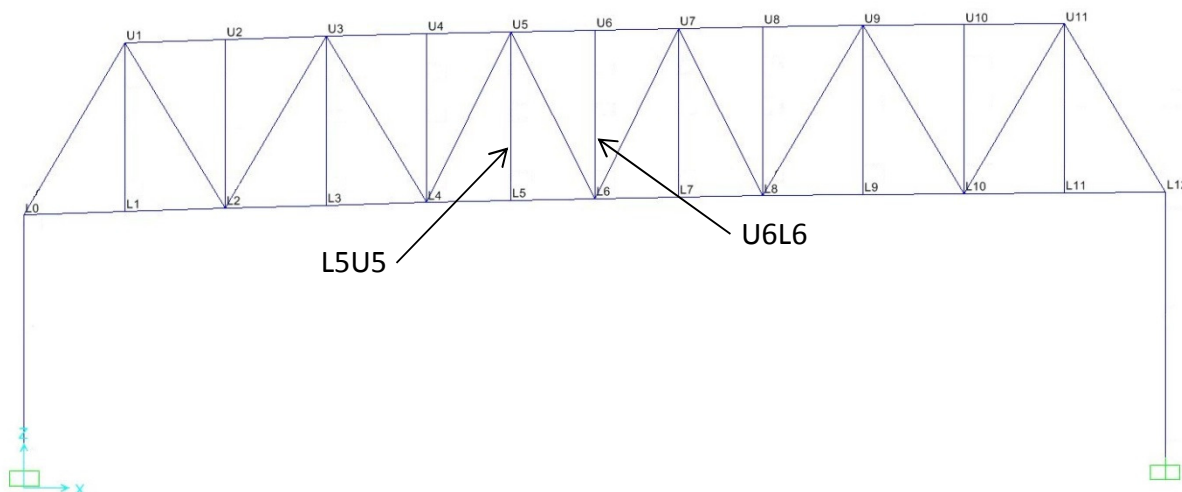


Figure 4-39: Little Mystic Elevation - Instrumented Verticals

In theoretical truss analysis, it is expected that the vertical members in this configuration should act as zero force members. Because it has been shown that the truss members behave more like frame elements than pins, the vertical members do resist some load. The structural analysis software appears to produce the expected results. But the collected data for the vertical members does not agree with the analytical data for gauges that are located near the i-joint of the members (Figure 4-42, Figure 4-43, Figure 4-44, Figure 4-45, Figure 4-48, Figure 4-49, and Figure 4-50). This is due to the additional moments that are induced into the vertical members due to the bending of the floor beams as the truck passes over it. This induced bending completely changes the results that are expected to be produced from the analytical model.

In order to track the induced bending through the vertical member, a finite element model was created. This model was a 3 span continuous beam that was intended to mimic the support that is provided by the bottom chord, the upper level of floor beams, the bottom of the portal frame bracing and the top chord (Figure 4-40).

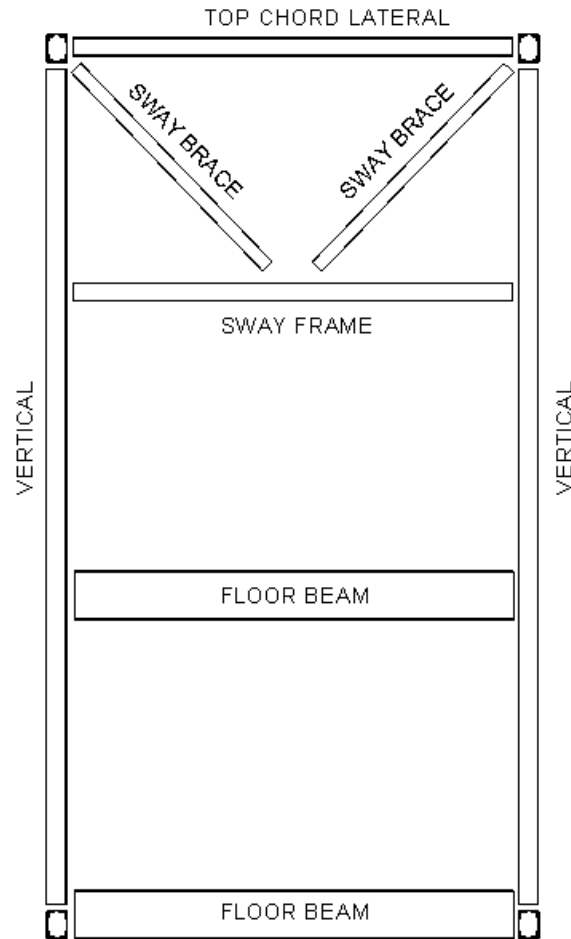


Figure 4-40: Little Mystic Sway Frame

A concentrated moment was placed at the left hand support. The moment diagram obtained from the analysis of this study can be found in Figure 4-41.

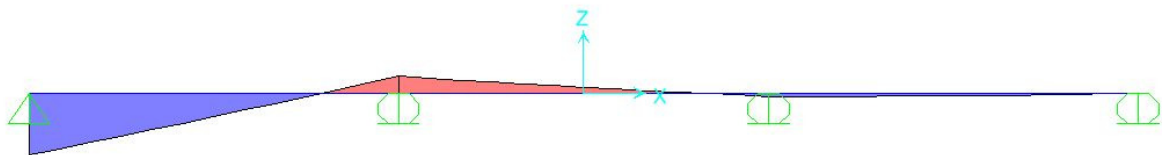


Figure 4-41: Vertical Member Moment Diagram

If the floor beams that connect both side trusses are considered to be fully fixed at the ends. When a truck runs over this floor beam, the fixed end moments place a torque on the bottom chord. This torque will attempt to find the stiffest load path throughout the structure. There are

two means to alleviate this torsion. The first path is through the bottom chord itself. This is an inefficient load path, as the torsional stiffness of the bottom chord is far smaller than the bending stiffness of the vertical member. The alternative is for the vertical member to take the torsion from the bottom chord in bending.

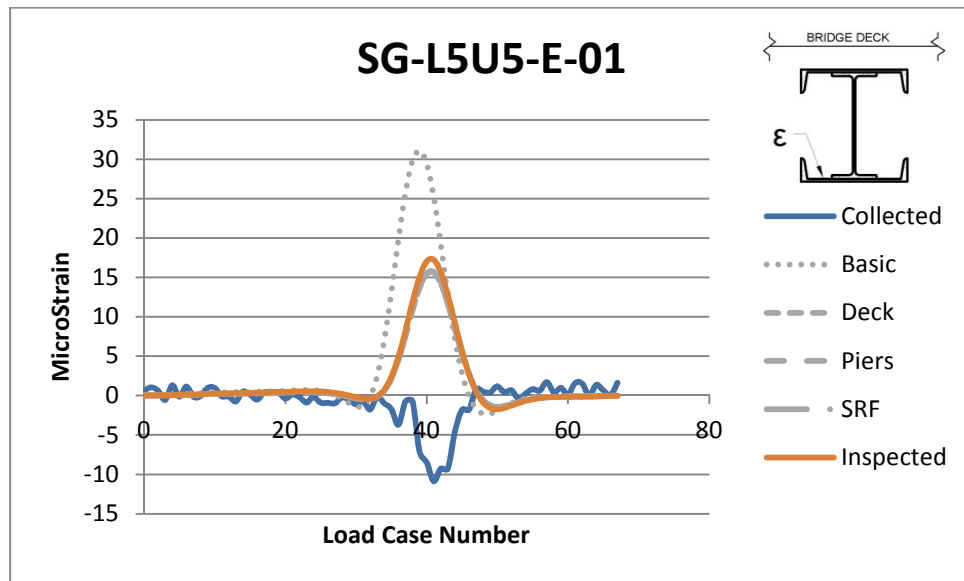


Figure 4-42: SG-L5U5-E-01 Strain vs Time

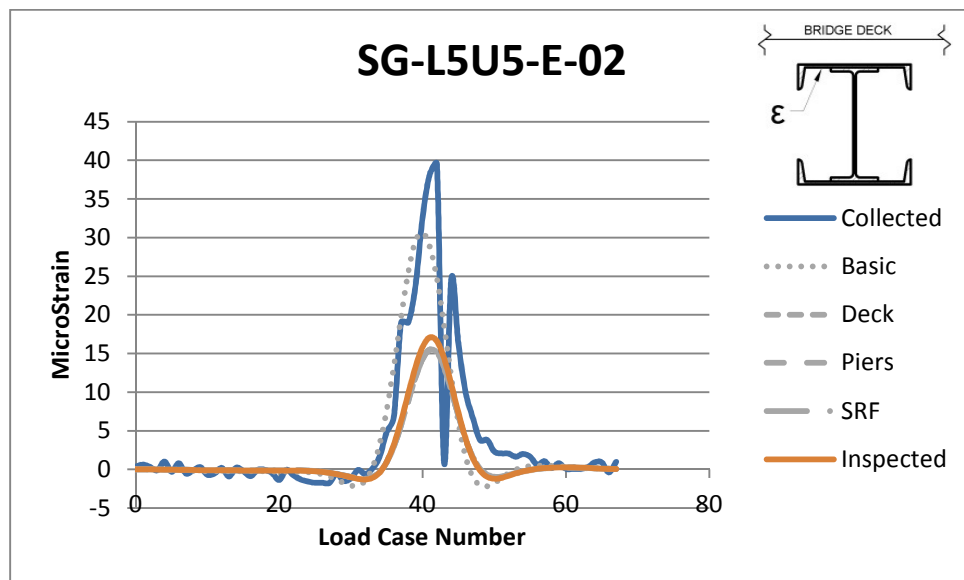


Figure 4-43: SG-L5U5-E-02 Strain vs Time

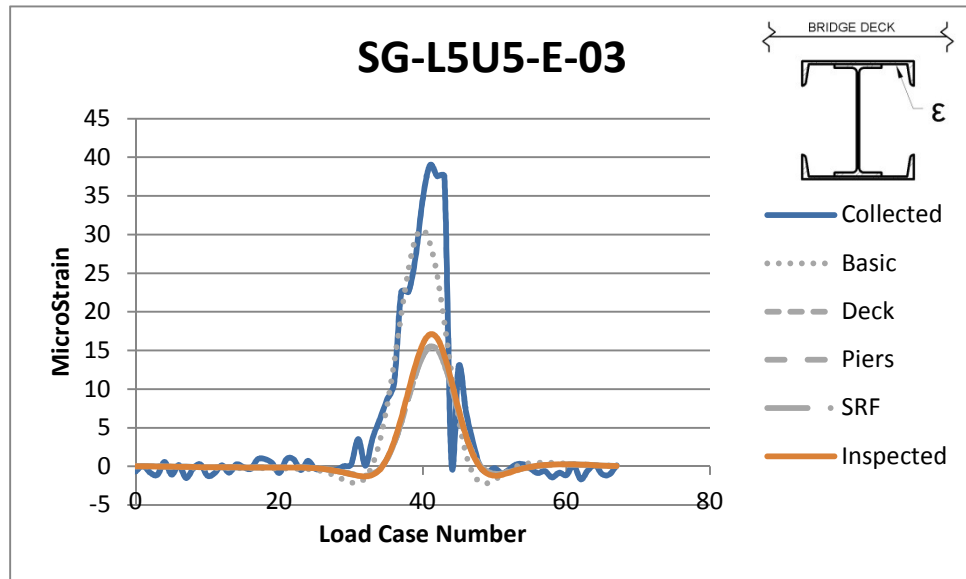


Figure 4-44: SG-L5U5-E-03 Strain vs Time

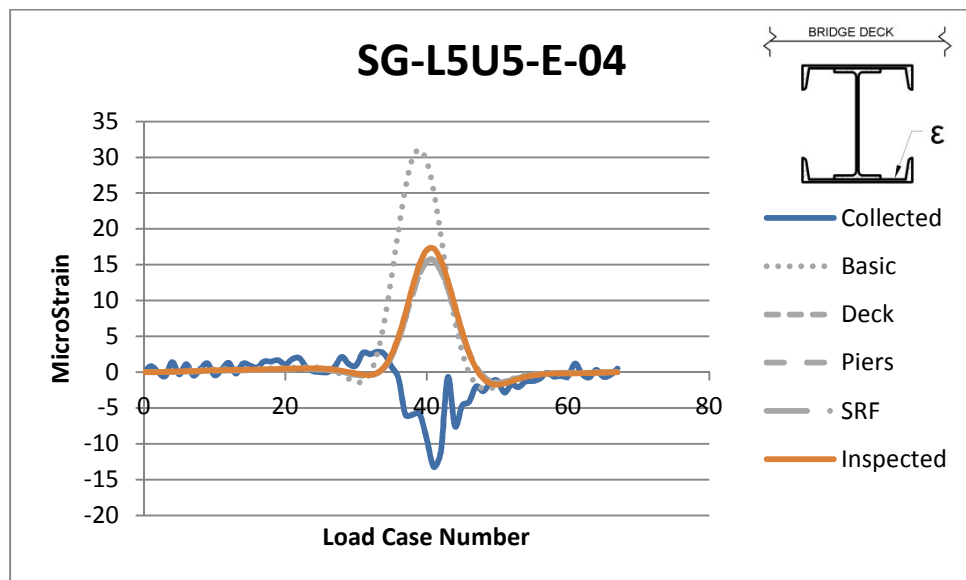


Figure 4-45: SG-L5U5-E-04 Strain vs Time

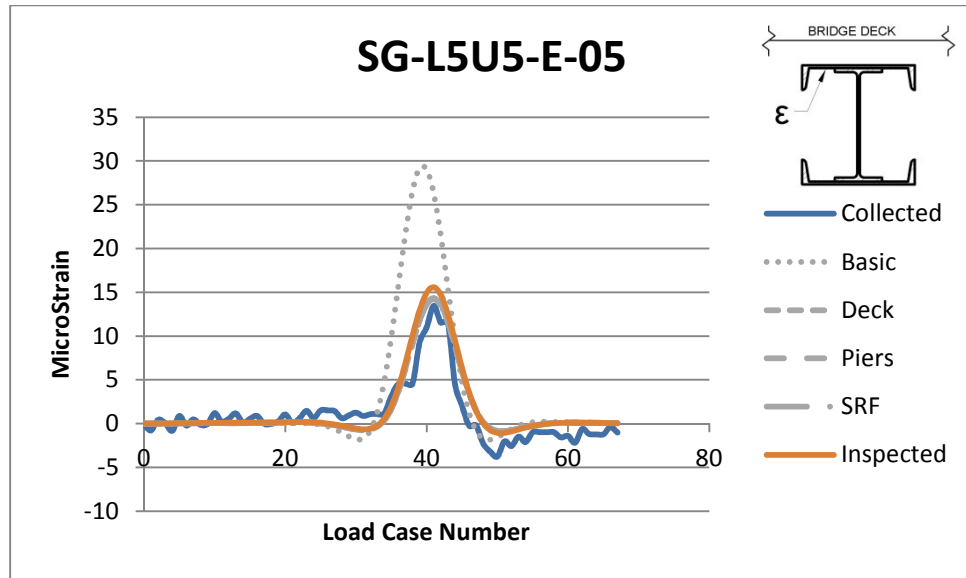


Figure 4-46: SG-L5U5-E-05 Strain vs Time

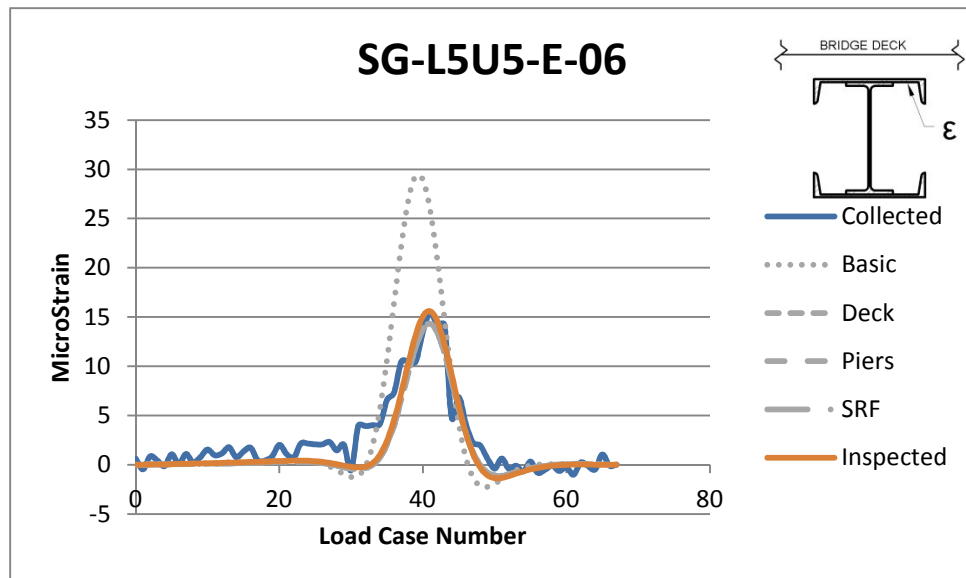


Figure 4-47: SG-L5U5-E-06 Strain vs Time

As noted earlier, all the vertical members are theoretically zero force members. This is confirmed by comparing the experimental strain with the theoretical strain for each of the gauges located near the j-joint of the member (Figure 4-51, Figure 4-52, Figure 4-53, and Figure 4-54). The reason that member L5U5 does not behave as a zero force member and experiences tension at the j end is due to the lack of diagonals that frame into the bottom chord at panel point 5. As the truck moves over panel point 5, the bottom chord begins to deflect downward

causing tension in the vertical member. When comparing the vertical at panel point 5 with the one at panel point 6, it can be seen that there is essentially no axial force in the vertical at panel point 6.

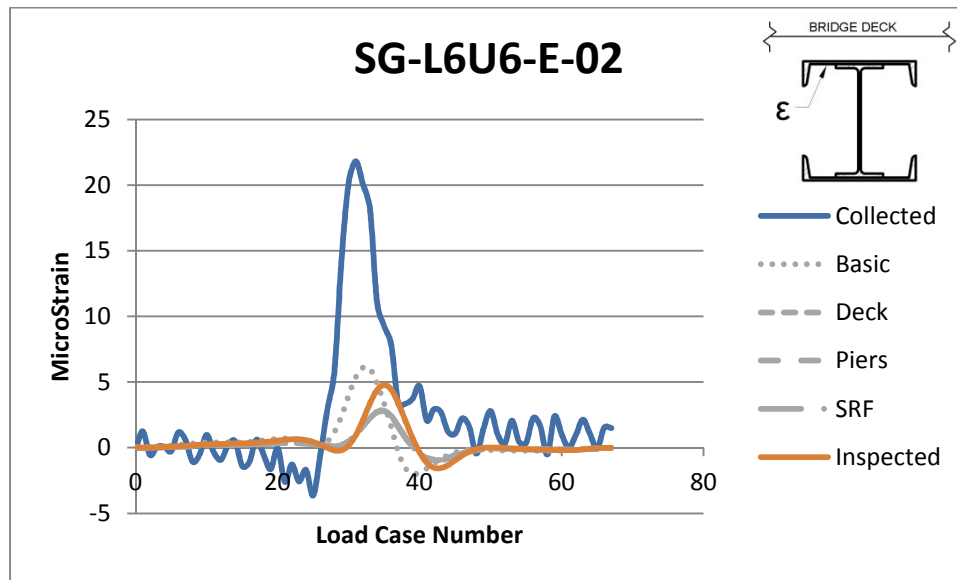


Figure 4-48: SG-L6U6-E-02 Strain vs Time

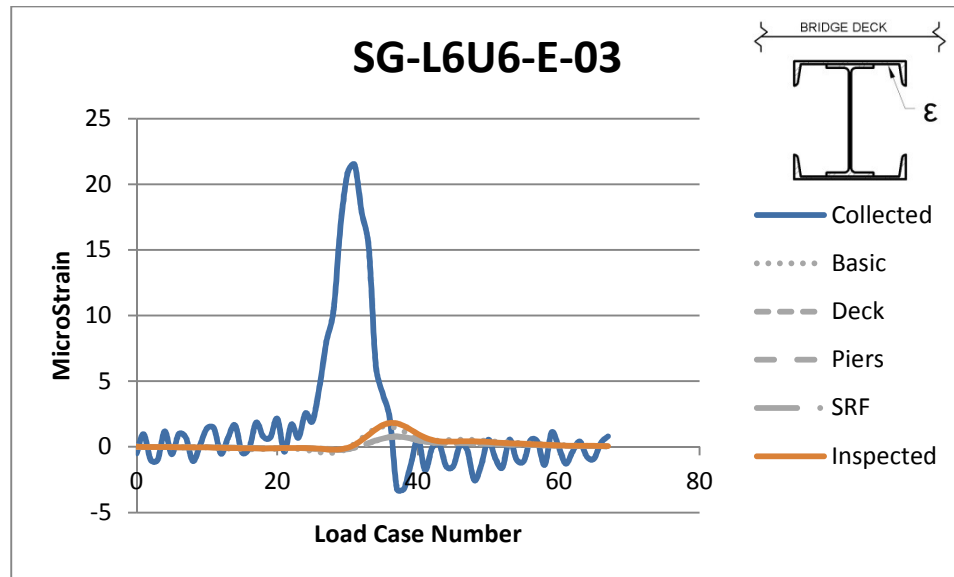


Figure 4-49: SG-L6U6-E-03 Strain vs Time

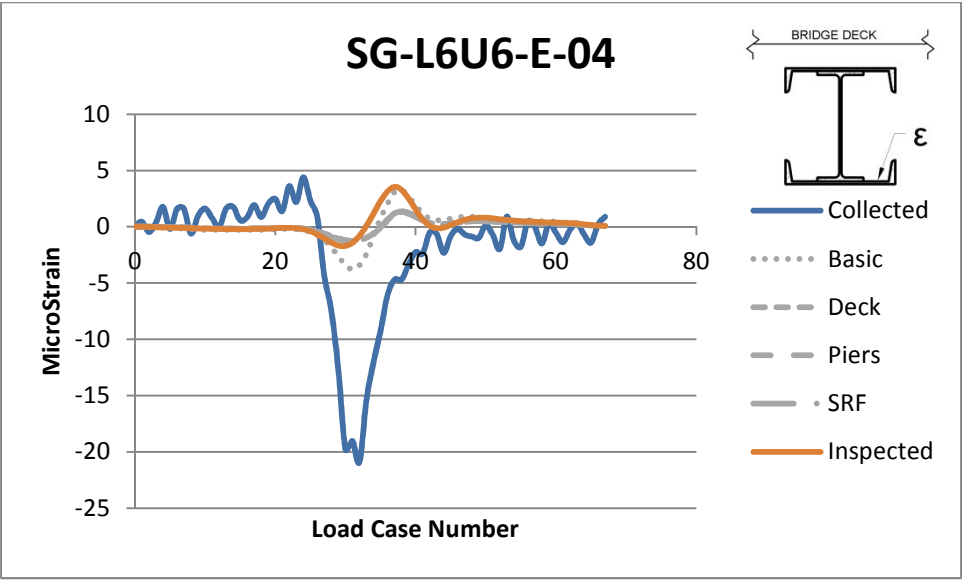


Figure 4-50: SG-L6U6-E-04 Strain vs Time

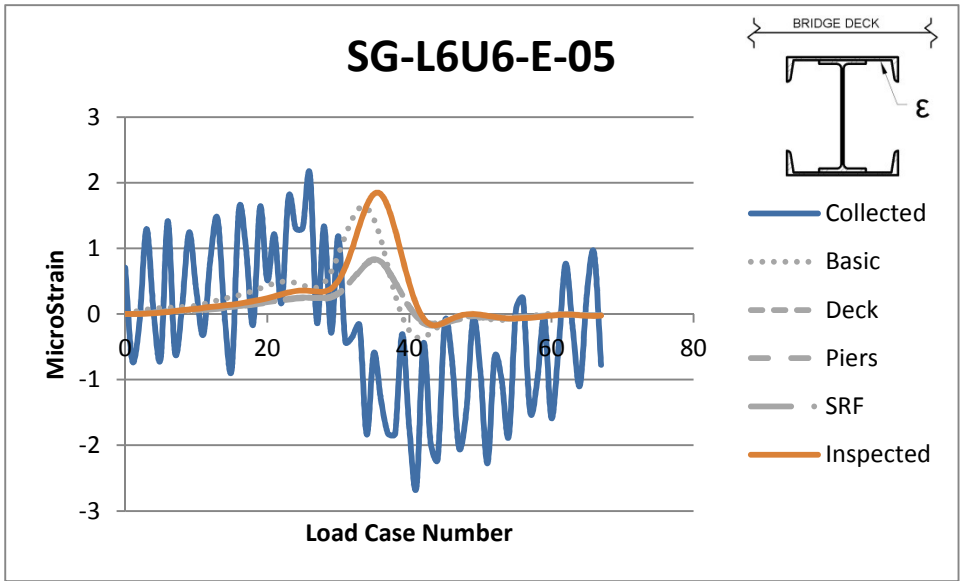


Figure 4-51: SG-L6U6-E-05 Strain vs Time

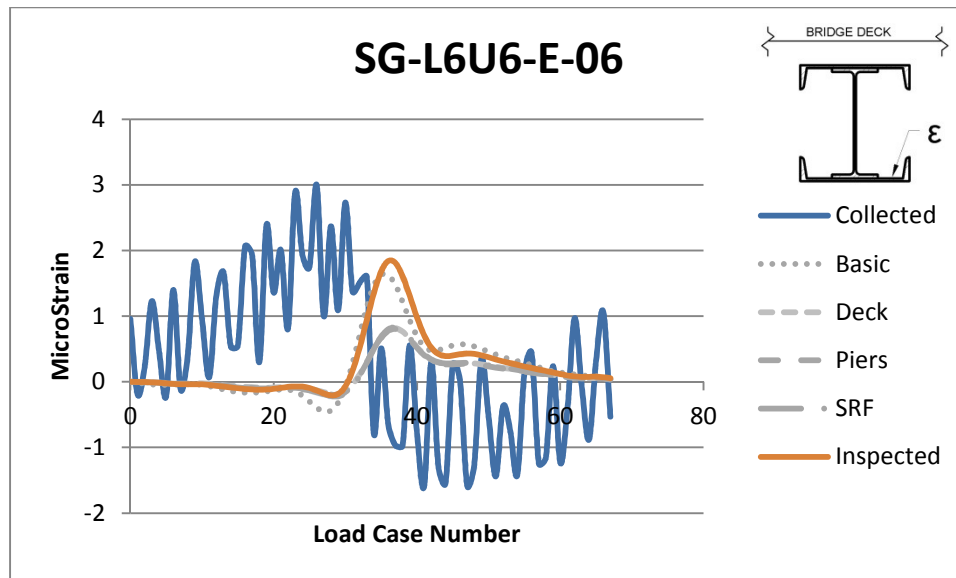


Figure 4-52: SG-L6U6-E-06 Strain vs Time

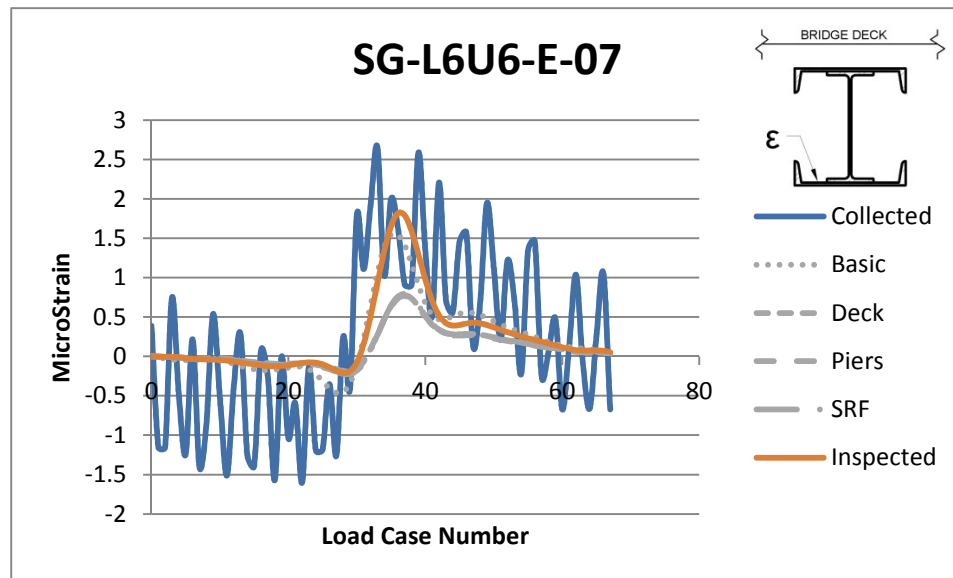


Figure 4-53: SG-L6U6-E-07 Strain vs Time

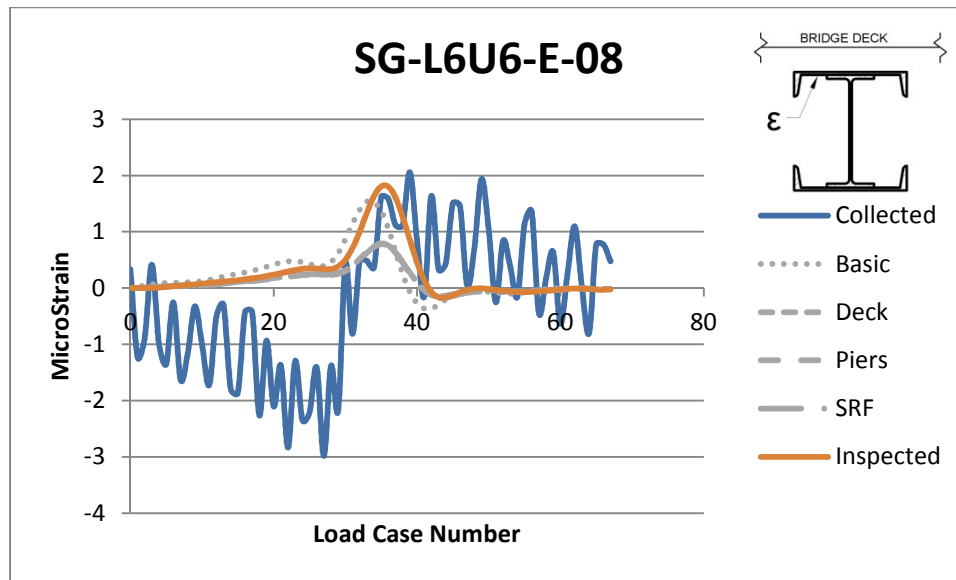


Figure 4-54: SG-L6U6-E-08 Strain vs Time

4.5.5 – Changes to Section Properties

A comparison was made between the section properties calculated using the 2008 inspection report of the Tobin Bridge and the model updating procedure, see Table 4-2: Comparison of Section Properties. The model updater presented in this research is based upon determining the inspected cross sectional area, then calculating the section properties based on a constant radius of gyration. All major chord members of the Little Mystic Span were updated based on the 2006 TranSystems bridge inspection. It can be seen that the calculated cross section properties are considerably lower than the section properties that were calculated using the model updating protocols. This is related to the fact that the engineers who had inspected and load rated the Little Mystic Span calculated the moment of inertia based upon the net effective section of the member in tension. While this is an acceptable assumption for tension members that never actually experience compression, the diagonals undergo both compression and tension and this assumption could potentially be overly conservative from a bridge management standpoint. Additionally, traditional load ratings are performed on an elemental basis. This basis typically does not allow for redistribution of loads as stiffnesses are reduced. However, in a performance-based model such as is being proposed, the structure could be rated as a system rather than the weakest of its components.

Table 4-2: Comparison of Section Properties

Member	From This Work Inspected Properties		Measured Inspected Properties
	Area	Moment of Inertia about Local Axis 2 (X)	Moment of Inertia about Local Axis 2 (X)
L4F-L5F	172.00	18799	16217
L5F-L6F	169.38	18513	16217

L5-L6	171.38	18731	16217
L6F-L7F	171.82	18779	16217
U5F-L5F	44.15	29131	956
L6F-U6F	26.44	17935	1246
U5F-L6F	31.32	2787	1524
L6F-U7F	31.88	2837	1524

Chapter 5: Conclusions/Future Work

5.1 – Conclusions

During this research, the Little Mystic Span of the Tobin Bridge was instrumented, load tested, and modeled. During previous work the model was verified and calibrated to match the collected data from a load test. This research applied additional modifications to the structural model that attempted to increase the accuracy of the model by incorporating updated section properties that were calculated based on the data collected during bridge inspections. The model, in general, more closely matched the data collected from the load test. While the changes that the model updater had made to the model are quite small, this relates more to the good condition of the structure than to any deficiencies in the model updating routines. It may seem that this procedure requires significant additional effort in order to complete. However, the methods in this research are not recommended to be used for all bridges. Signature span bridges are not designed or load rated through the use of AASHTO's approximate methods. In general, they already have some sort of computer model. If a model does not exist, analytical models can be quickly produced and prepared for analysis (Sanayei, Pheifer, Brenner, Bell, & Allen, 2010). Furthermore, most of the other steps in the process are already performed to some degree.

This protocol could also be used to evaluate construction loading conditions. This could have been used to evaluate the impact of additional loads that were placed on the I-35W Bridge in Minnesota while considering the actual section properties of the degraded members. (National Transportation Safety Board, 2008)

5.2 – Future Work

There is significant work that can be performed on this project. During the summer of 2010, a proposal was written for the instrumentation of the Big Mystic. The involve using significantly more sensors that are currently on the Little Mystic Span. Additionally, there were decisions made during the Little Mystic Span instrumentation that cause significant problems when trying to maintain the system. For example because the high speed data connection is located in the middle of the span, traffic must be diverted in order to service the instrumentation system. This has shown to be quite bothersome in the past few months because the computer system for the low speed data collection has become non-responsive, and the research team cannot reach the computer to fix it.

5.2.1 Improved Joint Analysis

In previous work, it was determined that the joints in the truss are not actually pinned connections but rather fully fixed. While this may be correct for some of the members, it may not be entirely true for all of the members. For instance, the chord members of the truss were shipped to the bridge site in lengths between 65 and 78 feet. Given that the panels are roughly 35 feet apart, the chord members cannot be anything but fixed joints. However, the members that frame into the chords, specifically the floor beams and the verticals may not be fully fixed. Further exploration would be required in order to determine the rotational fixity of each type of joint. This type of research could be combined with previous research by others to determine the rotational fixity of individual members.

5.2.1 Improved Acceptance Criteria

As previously mentioned, the objective function is a good tool that can be used to determine if one finite element model is more accurate than an updated finite element model. Its use is widely applicable when moving from an initial baseline model to a more exact model. However, when moving from a calibrated structural model to an inspected structural model, the changes are not done on a global basis that so many model updating procedures take. Each element is semi automatically updated individually.

5.3 – The Future of Bridge Condition Assessment

The future of bridge condition assessment will include smart sensing technology, self-diagnosing structural members and self-healing structural materials. However, through the use of integrated approaches that leverage the value of both visual inspection and advanced analysis tools, the process will certainly increase in speed. Due to the increasing omnipresence of computers, tablets, and smartphones, paper reporting and data collection should be retired as a means of record keeping. Companies such as Inspentech currently supplies software for the collection of condition data, element photos, and historic inspection reports. Additionally, the software aids in the creation of inspection reports but, there is currently no way to extract the information from the software as input to a structural analysis program for three dimensional system based analytical assessment of structural performance. Further integration will allow the bridge inspectors one more area where they can take a “hands off” approach to evaluation. The contribution of this work serves as a proof of concept to demonstrate the value that inspection data can add to structural modeling as well as a platform to develop future links

between inspection data and 3D modeling for analysis, visualization, and decision making.

Further research can lead to much more automation and speed.

5.4 – The Future of Bridge Modeling

Further research should be performed in the area of location based deterioration and analysis. A study was performed in order to evaluate the potential effect that current industry accepted practices have on the response of the bridge. Currently, it is standard practice to degrade the entirety of the structural member based upon areas of localized degradation (TranSystems, 2008). For instance, if a truss member has significant cross sectional area losses near one end, the entire member is analyzed as if that same cross sectional loss were present along the whole length. Based upon a preliminary sensitivity study, this assumption could quite conservative. As shown in Figure 5-1, an influence line for strain at a midspan bottom chord member, the partially degraded member actually has a higher strain value than the member. This result is in direct contradiction to the industry accepted assumption.

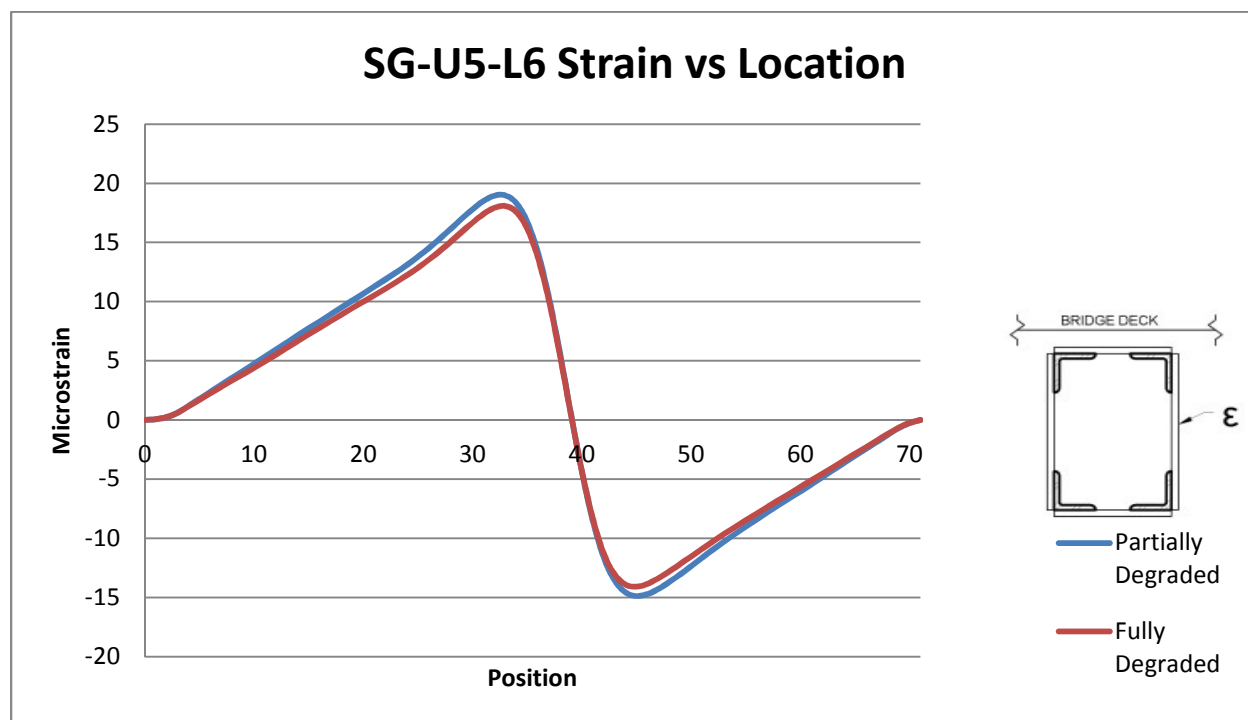


Figure 5-1: Effects of Localizing Deterioration

In this study, the SRF model of the Little Mystic Span was updated to include the inspection report data only for member U5-L6. This diagonal member was subdivided into four equal length sections, see Figure 5-2. In the first portion of this study, each of the four sections of the member had the section properties reduced before structural analysis was performed. In the second half of the study, only one section was given reduced cross sectional areas. The results of this analysis are shown in Figure 5-1. Analysis of this data has shown that when this more conservative approach is used, results were more than 19% higher than when localized deterioration was used.

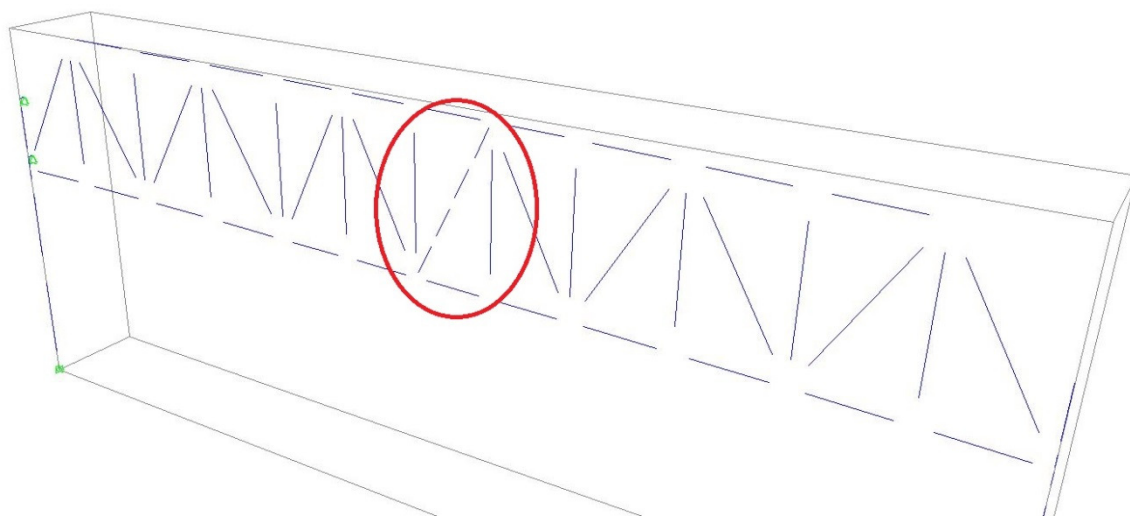


Figure 5-2: Subdivided Member U5-L6

Further investigation of this approach would be needed to determine all of the effects that this procedure has on the results of the structural analysis, however the initial results show that there could be significant impact if a more accurate methodology were used for the application of deterioration in finite element models. The proposed changes are not exceedingly difficult to implement. Considering the level of detail that bridge inspectors already utilize when developing field notes, it would not be difficult for the engineer performing the analysis to

apply this deterioration across the appropriate length of the member. Given that the large disparity between the current practice and the damage localization procedure, this could have a large impact on condition assessment.

5.5 – The Future of Bridge Management

Another area for improvement lies in permitting and construction loading. A major contribution to the failure of the I35W Bridge in Minneapolis, Minnesota was the high levels of construction load that was in place at the time of failure (National Transportation Safety Board, 2008). The asymmetric loading conditions that were present at the time of the collapse would have been quite simple to model using any number of finite element analysis packages. If an up-to-date, calibrated model had been available to quickly analyze the construction loading conditions, the tragic situation may have been avoided. Similarly, the I-5 Bridge in Skaggit, Washington was hit multiple times before it failed. (Baker, 2013). If these protocols were available to analyze the whole bridge, questions could have been asked as to what would happen if the bridge were struck again.

Finally, a move could be made from an elemental based load rating to a more performance based, system wide load rating. The proposed procedure, as mentioned earlier and noted again in Figure 5-3, uses finite element modeling to analyze the bridge and to develop the load rating. A system wide load rating is capable of capturing the actual capacity of the bridge rather than simply the capacity of the weakest element. This procedure has previously been carried out for the Powder Mill Bridge in Ware, Massachusetts. Using this procedure, researchers were able to

increase the load rating factor significantly compared to the use of the Load and Resistance Factor Rating as prescribed by the Manual for Bridge Evaluation, see Figure 5-4.

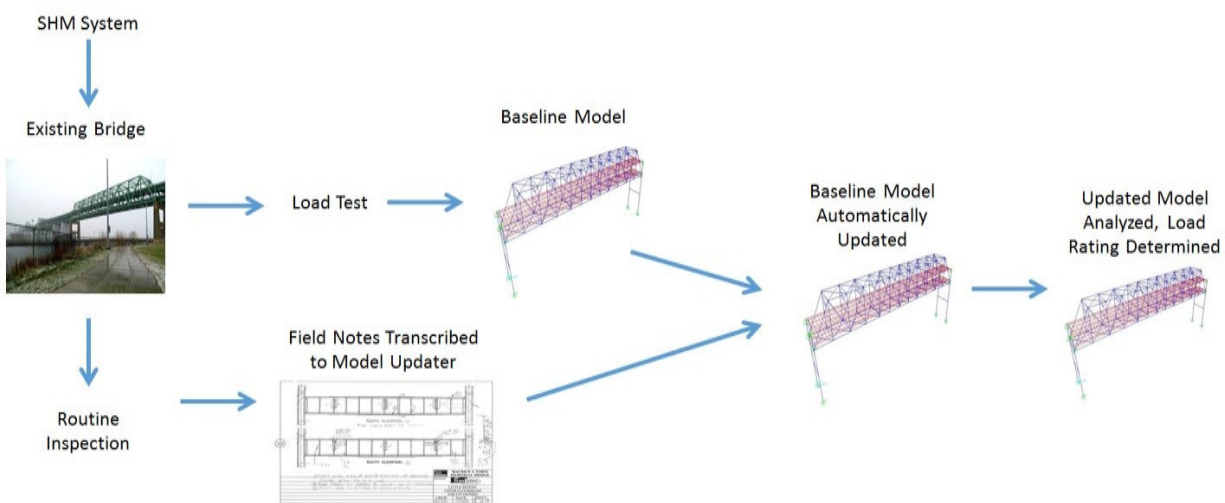


Figure 5-3: Element Based Model Updating and Load Rating Flowchart

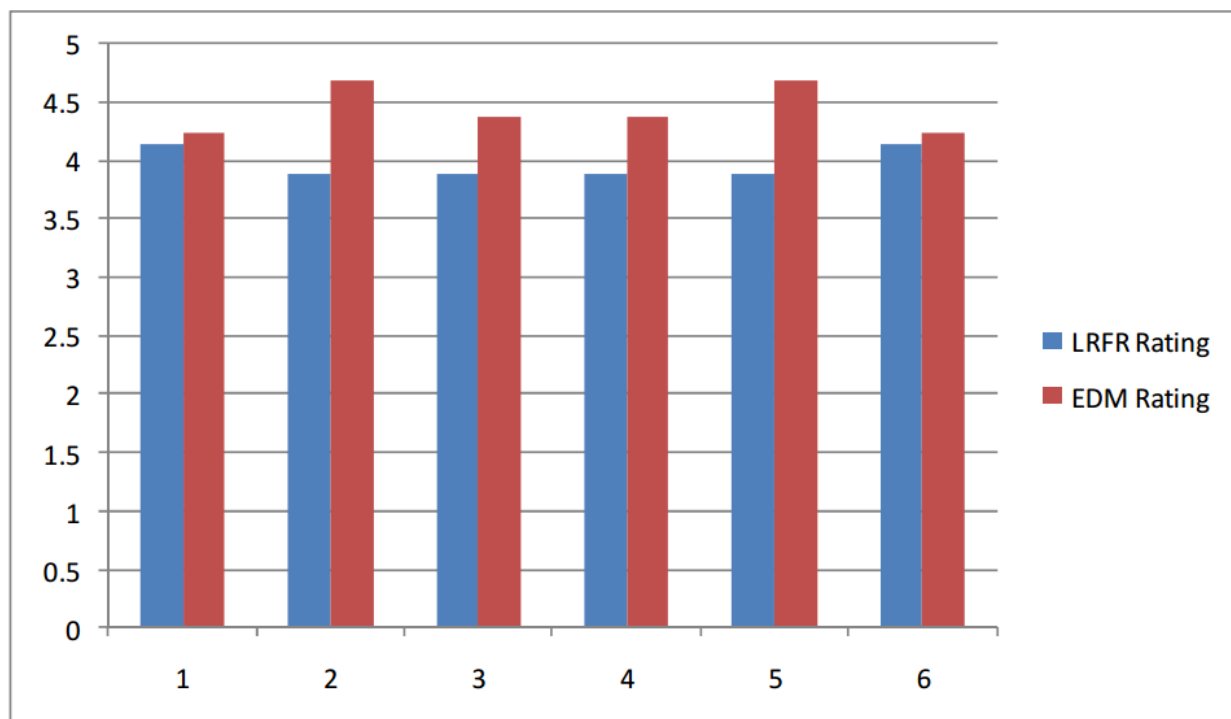


Figure 5-4: Comparison of LRFR and EDM Inventory Factors for Girders 1 through 6 (LeFebvre, 2010)

References

- AASHTO. (2004). LRFD Bridge Design Specifications Third Edition. *14.5 Bridge Joints*, pp. 14-8.
- AASHTO. (2008). *Bridging the Gap - Restoring and Rebuilding the Nation's Bridges*.
- AASHTO. (2011). *The Manual for Bridge Evaluation*. Washington, DC: American Association of State Highway and Transportation Officials.
- American Society of Civil Engineering. (2013). *2013 Report Card for America's Infrastructure*. Reston, VA: ASCE.
- ASCENH. (2011). *New Hampshire's Infrastructure Report Card*. Manchester, NH: ASCENH.
- Baker, M. (2013, 06 20). *Wash. DOT didn't flag caution on I-5 span*. Retrieved 04 19, 2014, from Seattle Times:
http://seattletimes.com/html/localnews/2021230837_apusbridgecollapsecaution.html
- Barrish, R. A., Grimmelsman, K. A., & Aktan, A. E. (2000, 06). Instrumented Monitoring of The Commodore Barry Bridge. *Society of Photo-optical Instrumentation Engineers*, 3995, 112-126.
- Bell, E. S., & Sipple, J. (2009). *In-Service Performance Monitoring of a CRFP Reinforced HPC Bridge Deck*. Concord, NH: New Hampshire Department of Transportation.
- Bell, E. S., Sanayei, M., Javdekar, C. N., & Slavsky, E. (2007). Multiresponse Parameter Estimation for Finite-Element Model Updating Using Nondestructive Test Data. *Journal of Structural Engineering - ASCE*, 1067-1079.
- Bowman, M. M. (2002). *Load Testing of the Carbon FRP Grid Reinforced Concrete Bridge Deck on the Rollins Road Bridge, Rollinsford, New Hampshire*. Durham, NH: University of New Hampshire.
- Branco, F. A., & Mendes, P. A. (1993). Thermal Actions for Concrete Bridge Design. *Journal of Structural Engineering*, 119(8), 2313 -2331.
- Brownjohn, J. M., Moyo, P., Omenzetter, P., & Chakraborty, S. (2005). Lessons from monitoring the performance of highway bridges. *Structural Control and Health Monitoring*, 12:227-244.
- Chensiyuan. *Tobin Bridge Mystic River Boston*. Boston, MA.
- Chung, W., & Sotelino, E. (2006). Three-Dimensional Finite Element Modeling of Composite Bridge Girders. *Engineering Structures*, 63-71.
- Computer Structures, Inc. (2007, October). CSI Analysis Reference Manual for SAP2000®, ETABS®, and SAFE™. Berkeley, California, USA.
- Dietrich, J. *Commodore Barry Bridge From Ferry Rd*. WikiMedia.
- Farhey, D. N. (2005). Bridge Instrumentation and Monitoring for Structural Diagnostics. *Structural Health Monitoring*, 301-318.
- Farhey, D. N. (2007). Quantitative Assessment and Forecast for Structurally Deficient Bridge Diagnostics. *Structural Health Monitoring*, 39-48.
- Fay, Spoffard, & Thorndike, LLC. (2007). Plan and Profile of Bridge Replacement No. B-02-012.
- Fu, G., Feng, J., & Dekelbab, W. (2003). *NCHRP Report 495 - Effect of Truck Weight on Bridge Network Costs*. Washington, D.C.: Transportation Research Board.
- Garcia-Palencia, A. J., & Santini-Bell, E. (2013). *Structural Model Updating Using Dynamic Data*. University of New Hampshire , Department of Civil Engineering, Durham, NH.

- Garcia-Palencia, A. J., & Santini-Bell, E. (2014). *A Frequency Response Functions-Based Model Updating Algorithm for Condition Assessment of In-Service Bridges*. University of New Hampshire, Department of Civil Engineering. Durham, NH: University of New Hampshire.
- Google. (2013). *Barre, MA*. Retrieved June 16, 2013, from Google Maps:
<https://maps.google.com/?ll=42.43562,-70.894775&spn=3.725538,8.453979&t=m&z=8>
- Grimson, J. L., Commander, B. C., & Ziehl, P. H. (2008). Superload Evaluation of the Bonnet Carre Spillway Bridge. *Journal of Performance of Constructed Facilities - ASCE*, 22(4), 253-263.
- Guan, H., Karbhari, V. M., & Sikorsky, S. C. (2007, August). Long-term Structural Health Monitoring System for a FRP Composite Highway Bridge Structure. *Journal of Intelligent Material Systems and Structures*, Vol. 18, 809-823.
- Hearn, G. (2007). *NCHRP Synthesis 375 - Bridge Inspection Practices*. Washington, D.C.: Transportation Research Board.
- Howell, D. A., & Shenton III, H. W. (2006). System for In-Service Strain Monitoring of Ordinary Bridges. *Journal of Bridge Engineering - Vol. 16, No. 6*, 673-680.
- Jang, S., Li, J., & Spencer, B. F. (2013, July). Corrosion Estimation of a Historic Truss Bridge Using Model Updating. *Journal of Bridge Engineering*, 678-689.
- Karbhari, V. M., Chin, J. W., Hunston, D., Benmokrane, B., Juska, T., Morgan, R., et al. (2003). Durability Gap Analysis for Fiber-Reinforced Polymer Composites in Civil Infrastructure. *Journal of composites for construction*, 7(3), 238-247.
- LeFebvre, P. J. (2010). The Instrumentation, Testing, and Structural Modeling of a Steel Girder Bridge for Long-Term Structural Health Monitoring.
- Leshko, B. J. (2005, October). Revised National Bridge Inspection Standards (NBIS). *STRUCTURE Magazine*.
- Lord, J.-F., Ventura, C. E., & Dascotte, E. (2004). Automated Model Updating Using Ambient Vibration Data from a 48-Story Building in Vancouver.
- Mason County, WV. (n.d.). *The Silver Bridge*. Retrieved 10 30, 2007, from Infamous Bridge Disasters: <http://filebox.vt.edu/users/aschaeff/silver/silver.html>
- MementoMori. *Tobin Bridge in fog and snow*. Boston, MA.
- Microsoft. (2010). Excel Help File Version 14.0.6129.5000. Redmond, WA, USA: Microsoft.
- Moorthy, S., & Roeder, C. W. (1992). Temperature-Dependent Bridge Movements. *Journal of Structural Engineering*, 118(4), 1090-1105.
- National Climatic Data Center. (n.d.). *Snowfall - Average Total in Inches*. Retrieved August 18, 2008, from <http://lwf.ncdc.noaa.gov/oa/climate/online/ccd/snowfall.html>
- National Institute of Standards and Technology. (2009, July 8). <http://www.nist.gov>. Retrieved October 25, 2013, from The Collapse of the Silver Bridge:
<http://museum.nist.gov/exhibits/silverbridge/eyebars.htm>
- National Transportation Safety Board. (1970). *Collapse of U.S. 35 Highway Bridge*. Highway Accident Report, Washington, DC.
- National Transportation Safety Board. (2008). *Collapse of I35W Highway Bridge*. Washington, DC: National Transportation Safety Board.
- NHASCE. (2006). *2006 Report Card for New Hampshire's Infrastructure*. NHASCE.
- NHDOT. (2008, August 5-6). *New Hampshire bridges and related maintenance issues*. Northeast Bridge Preservation Partnership Meeting, Worcester, Massachusetts.

- NHDOT Bureau of Bridge Design. (1999, July). Rollins Road Bridge Over B&M Railroad and Main Street Plans.
- NHDOT Bureau of Bridge Design. (2007). *Bridge Inspection Report - Rollinsford 091/085*. NHDOT.
- Office of Bridge Technology. (2008, August 18). *IBRC - Bridge*. Retrieved from FHWA: <http://www.fhwa.dot.gov/bridge/ibrc/>
- Panduit. (2004). *The Evolution of Copper Cabling Systems from Cat5 to Cat5e to Cat6*. Panduit.
- Peeters, B., & De Roeck, G. (2001). One-year monitoring of the Z24-Bridge: environmental effects versus damage events. *Earthquake Engineering and Structural Dynamics*, 30(2), 149-171.
- Petroski, H. (2007, August 4). Learning from bridge failure. *Los Angeles Times*.
- Phares, B. M., Rolander, D. D., Graybeal, B. A., & Washer, G. A. (2000). Studying the Reliability of Bridge Inspection. *Public Roads*, 64(3).
- Robert-Nicoud, Y., Raphael, B., Burdet, O., & Smith, I. F. (2005). Model Identification of Bridges Using Measurement Data. *Computer-Aided Civil and Infrastructure Engineering*(20), 118-131.
- Rosenstrauch, P. L., Sanayei, M., & Brenner, B. R. (2013, March). Capacity analysis of gusset plate connections using the Whitmore, block shear, global section shear, and finite element methods. *Engineering Structures*, 48, 543-557.
- Salmon, C. G., & Johnson, E. (1996). *Steel Structures: Design and Behavior, Emphasizing Load and Resistance Factor Design* (Fourth Edition ed.). (T. M. Slaughter, Ed.) New York, NY, USA: Harper Collins.
- Sanayei, M., Bell, E. S., Javdekar, C. N., Edelmann, J. L., & Slavsky, E. (2006). Damage Localization and Finite-Element Model Updating Using Multiresponse NDT Data. *ASCE Journal of Bridge Engineering*, 11(6), 688-689.
- Sanayei, M., Imbaro, G. R., McClain, J. A., & Brown, L. C. (1997). Structural Model Updating Using Experimental Static Measurements. *Journal of Structural Engineering*, 792-798.
- Sanayei, M., Pheifer, E., Brenner, B., Bell, E., & Allen, W. M. (2010). *Structural Modeling, Analysis, and Instrumentation of the Maurice J Tobin Memorial Bridge*. Tuft's University.
- Santini-Bell, E., Lefebvre, P. J., Sanayei, M., Brenner, B., Sipple, J. D., & Peddle, J. (2013). Objective Load Rating of a Steel-Girder Bridge Using Structural Modeling and Health Monitoring. *Journal of Structural Engineering*, 1771-1779.
- Santini-Bell, E., Sanayei, M., Brenner, B., Sipple, J., & Blanchard, A. (2008). Nondestructive testing for design verification of Boston's Central Artery underpinning frames and connections. *Bridge Structures - Assessment, Design and Construction*, 4(2), 87-98.
- SAP2000. (2011). Version 15.0.1 Ultimate . Berkely, California, USA: Computer and Structures, Inc.
- Schlune, H., Plos, M., & Gylltoft, K. (2009, March 10). Improved Bridge Evaluation Through Finite Element Model Updating Using Static and Dynamic Measurement. *Engineering Structures*, 1477-1485.
- Sipple, J. (2008, April 26). *2008 Structures Congress Presentation*. Vancouver, BC.
- Stanton, J. F., Roeder, C. W., & Mackenzie-Helnwein, P. (2004). *Rotational Limits for Elastomeric Bearings Appendix F*. Washington: Transportation Research Board.

- Stanton, J. F., Roeder, C. W., Mackenzie-Helnwein, P., White, C., Kuester, C., & Craig, B. (2008). *NCHRP Report 596 - Rotational Limits for Elastomeric Bearings*. Washington, D.C.: Transportation Research Board.
- Structurae. (1999, 11 21). *Commodore Barry Bridge*. Retrieved 03 14, 2014, from International Database for Civil and Structural Engineering:
<http://structurae.net/structures/data/index.cfm?ID=s0000560>
- Taly, N. (1998). *Design of Modern Highway Bridges*. New York: McGraw-Hill.
- The D.S. Brown Company. (2008, October 09). *The D.S. Brown Company Corporate Website*. Retrieved from <http://www.dsbrown.com/>
- TranSystems. (2008). *Tobin Bridge Little Mystic Span Rerating*. Boston: TranSystems.
- U.S. Department of Transportation. (2006). *2006 Status of the Nation's Highways, Bridges, and Transit - Conditions and Performance*.
- Wilhelm Ernst & Sohn Verlag. (2014, 7 29). *Tobin Memorial Bridge*. Retrieved 8 3, 2014, from Structurae: <http://structurae.net/structures/tobin-memorial-bridge>
- Zhang, Z., & Aktan, A. E. (1997). Different Levels of Modeling for the Purpose of Bridge Evaluation. *Applied Acoustics*, 189-204.

Appendices

Appendix 1 User's Guide.....	94
Appendix 2: Sensor Data Sheets	96
Appendix 3: Additional Strain vs Time Graphs	104
Appendix 4: VBA Routines	123

Appendix 1 User's Guide

User's Guide Table of Contents

A1.1 – Introduction	94
A1.2 - Model Setup	94
A1.3 - Spreadsheet Setup	95
A1.4 – Execution	95
A1.5 - Post Processing.....	96

A1.1 – Introduction

This guide is intended to provide instructions to users of the model updating software as well as all the accompanying routines that aid in the model updating procedure. There are several caveats to using the model updater. First is that the names of the members that are to be updated must be known. This might not seem like a large caveat, however, this proof of concept was performed by updating just 90 frame elements. Considering that finite element models can easily have thousands of elements, the problem can quickly become out of hand. This problem was solved in the case study by using the member names that were assigned during the design phase.

Additionally, the software is only designed to update frame elements. The user can, at his or her discretion, modify the code in order to update other types of elements, but this research only focused on frame elements.

A1.2 - Model Setup

The model updating software requires little initial setup. As previously mentioned, the names of the members that will be updated must be known. Additionally, all of the members should have

the same section properties. This may sound counter intuitive, but the members achieve different calculated section properties by using property modifiers. This is done in order to ease the calculations performed by the VBA routines. Additionally, updating frame section properties is a much more complicated task to program.

A1.3 - Spreadsheet Setup

When setting up the spreadsheets, the first task is to select the “Inspection_Data” worksheet. This is the location where the members that have been inspected will be noted. The names of the members are required to be placed starting in cell B5. The member’s geometry can be input in column C. Although the “Geometry” column is not required to be used, it can aid in organizing the calculations. The geometry column is intended to indicate the general shape of the member, box, wide flange, channel, etc.

Finally, the estimated cross sectional area of the inspected member should be placed in column D. This number is not the original cross sectional area, but the effective cross section after taking losses such as rust or other corrosion.

A1.4 – Execution

After the model and the spreadsheets have been setup, the next step is to execute the updating routine. This is as simple as clicking the “Execute” button and selecting the model that the user will be updating.

A1.5 - Post Processing

As there is no structural being performed on the model, post processing is minimal, though the user is encouraged to check the section properties after they have been updated.

Appendix 2: Sensor Data Sheets

This section contains technical data sheets for the sensors installed on the Little Mystic Span. Sensors include (in order of spec sheet):

- Single Strain Gauge, Omega Engineering: # KFG-5-350-C1-11L3M3R
- Strain Gauge Rosette, Omega Engineering: # KFG-5-350-D17-11L3M3S
- Tiltmeter, Digikey: # 551-1018 ND
- Accelerometer, Dytran: # 7523A1
- Thermistor: Geokon: # 3800

PRECISION STRAIN GAGE

PRE-WIRED STRAIN GAGES



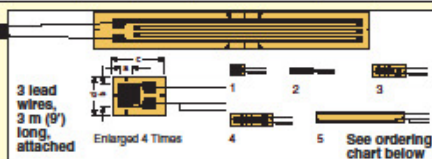
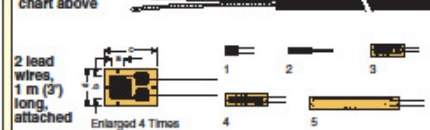
MOST POPULAR MODELS HIGHLIGHTED!

To Order (Specify Model Number)

ENCAPSULATED WITH 2 LEAD WIRES, 1 m (3') LONG, ATTACHED

MODEL NO.	PRICE PER PKG OF 10	NOM. RESIS- TANCE (Ω)	DIMENSIONS mm (in) [†]				MAX V (V _{rms})	TERMINATION	TEMP COMP.	FIG.
			GRID		CARRIER					
			A	B	C	D				
KFG-02-120-C1-11 L1 M2R	\$140	120	0.2 (0.008)	1.3 (0.051)	3.3 (0.13)	2.4 (0.094)	1	2 wire	STE	1
KFG-1N-120-C1-11L1M2R	109	120	1.0 (0.039)	0.7 (0.028)	4.2 (0.17)	1.4 (0.055)	1.5	2 wire	STE	2
KFG-2N-120-C1-11L1M2R	94	120	2.0 (0.079)	0.9 (0.035)	5.3 (0.21)	1.4 (0.055)	2	2 wire	STE	2
KFG-3-120-C1-11L1M2R	88	120	3.0 (0.12)	1.3 (0.051)	7.4 (0.29)	2.8 (0.11)	4	2 wire	STE	3
KFG-3-350-C1-11L1M2R	121	350	3.0 (0.12)	1.3 (0.051)	7.4 (0.29)	2.8 (0.11)	15	2 wire	STE	3
KFG-5-120-C1-11L1M2R	80	120	5.0 (0.2)	1.4 (0.055)	9.4 (0.37)	2.8 (0.11)	8	2 wire	STE	3
KFG-5-350-C1-11L1M2R	124	350	5.0 (0.2)	1.4 (0.055)	9.4 (0.37)	2.8 (0.11)	20	2 wire	STE	4
KFG-10-120-C1-11L1M2R	100	120	10.0 (0.39)	3.0 (0.12)	16.0 (0.63)	5.2 (0.2)	15	2 wire	STE	4
KFG-30-120-C1-11 L1M2R	119	120	30.0 (1.18)	3.3 (0.13)	37.0 (1.46)	5.2 (0.2)	25	2 wire	STE	5

See ordering chart above



MOST POPULAR MODELS HIGHLIGHTED!

To Order (Specify Model Number)

ENCAPSULATED WITH 3 LEAD WIRES, 3 m (9') LONG, ATTACHED

MODEL NO.	PRICE PER PKG OF 10	NOM. RESIS- TANCE (Ω)	DIMENSIONS mm (in) [†]				MAX V (Vrms)	TERMINATION	TEMP COMP.	FIG.
			GRID		CARRIER					
			A	B	C	D				
KFG-02-120-C1-11L3M3R	\$184	120	0.2 (0.008)	1.3 (0.051)	3.3 (0.13)	2.4 (0.094)	1	3 wire	STE	1
KFG-1N-120-C1-11L3M3R	153	120	1.0 (0.039)	0.7 (0.028)	4.2 (0.17)	1.4 (0.055)	1.5	3 wire	STE	2
KFG-2N-120-C1-11L3M3R	138	120	2.0 (0.079)	0.9 (0.035)	5.3 (0.21)	1.4 (0.055)	2	3 wire	STE	2
KFG-3-120-C1-11L3M3R	131	120	3.0 (0.12)	1.3 (0.051)	7.4 (0.29)	2.8 (0.11)	4	3 wire	STE	3
KFG-3-350-C1-11L3M3R	165	350	3.0 (0.12)	1.3 (0.051)	7.4 (0.29)	2.8 (0.11)	15	3 wire	STE	3
KFG-5-120-C1-11L3M3R	124	120	5.0 (0.2)	1.4 (0.055)	9.4 (0.37)	2.8 (0.11)	8	3 wire	STE	3
KFG-5-350-C1-11L3M3R	165	350	5.0 (0.2)	1.4 (0.055)	9.4 (0.37)	2.8 (0.11)	20	3 wire	STE	4
KFG-10-120-C1-11L3M3R	145	120	10.0 (0.39)	3.0 (0.12)	16.0 (0.63)	5.2 (0.2)	15	3 wire	STE	4
KFG-30-120-C1-11L3M3R	163	120	30.0 (1.18)	3.3 (0.13)	37.0 (1.46)	5.2 (0.2)	25	3 wire	STE	5

DISCOUNT SCHEDULE	
1 to 10 pkgs	Net
11 to 24 pkgs	.5%
25 to 49 pkgs	.10%
50 and up and OEM	Consult Factory

[†] For dimensions key, see page E-18. Note: For strain gage accessories see pages E-56 to E-59.
Ordering Example: KFG-02-120-C1-11L1M2R, package of 10 pre-wired strain gages, encapsulated with 2 lead wires attached, \$140.



PRECISION STRAIN GAGE PRE-WIRED, STACKED (ROUND CARRIER) RECTANGULAR ROSETTE

KFG Series

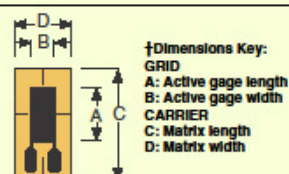
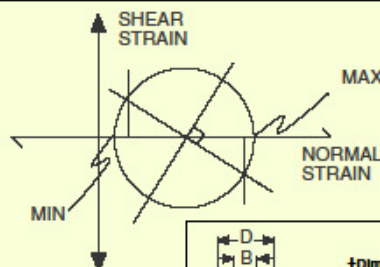
Starts at
\$286
Pkg/10

Rosettes are used to compute the state of stress at a particular point. The plotted results will form a Mohr circle, which gives the value and orientation of principal strains.

Termination

2 Wire: 2 lead wires, 1 m (3') attached
3 Wire: 3 lead wires, 3 m (9') attached
(minimize lead wire resistance effects)

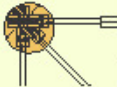

Temperature Compensation
STE Steel 10.8 ppm/C



Custom-Designed
Strain Gages
Available!
No Minimum Order.
Consult Engineering.

☐ MOST POPULAR MODELS HIGHLIGHTED!

To Order (Specify Model Number)

		MODEL NO.	PRICE PER PKG OF 10	NOM. RESIS- TANCE (Ω)	DIMENSIONS mm (in) ¹				MAX PERMITTED BRIDGE ENERGIZING VOLTAGE (Vrms)	TERMINATION	TEMP COMP.
					GRID		CARRIER				
					A	B	C	D			
0°/45°/90° ENCAPSULATED WITH 2 LEAD WIRES 1 m (3') LONG—MATCHED TO STEEL											
	KFG-1-120-D17-11L1M2S	\$389	120	1.0 (0.039)	1.2 (0.047)	5.0 (0.2)	—	1.5	2 Wire	STE	
	KFG-2-120-D17-11L1M2S	286	120	2.0 (0.079)	1.3 (0.051)	8.0 (0.31)	—	2	2 Wire	STE	
	KFG-3-120-D17-11L1M2S	286	120	3.0 (0.12)	1.3 (0.051)	10.0 (0.39)	—	4	2 Wire	STE	
	KFG-3-350-D17-11L1M2S	419	350	3.0 (0.12)	1.3 (0.051)	10.0 (0.39)	—	15	2 Wire	STE	
	KFG-5-120-D17-11L1M2S	286	120	5.0 (0.2)	1.4 (0.055)	11.0 (0.43)	—	8	2 Wire	STE	
	KFG-5-350-D17-11L1M2S	419	350	5.0 (0.2)	1.4 (0.055)	11.0 (0.43)	—	20	2 Wire	STE	
0°/45°/90° ENCAPSULATED WITH 3 LEAD WIRES 3 m (9') LONG—MATCHED TO STEEL											
	KFG-1-120-D17-11L3M3S	\$523	120	1.0 (0.039)	1.2 (0.047)	5.0 (0.2)	—	1.5	3 Wire	STE	
	KFG-2-120-D17-11L3M3S	419	120	2.0 (0.079)	1.3 (0.051)	8.0 (0.31)	—	2	3 Wire	STE	
	KFG-3-120-D17-11L3M3S	419	120	3.0 (0.12)	1.3 (0.051)	10.0 (0.39)	—	4	3 Wire	STE	
	KFG-3-350-D17-11L3M3S	549	350	3.0 (0.12)	1.3 (0.051)	10.0 (0.39)	—	15	3 Wire	STE	
	KFG-5-120-D17-11L3M3S	419	120	5.0 (0.2)	1.4 (0.055)	11.0 (0.43)	—	8	3 Wire	STE	
	KFG-5-350-D17-11L3M3S	549	350	5.0 (0.2)	1.4 (0.055)	11.0 (0.43)	—	20	3 Wire	STE	

DISCOUNT SCHEDULE

1 to 10 pkgs	Net
11 to 24 pkgs	5%
25 to 49 pkgs	10%
50 and up and OEM	Consult Factory

Note: For strain gage accessories see pages E-56 to E-59.

Ordering Example: KFG-2-120-D17-11L3M3S, package of 10 pre-wired rosette strain gages, encapsulated with 3 lead wires attached to each element, with temperature characteristics matched to steel, \$419.



SCA121T Series Stand Alone Inclinerometer

Dual Axis Analog Output

FEATURES

- Silicon 3D MEMS sensor
- 0.1° accuracy
- Resolution <0.001°
- Operating temperature range -40...+85°C
- Long term stability <0.02°
- Shock resistance 20 000 g
- Sensing element 3 dB @ 18 Hz
- Main dimensions 30x30x13 mm size, single or dual axis
- Voltage output
- RoHS compatible

BENEFITS

- Excellent long term stability
- Sensing element controlled frequency response
- Outstanding shock durability
- Harsh environment robustness

APPLICATIONS

- Platform tilt measurement
- Equipment and instrument condition monitoring
- Inclination based position measurement
- Rotational orientation measurement

For customised product please contact VTI Technologies

ELECTRICAL CHARACTERISTICS

Parameter	Condition	Min.	Typ	Max.	Units
Supply voltage	Unregulated or regulated electronic	7	16	35	V
Current consumption		4.5	5	5.25	mA
Output load	Resistive	10			kΩ
	Capacitive			20	nF

PERFORMANCE CHARACTERISTICS

Parameter	Condition	SCA121T-D03	SCA121T-D07	SCA121T-D05	Units
Measuring range ¹		±90	±30	±90	°
Supply voltage		7...35	7...35	5±0.25	V
Measuring axis	6-axis (3 inclination)	X/Y	X/Y	X/Y	
Offset A, 1	Output at 0°	2.5	2.5	2.5	V
Offset zero point error ¹⁵	Max. deviation	1	1	1	°
Offset temperature error	0.70°C	±0.2	±0.2	±0.2	°
	-25...85°C	±0.6	±0.6	±0.6	°
Sensitivity		2	4	2	V/g
		35	70	35	mV/g (offset pos.)
Sensitivity temperature error ¹⁶	0.70°C	-0.8...0.3	-0.8...0.3	-0.8...0.3	%
	-25...85°C	-1.5...0.5	-1.5...0.5	-1.5...0.5	%
Nonlinearity	Sine output	N/A	0.1	N/A	°
Frequency response -3 dB ¹⁷		8	18	8	Hz
Cross-axis sensitivity ¹⁸		3	3	3	%

Typical values unless otherwise specified.

Note 1: The measuring range is limited by the sensitivity and offset.

Note 2: Offset specified as Output @ 0°.

Note 3: The frequency response is determined by the sensing element's internal gas damping.

The output has true DC (0 Hz) response.

Note 4: The cross-axis sensitivity determines how much inclination, perpendicular to the measuring axis, couples to the output.

Note 5: For optimum zero point accuracy mounting angle of the part can be adjusted.

MEASURING DIRECTIONS

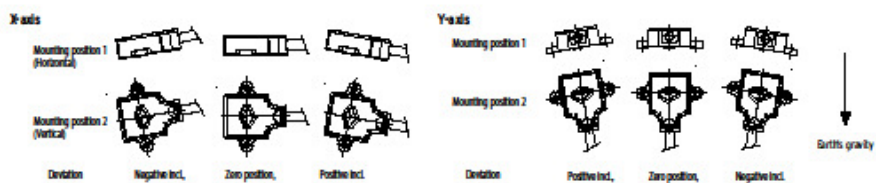


Figure 1. Positions

Notes:

- It is important that the part is parallel to the mounting plane, and that the output equals the zero value when sensor is in zero position.
- Zero position: Please note the picture above which provides information on how the output of the inclinometer behaves in different circumstances when assembled. Please also note that you can rotate the part around the measuring plane for optimum mounting location.

SCA121T Series

ELECTRICAL CONNECTION

SCA121T series

Wire color	Name	Function
Blue	GND	Ground
Red	V _{cc}	Power supply
Yellow	Out X	X-axis output
Green	Out Y	Y-axis output
White		Not connected

MECHANICAL SPECIFICATION

Cable length: 003, 007 30 cm
 005 10 cm
 Total weight: Approx. 60 grams
 Protection class: IP66
 Housing: Zinc casting with passivation

MOUNTING

The sensor module is to be mounted on a flat and smooth surface with 2 screws, dimension M4. Mounting torque 5 ±1 Nm.

SENSOR DIMENSIONS

Dimensions in mm.

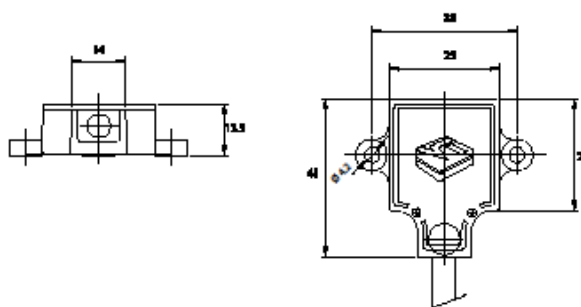


Figure 2.

VOLTAGE TO ANGLE CONVERSION

$$\text{Inclination angle} = \arcsin \left(\frac{V_{\text{out}} - \text{Offset}}{\text{Sensitivity}} \right)$$

where:

V_{out} = analog output [V]

Offset = 25 V_{cc} output at 0° inclination position

Sensitivity = sensitivity of device [V/g]

VTI Technologies Oy
 Myllytieventie 6
 P.O. Box 27
 FI-05021 Vantaa
 Finland
 Tel. +358 9 879 181
 Fax +358 9 879 1890
 sales@vti.fi

VTI Technologies Oy
 Runkkuritien 2
 Reinholdstraße 72-94
 D-65229 Frankfurt am Main
 Germany
 Tel. +49 69 676 786 880
 Fax +49 69 676 882 19
 sales@vti.de

VTI Technologies, Inc.
 One Park Lane Drive
 Suite 104 - East Tower
 Dearborn, MI 48126
 USA
 Tel. +1 313 425 0850
 Fax +1 313 425 0860
 sales@vtitechnologies.com

VTI
 TECHNOLOGIES

PROPRIETARY AND CONFIDENTIAL

THIS DRAWING IS THE PROPERTY OF DYTRAN. IT IS TO BE USED FOR THE PURPOSES SPECIFIED ONLY. IT IS NOT TO BE REPRODUCED OR TRANSMITTED IN ANY FORM OR BY ANY MEANS, ELECTRONIC OR MECHANICAL, WITHOUT PERMISSION OF DYTRAN. THIS DRAWING IS UNCLASSIFIED.

REVISIONS

REV.	ECN	DESCRIPTION	BY/DATE	CHK	APPR
A	5112	INITIAL RELEASE	03/07/02	CES	PML
B	5203	REVISED POLARITY MARKING	05/05/08	RA	DV
C	5630	ADDED X,Y,Z ARROWS	12/01/08	JS	RA-DV

BLACK: GRN
RED: +EXCITATION
GREEN: +SIGNAL X
YELLOW: +SIGNAL Y
BLUE: +SIGNAL Z
WHITE: SELF TEST

WIRING DIAGRAM

7523A1

DC ACCELEROMETER, TRIAXIAL, 2g

MASTER COPY - ONLY IF IN RED

CONTRACT NO.

APPROVALS

APPROVALS	DATE
ORIG PML	10/18/07
CHK CES	03/19/08
APP PML	03/21/08

MATERIAL: ALUMINUM ALLOY

FINISH:

DO NOT SCALE DRAWING

SCALE: 4:1

SHEET 1 of 1



SPECIFICATIONS, SERIES 7523A TRIAXIAL ACCELEROMETER

PERFORMANCE

	A1	A3	A5	UNITS
Input	±2	±1	±50	g
Output, bias, ±20%	2.5	2.5	2.5	V
Output range	±1.1	±1.4	±1.8	V
Bandwidth, X & Y Axes	0-1500	0-1500	0-400	Hz
Z Axis	0-500	0-1500	0-400	Hz
Sensitivity	550	93	36	mV/g
Output Noise, nom.	3	10	40	mGrms
Output Impedance	3500	3500	<500	Ω

PERFORMANCE FOR ALL MODEL NUMBERS (Tc=+25°C)

	MIN	NOM	MAX	UNITS
Maximum Mechanical Shock			4000	g peak
Resonance Frequency		5000		Hz
Transverse Sensitivity			2	%
Operating Temperature	-55		+125	°C
Compensated Temperature Range (CTR)	-20		+70	°C
Thermal Zero in CTR			0.03	% FS/°C
Thermal Sensitivity Drift in CTR			0.02	% FS/°C
Storage Temperature	-55		-150	°C
Non-Linearity			0.3	%
Excitation, regulated	4.8		5.2	VDC
Current consumption		4.5		mA

PHYSICAL PARAMETERS FOR ALL MODEL NUMBERS

Case Material	anodized aluminum			
Cable Length	A1	A3	A5	UNITS
	79	77	79	Inch
Mounting Provision	two M2 screws (provided)			
	MIN	A1	A3	NOM
Case Length				A5
Case Width				0.59
Case Height				0.59
Mounting Hole Spacing		0.30	0.30	0.59
Mass				10
				grams

NOTES:

SUPPLIED ACCESSORIES:

A1 (2) Mounting Screws (Model 6722), M2 x 12 flathead
 A3, A5 (2) Mounting Screws (Model 6914), M2 x 20 flathead



The World Leader in Vibrating Wire Technology™

Model 3800 Thermistor Probe

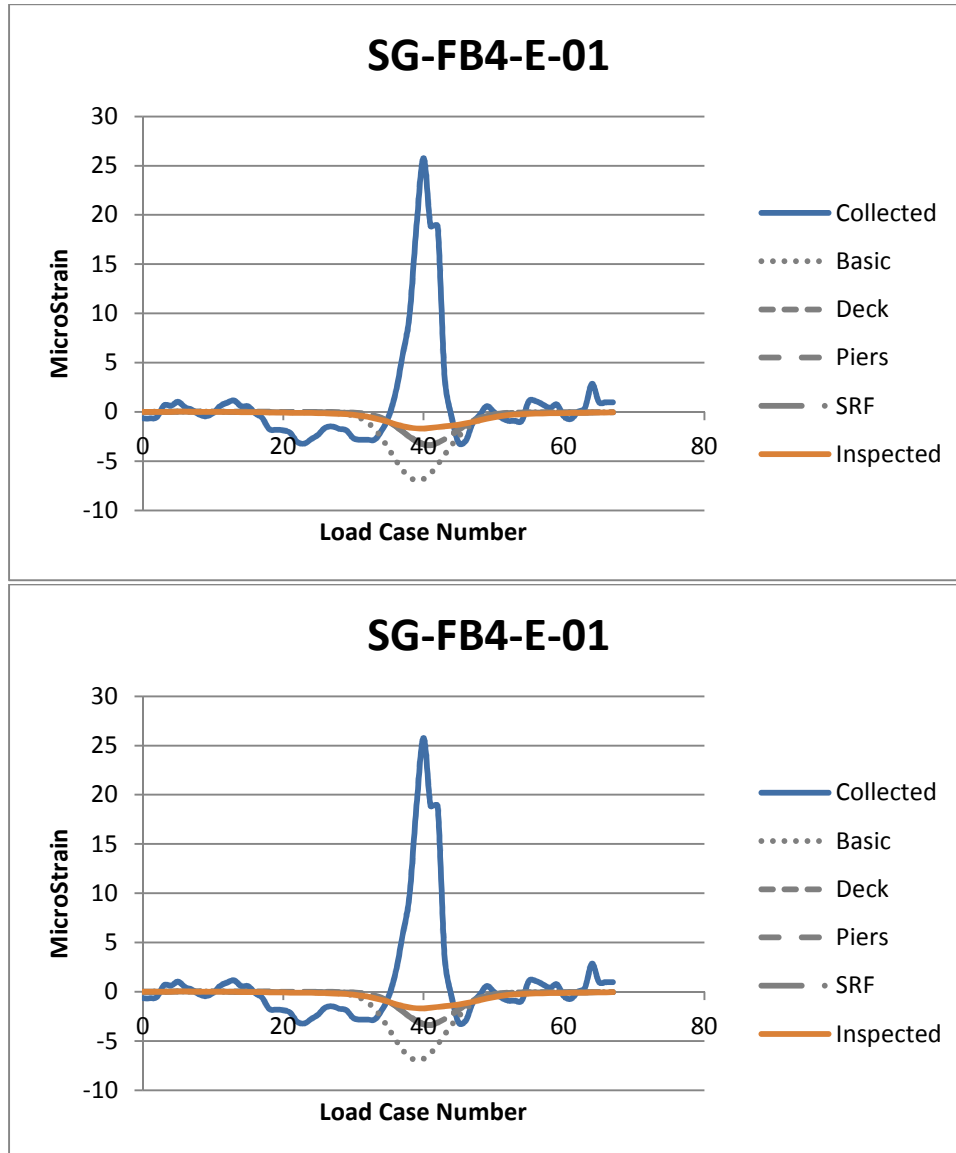


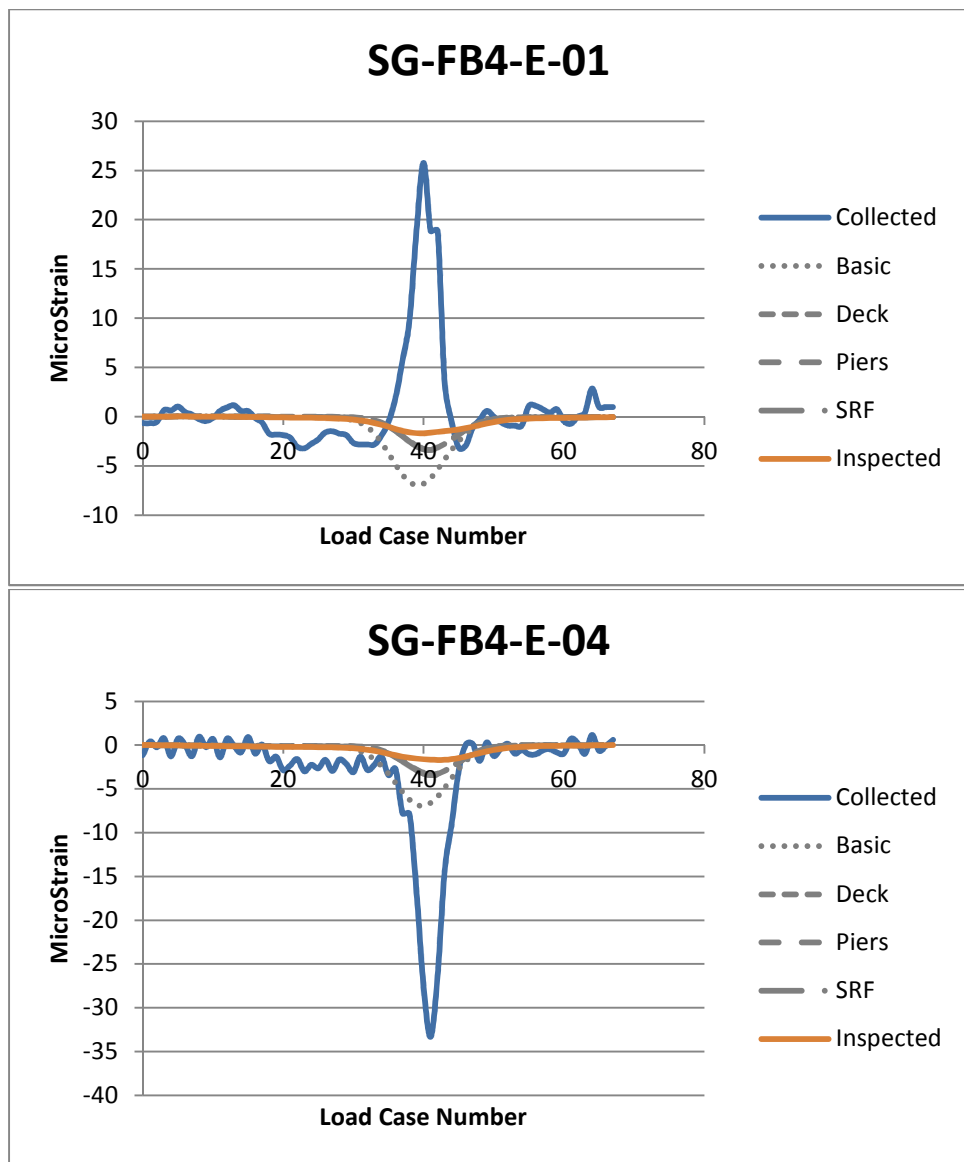
The Model 3800 Thermistor Probe consists of an interchangeable thermistor bead (Model 3800-1-1-1) mounted inside a rugged PVC (Model 3800-1-1) or stainless steel (Model 3800-2-1) housing. They are used for remote readings, such as measuring hydration and cooling temperatures in placement of mass concrete.

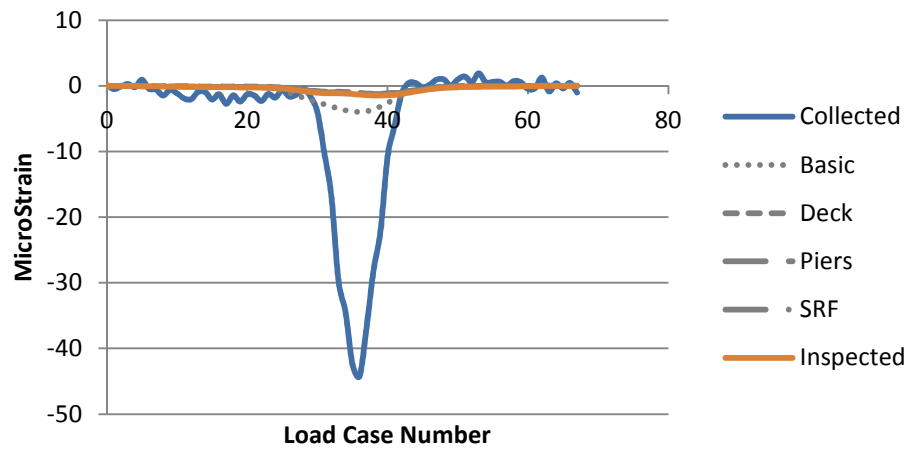
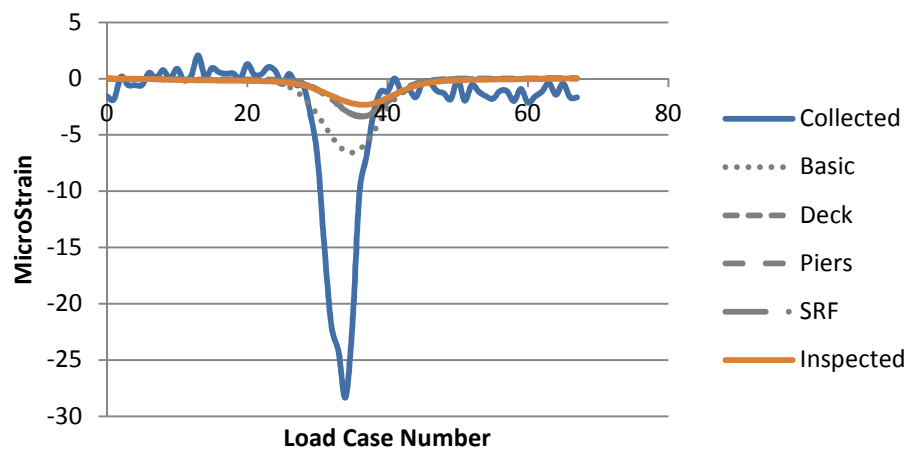
Specifications	3800-1-1	3800-2-1
Standard Range	-50°C to +150°C	-50°C to +150°C
Resolution	0.1°C	0.1°C
Accuracy ¹	±0.5°C	±0.5°C
Temperature Range	-20°C to +80°C	-20°C to +80°C
Length × Diameter	50 × 12 mm	50 × 12 mm

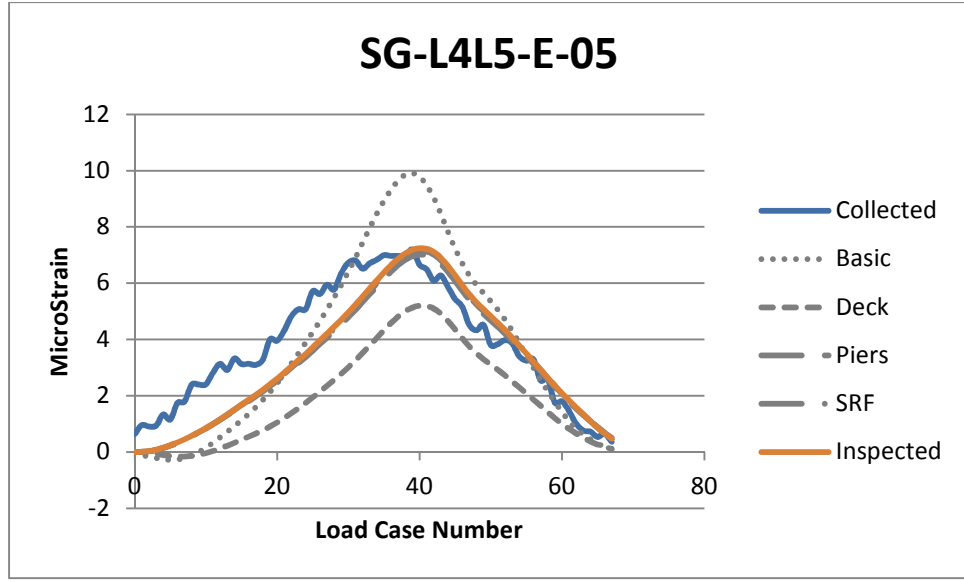
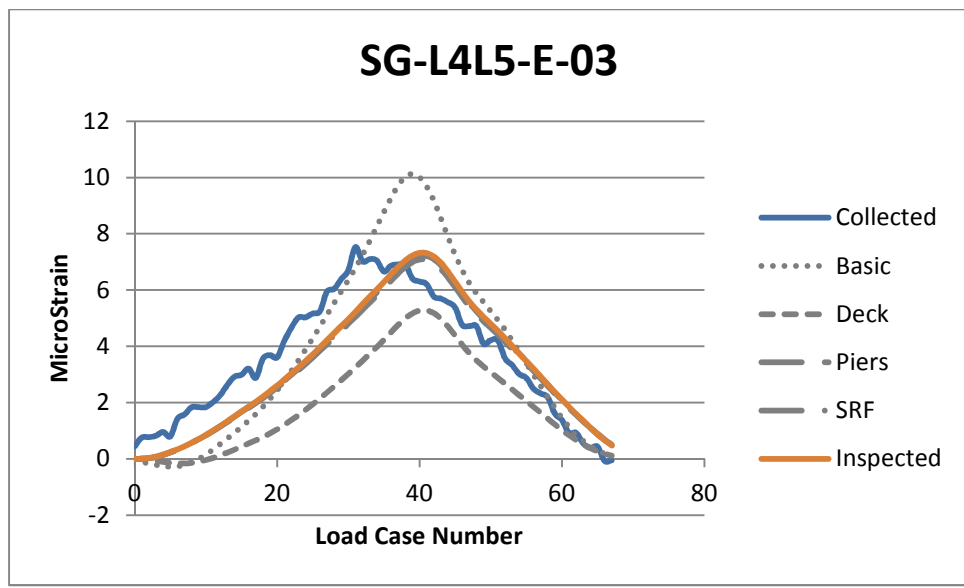
¹Accuracy of ±0.2°C available on request.

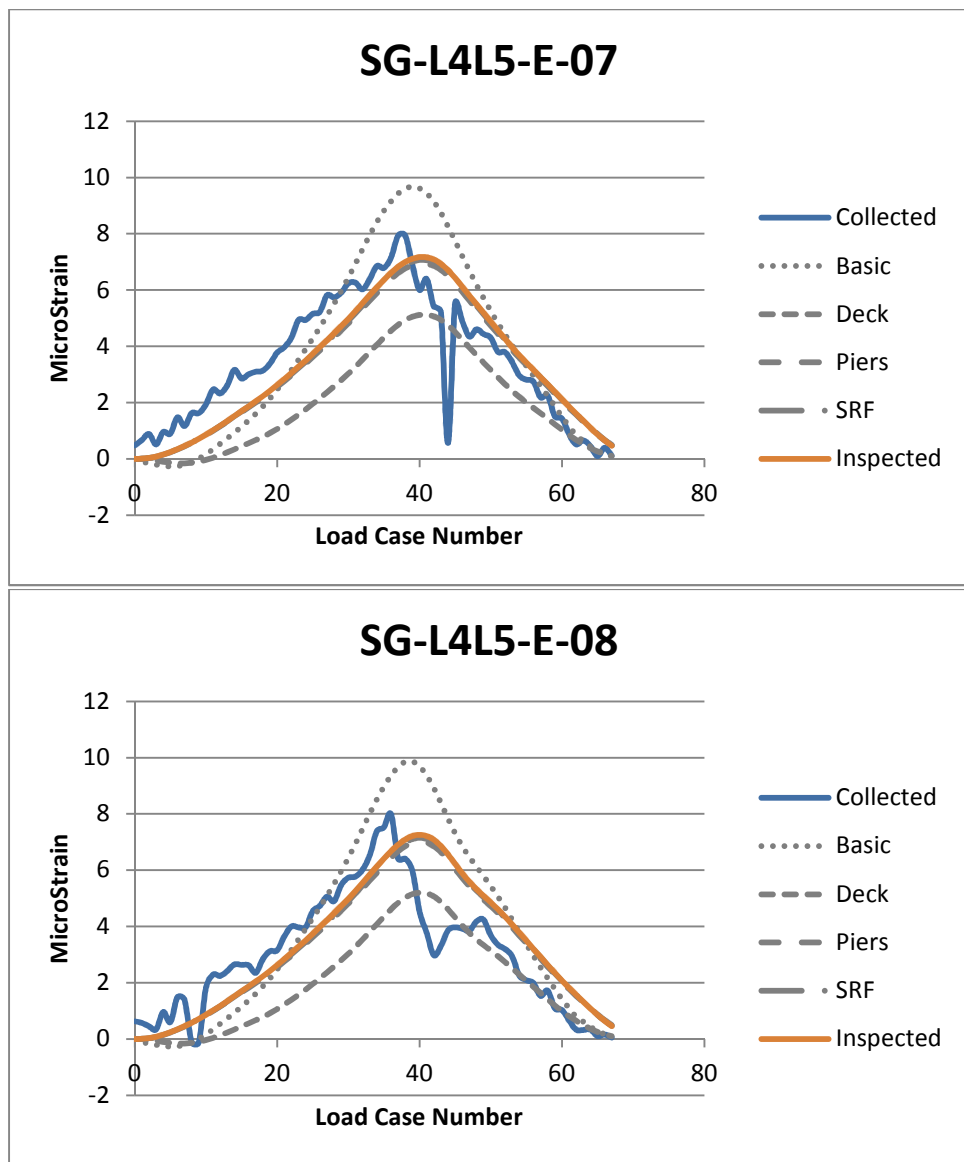
Appendix 3: Additional Strain vs Time Graphs

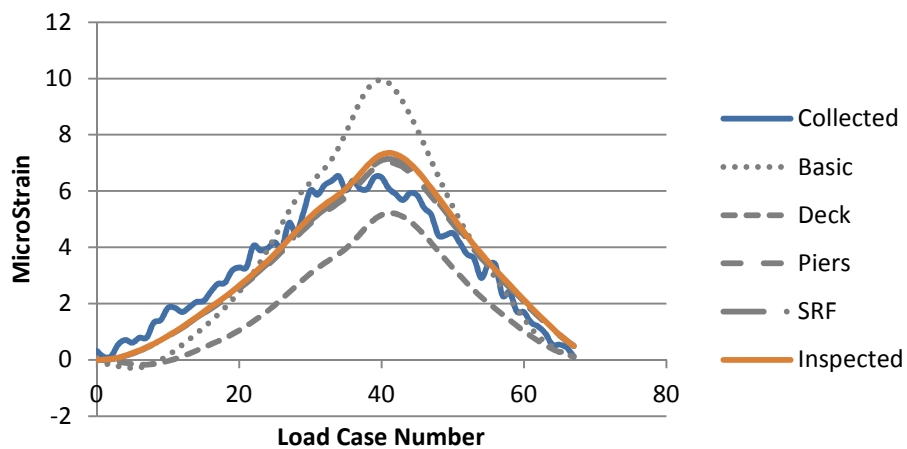
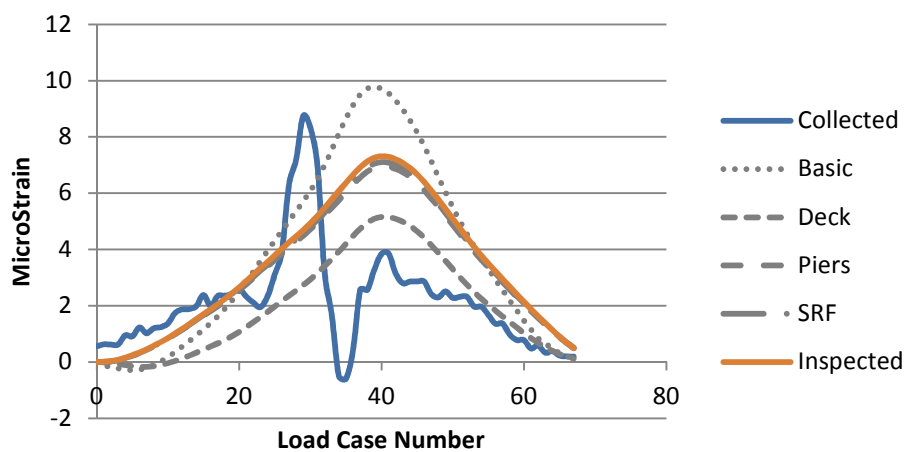


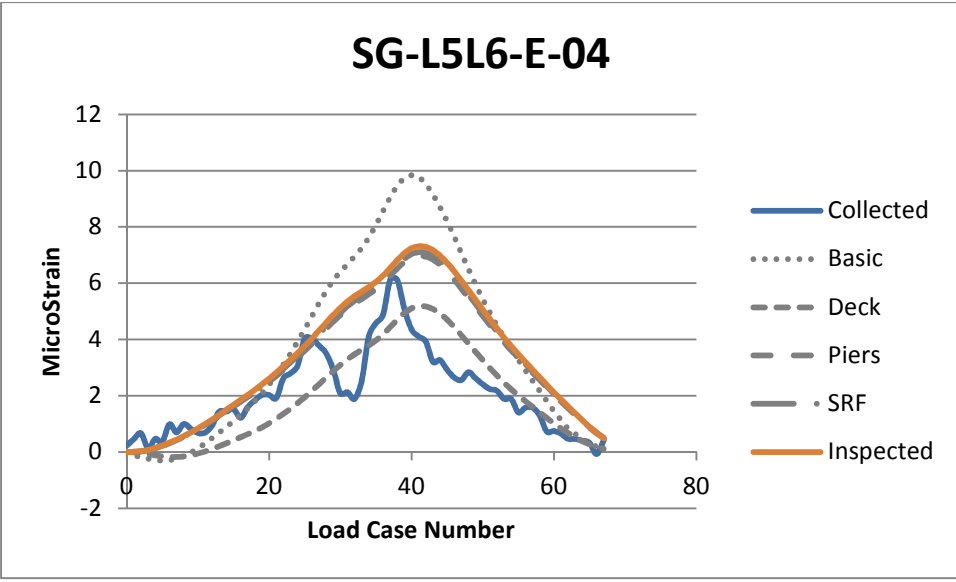
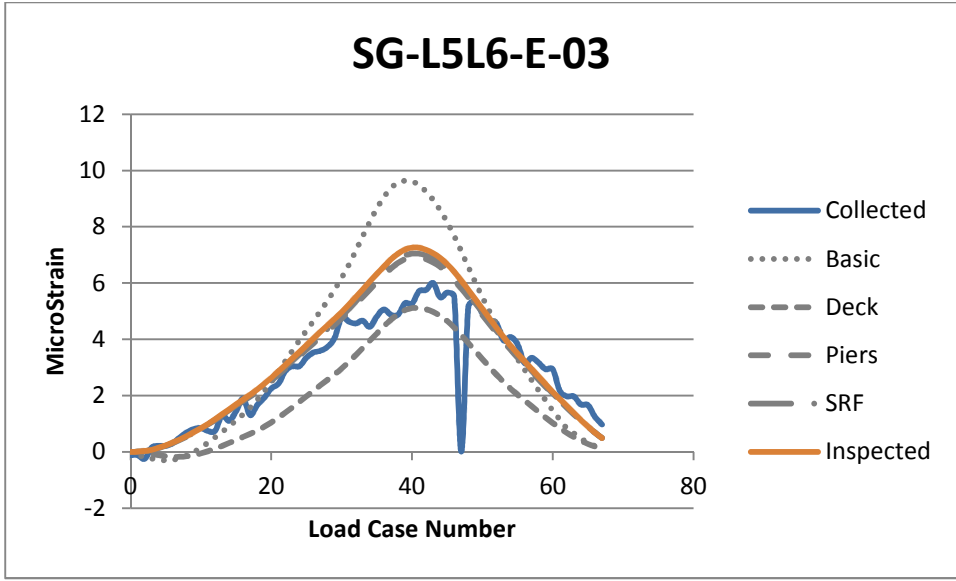


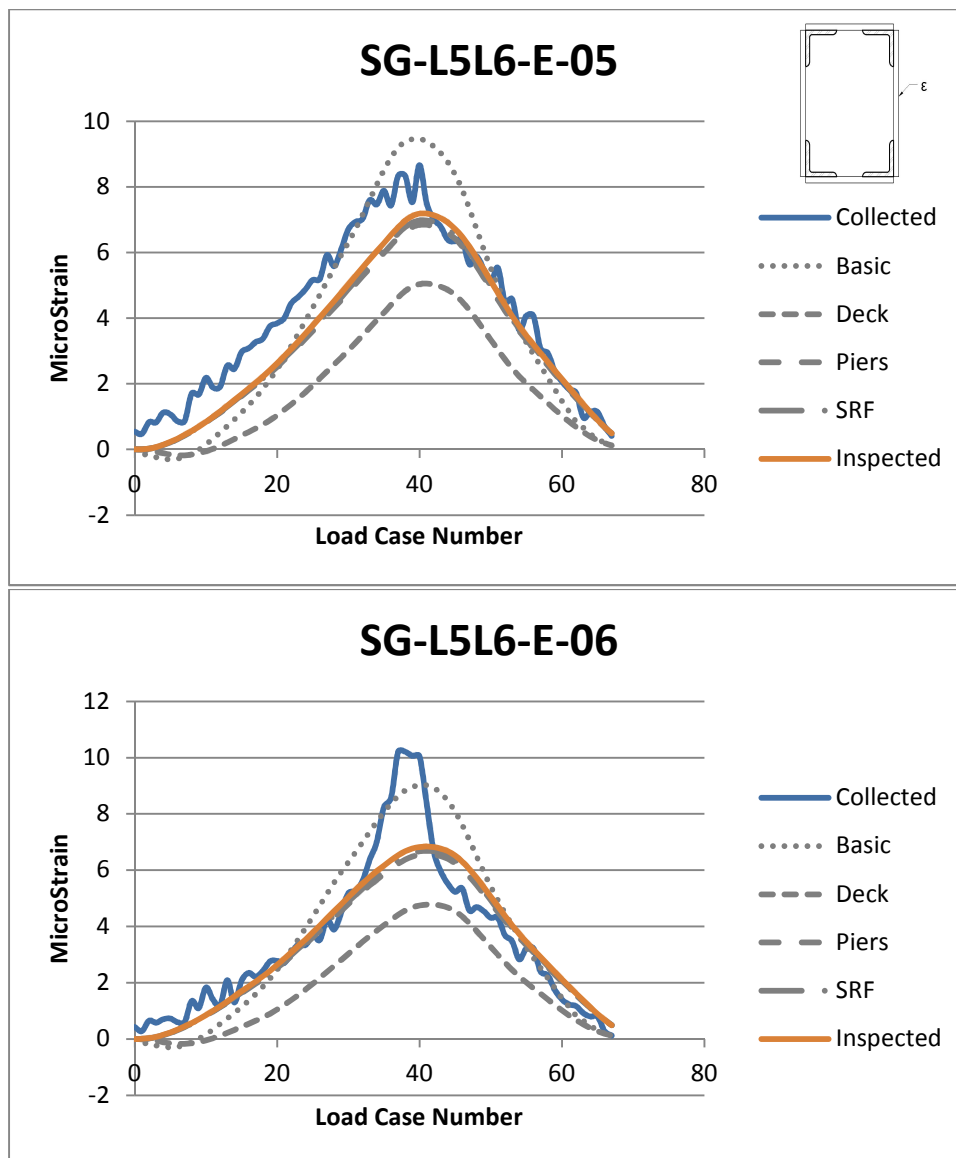
SG-FB5-E-01**SG-FB5-E-02**

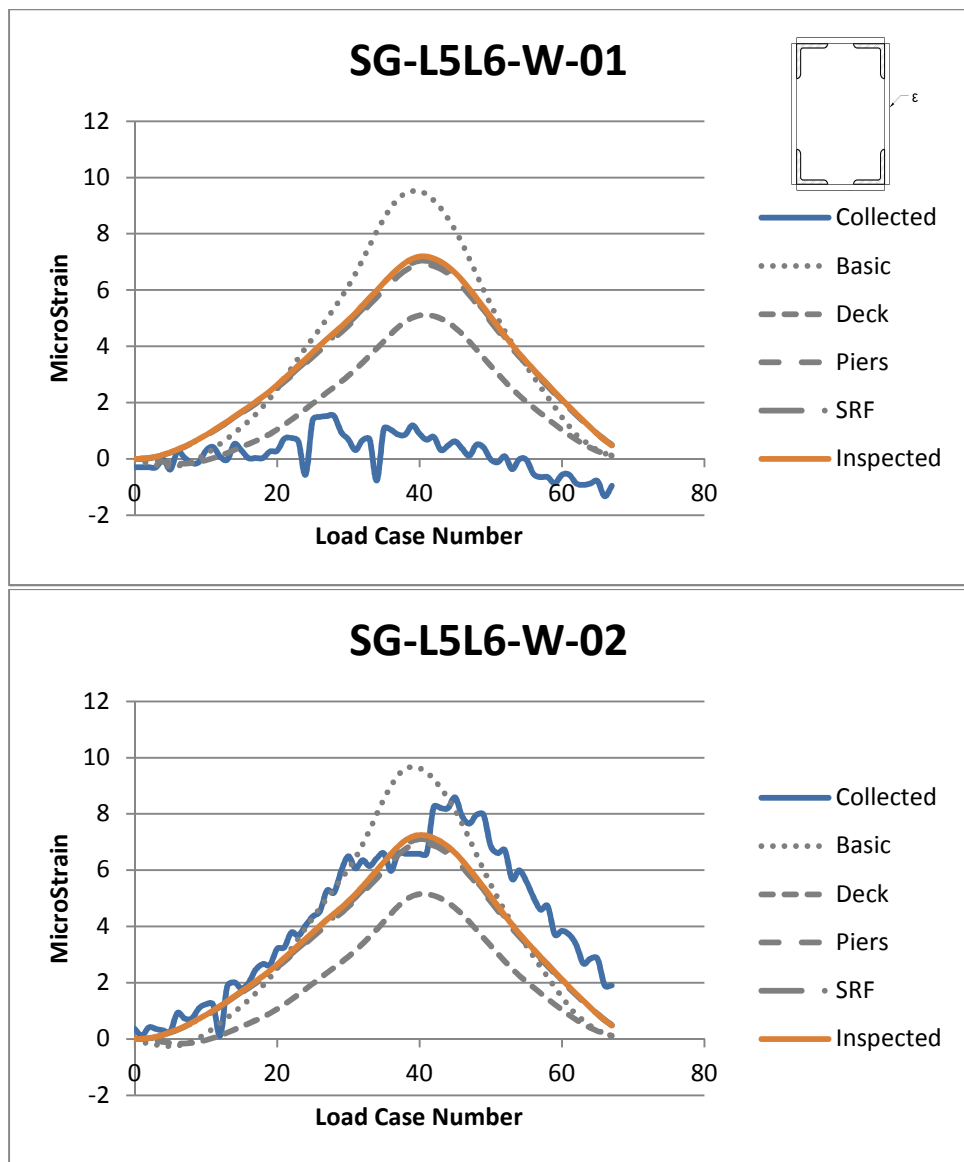


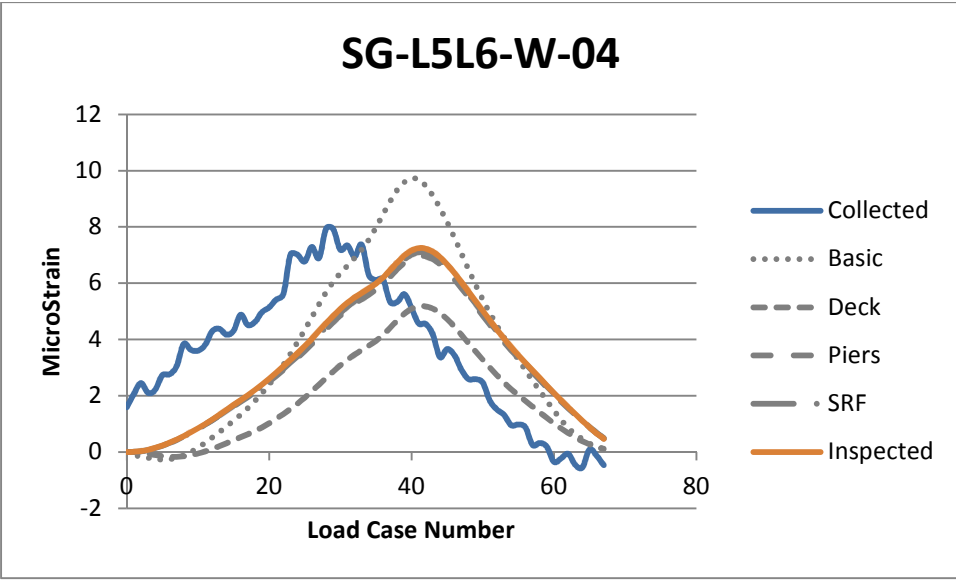
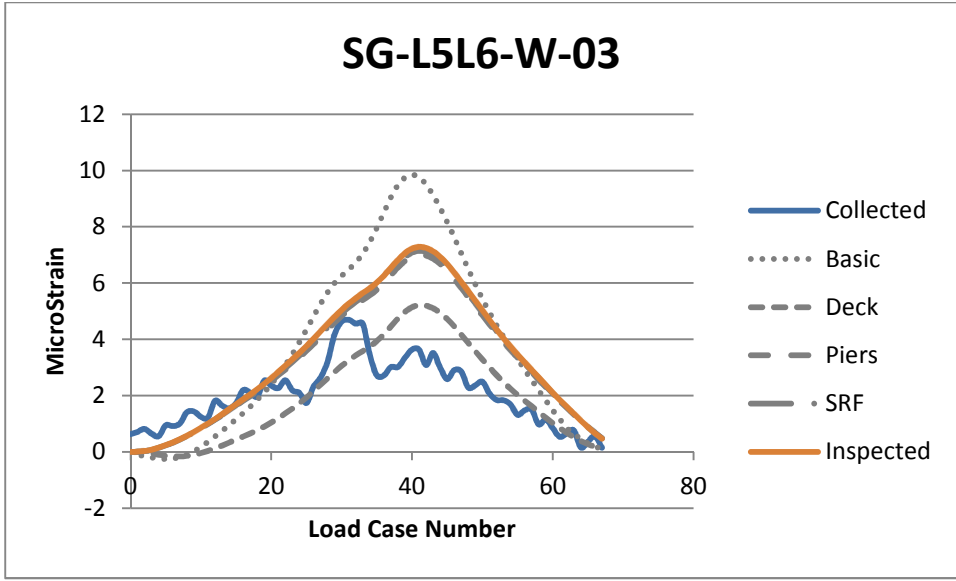


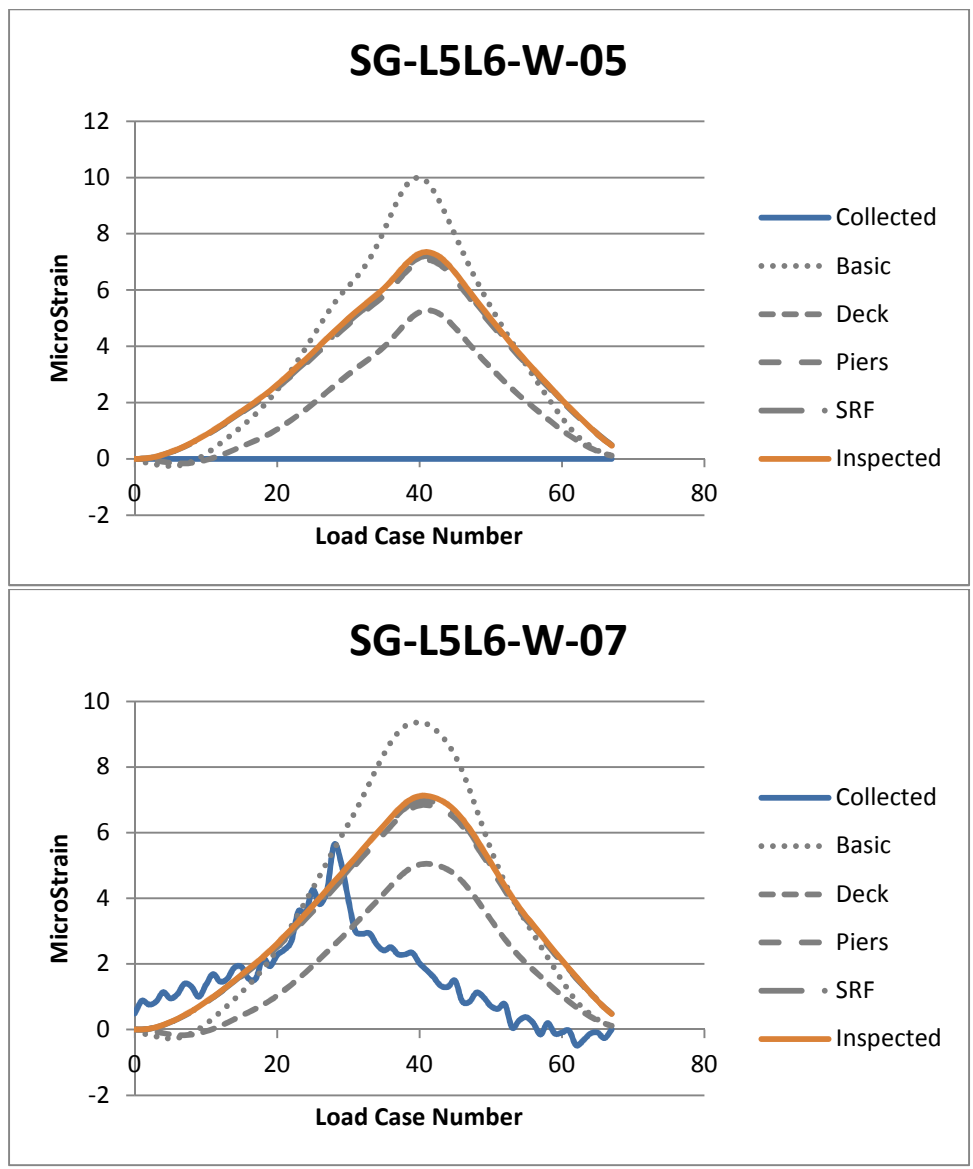
SG-L5L6-E-01**SG-L5L6-E-02**

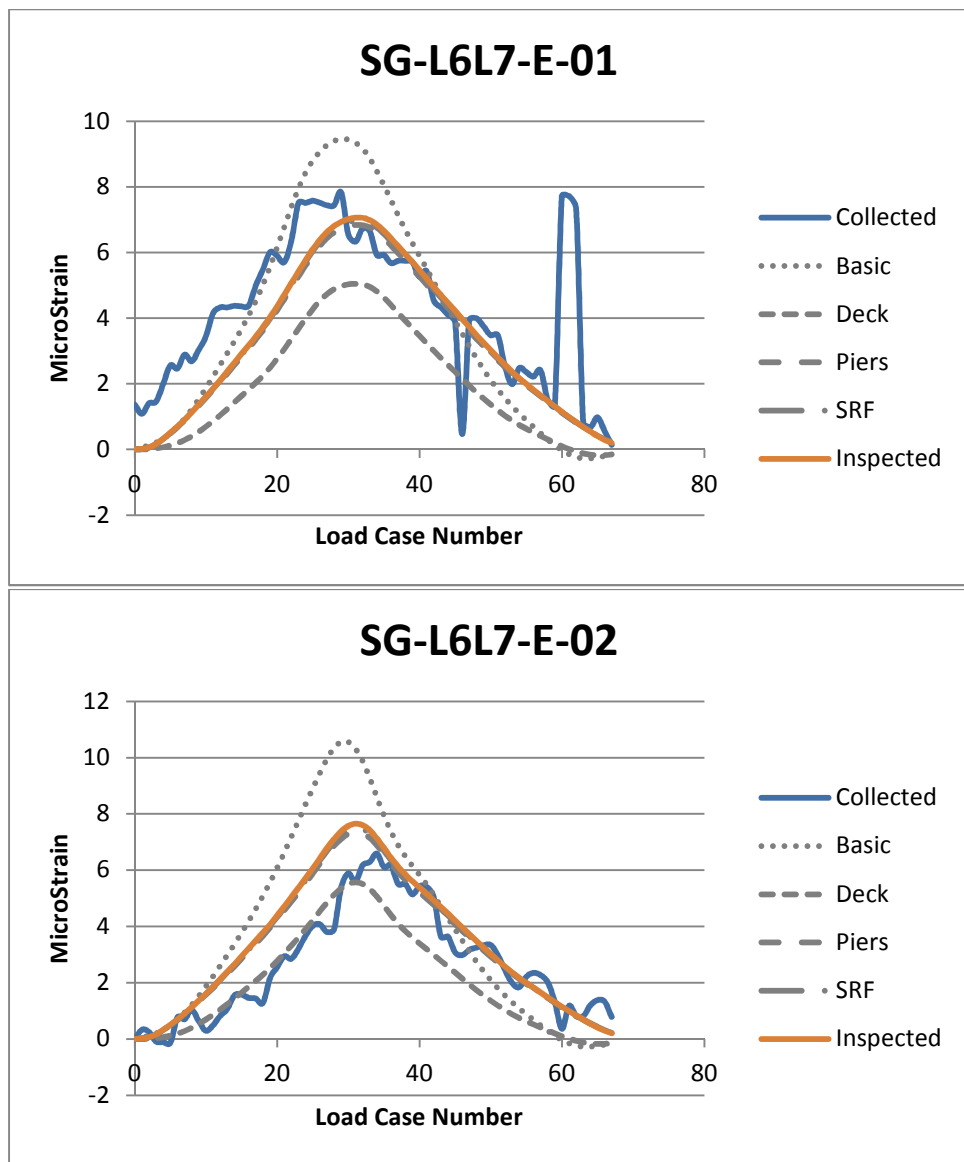


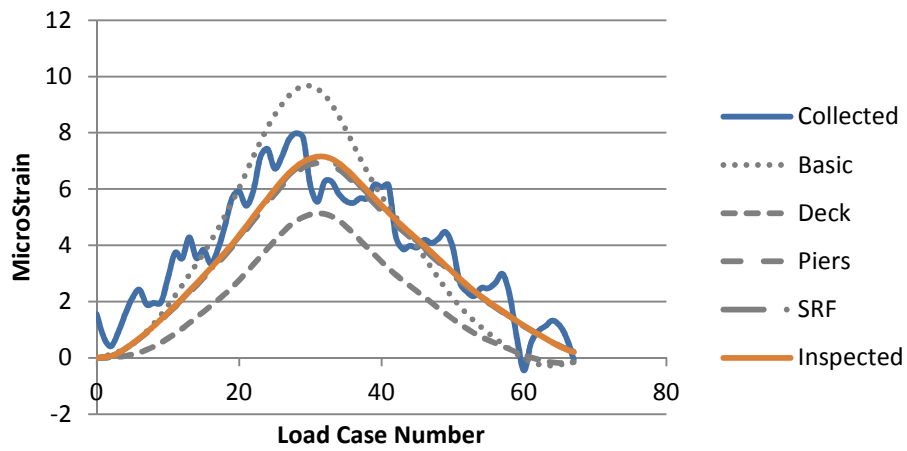
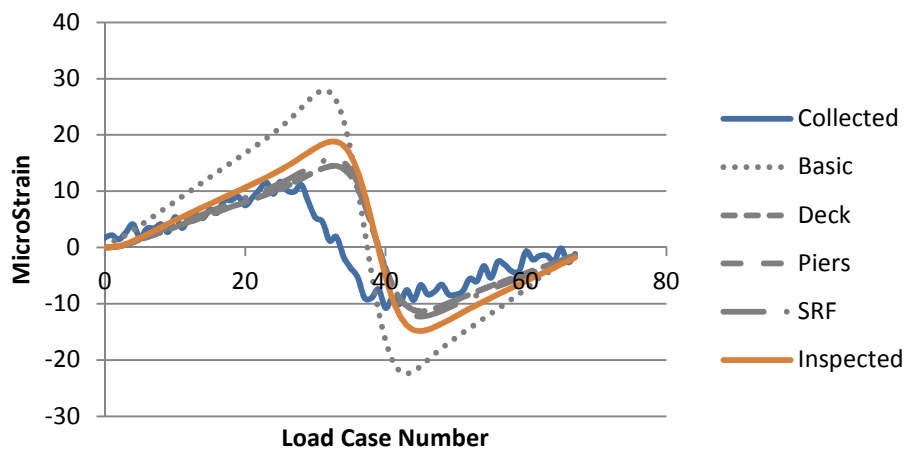


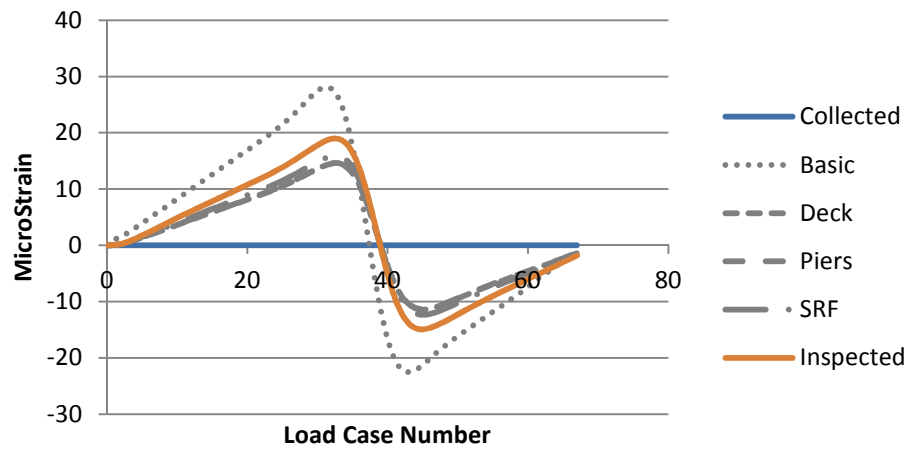
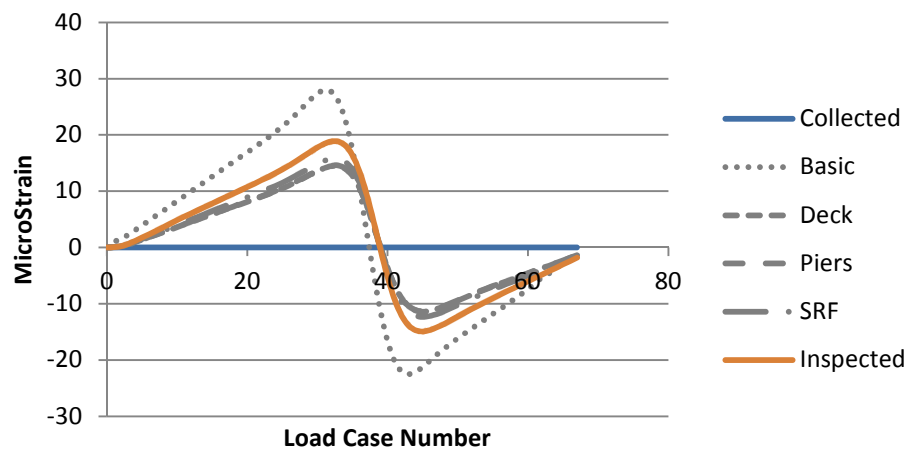


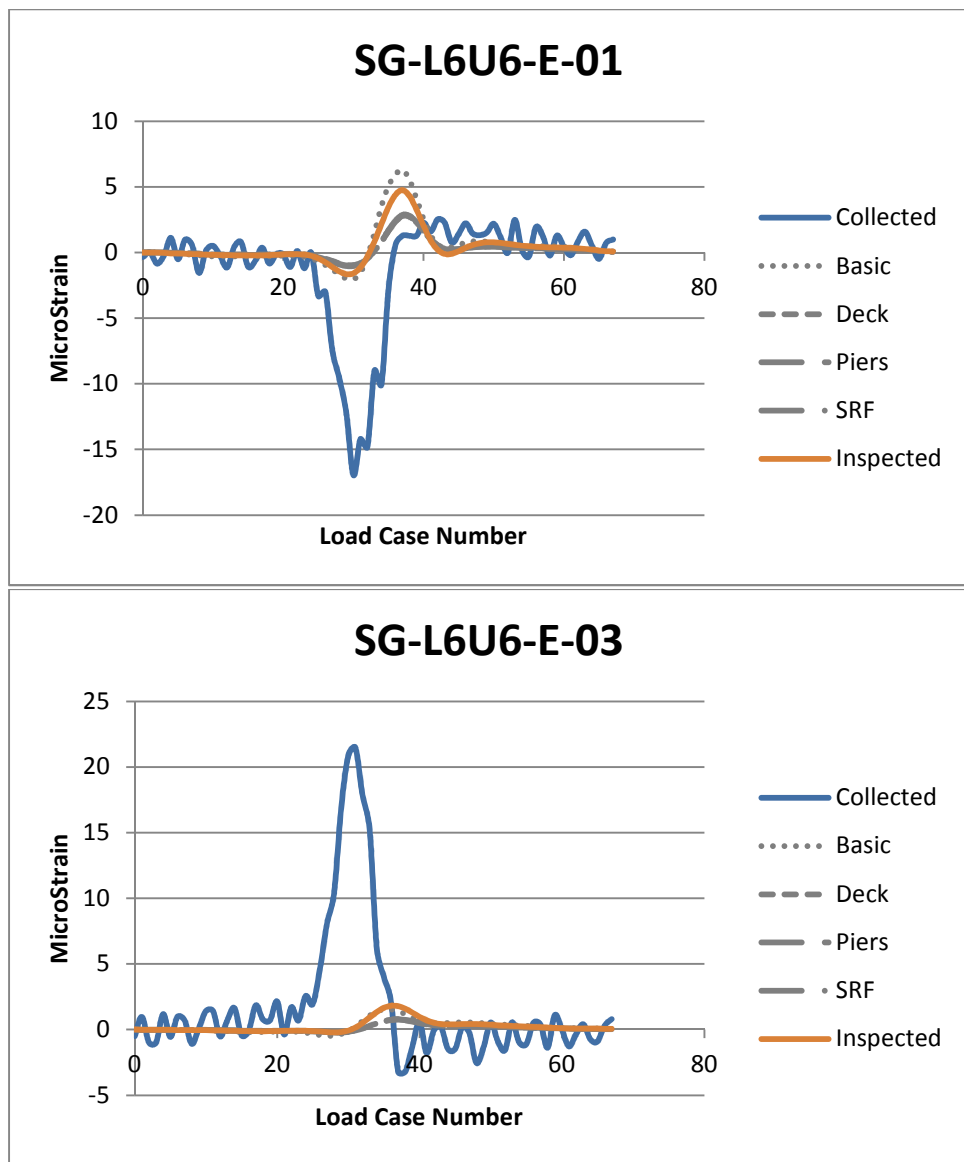


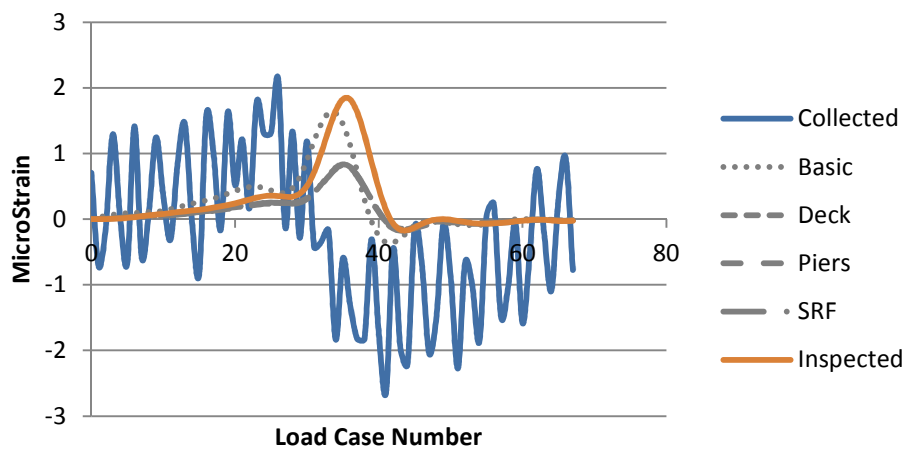
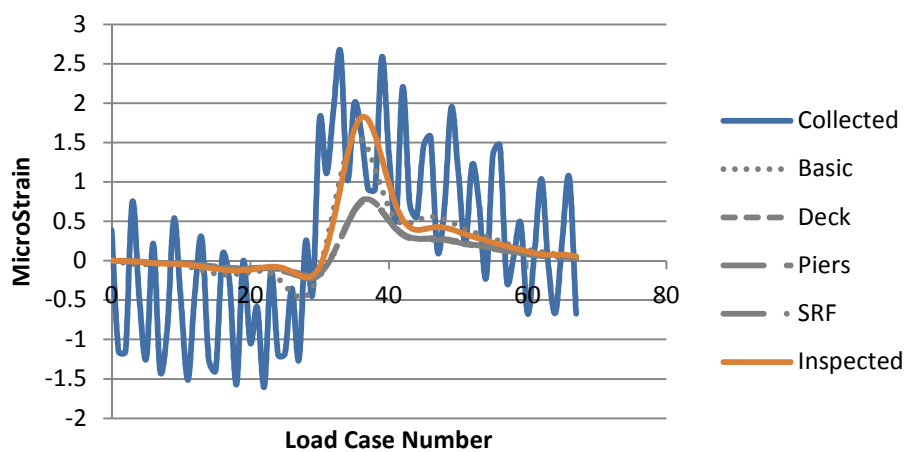


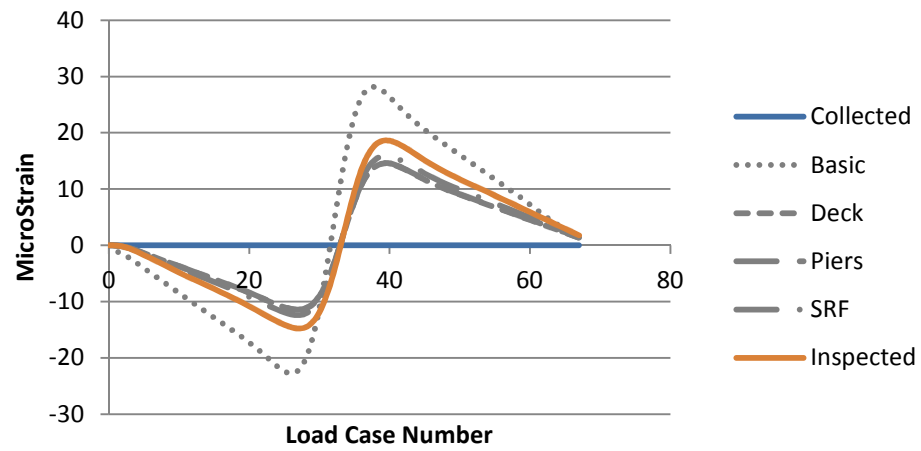
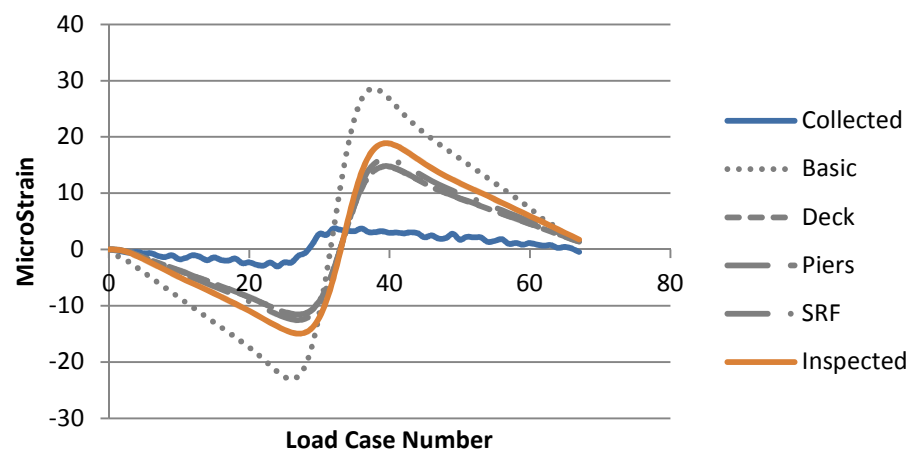


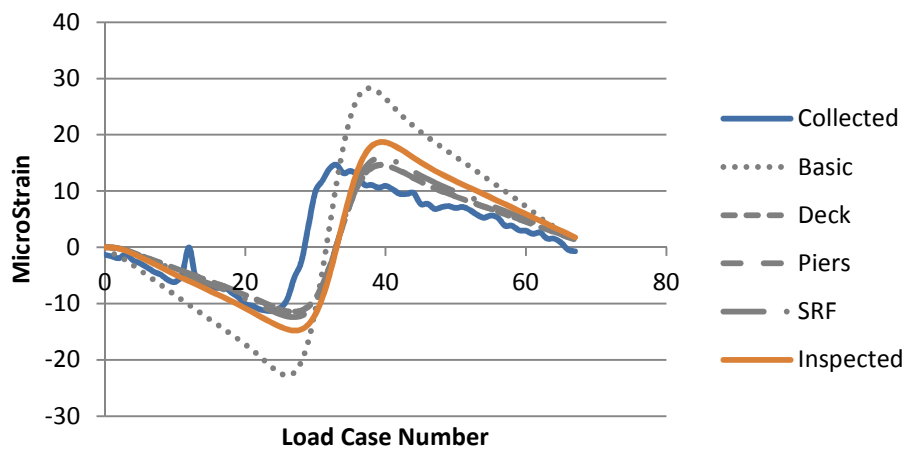
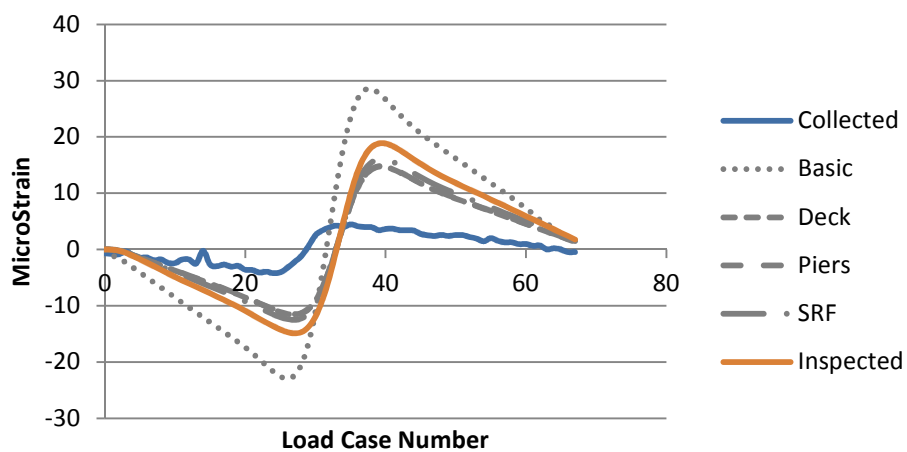
SG-L6L7-E-07**SG-L6U5-E-01**

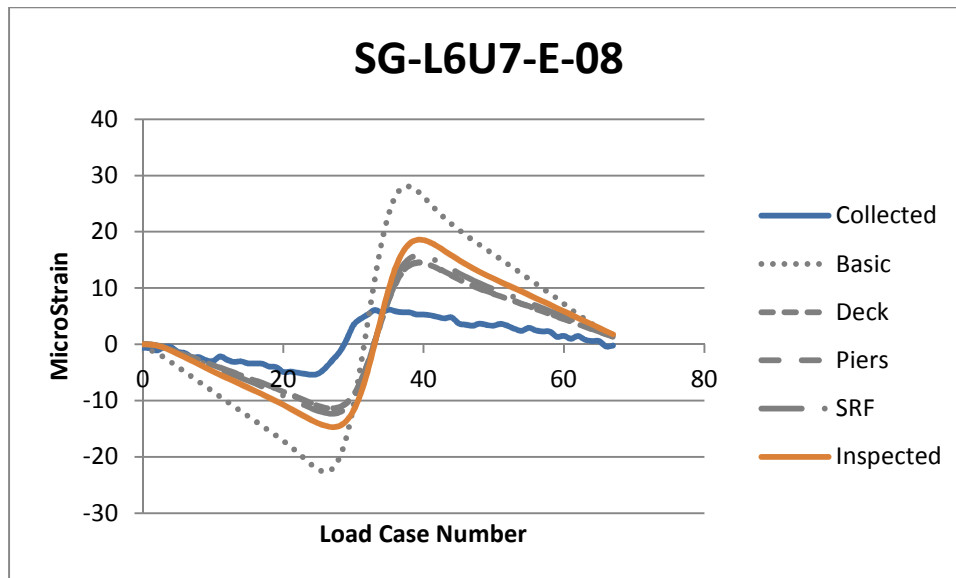
SG-L6U5-E-02**SG-L6U5-E-07**



SG-L6U6-E-05**SG-L6U6-E-07**

SG-L6U7-E-03**SG-L6U7-E-04**

SG-L6U7-E-05**SG-L6U7-E-06**



Appendix 4: VBA Routines

Model Updating Protocol

Option Explicit

Option Base 0

Sub GetMemberInfo()

 'dimension variables

 Dim SapObject As SAP2000v15.SapObject

 Dim SapModel As cSapModel

 Dim FileName As String

 Dim ret As Long

 Dim membername As String

 Dim lastrow As Long

 Worksheets("From_SAP").Activate

 lastrow = Range("A2").End(xlDown).Row

 Range("A2:l" & lastrow).ClearContents

 Application.ScreenUpdating = True

 Application.ScreenUpdating = False

 'Request filename of model

 FileName = Application.GetOpenFilename("SAP2000 files (*.sdb), *.sdb", 1, "Open", , False)

 'Create an instance of the Sap2000 object

 Set SapObject = New SAP2000v15.SapObject

 'Start the Sap2000 application

 SapObject.ApplicationStart

 'Create the SapModel object

 Set SapModel = SapObject.SapModel

 'Initialize Model

 ret = SapModel.InitializeNewModel

 'Open the existing Model

 ret = SapModel.File.OpenFile(FileName)

```

'Hide SAP
ret = SapObject.Hide

'get frame object names
Dim NumberNames As Long
Dim MemberNames() As String
ret = SapModel.FrameObj.GetNameList(NumberNames, MemberNames)

'Output Array to Excel
Worksheets("From_SAP").Activate
Range("A2:A" & UBound(MemberNames) + 1) =
WorksheetFunction.Transpose(MemberNames)

'Get frame object data
Dim Modifiers(7) As Double
Dim i As Double
Worksheets("From_SAP").Activate
Range("A2").Activate
i = 2
Dim j As Integer
Do Until i = UBound(MemberNames, 1) + 2
    ret = SapModel.FrameObj.GetModifiers(ActiveCell, Modifiers)
    j = 0
    For j = 2 To 9
        Cells(i, j) = Modifiers(j - 2)
        'Range("B" & i & ":I" & i) = Modifiers(j)
    Next j
    ActiveCell.Offset(1, 0).Activate
    i = 1 + i
Loop

'Copy Inspected Members to "To_SAP" worksheet
Worksheets("Inspection_Data").Activate
Range("B5").Activate
j = 2
Do Until ActiveCell.Value = ""
    If ActiveCell = "Member" Or ActiveCell = "." Then
        ActiveCell.Offset(1, 0).Activate
    Else
        Worksheets("To_SAP").Range("A" & j) = ActiveCell.Value
        ActiveCell.Offset(1, 0).Activate
        j = j + 1
    End If
Loop

```

```

Range("B5").Activate
SapModel.SetModelsLocked (False)

'Assign modifiers to SAP model
Worksheets("To_SAP").Activate
Range("A2").Activate
Dim Updated_Modifiers(7) As Double
Do Until ActiveCell = ""
    membername = ActiveCell.Value
    ActiveCell.Offset(0, 1).Activate
    Updated_Modifiers(0) = ActiveCell
    ActiveCell.Offset(0, 1).Activate
    Updated_Modifiers(1) = ActiveCell
    ActiveCell.Offset(0, 1).Activate
    Updated_Modifiers(2) = ActiveCell
    ActiveCell.Offset(0, 1).Activate
    Updated_Modifiers(3) = ActiveCell
    ActiveCell.Offset(0, 1).Activate
    Updated_Modifiers(4) = ActiveCell
    ActiveCell.Offset(0, 1).Activate
    Updated_Modifiers(5) = ActiveCell
    ActiveCell.Offset(0, 1).Activate
    Updated_Modifiers(6) = ActiveCell
    ActiveCell.Offset(0, 1).Activate
    Updated_Modifiers(7) = ActiveCell
    'ret = SapModel.FrameObj.SetSelected(membername, True)
    ret = SapModel.FrameObj.SetModifiers(membername, Updated_Modifiers)
    If Not ret = 0 Then
        MsgBox ("Fail at " & Range("A" & ActiveCell.Row))
        Debug.Assert False
    End If
    ActiveCell.Offset(1, -8).Activate
Loop
Range("A2").Activate

'Save SBD file
Dim SaveFile As Variant
Dim filepath As String
Dim sapname As String
Dim slash_location As Long
Dim root_location As String
Dim sap_extension As String
filepath = ActiveWorkbook.Path & "\\Little Mystic\\Updated Models\\"
'find location of last \ from left

```

```

slash_location = InStrRev(FileName, "\")
'number of characters from slash to the right
sapname = Right(FileName, Len(FileName) - slash_location)
'add "Updated" to end of sapname
sap_extension = Right(sapname, 4)
sapname = Left(sapname, Len(sapname) - 4)
sapname = sapname & "_Updated" & sap_extension
'Unhide SAP
ret = SapObject.Unhide

SaveFile = filepath & sapname
ret = SapModel.File.Save(SaveFile)

'Close Sap2000
SapObject.ApplicationExit False
Set SapModel = Nothing
Set SapObject = Nothing
Application.ScreenUpdating = True
Worksheets("From_SAP").Activate

End Sub

```